

Tropical methods for stable Horikawa surfaces

Jonny Evans

Angelica Simonetti

Giancarlo Urzúa

May 7, 2024

Abstract

There are many strata in the KSBA boundary of the moduli space of octic double planes ($K^2 = 2$, $p_g = 3$). We use methods from tropical and toric geometry to show that only three of these correspond to surfaces with at worst quotient singularities.

1 Introduction

§1.1 This paper has been written to illustrate the power of techniques from tropical geometry and mirror symmetry for studying the KSBA moduli space of surfaces on or near the Noether line. We focus on the case of surfaces with $K^2 = 2$ and $p_g = 3$, where we are able to give a complete classification of the strata in the KSBA boundary corresponding to normal surfaces with at worst cyclic quotient singularities: there are three such strata, and we completely understand the singularities which appear (see Theorem §1.8). The integral affine geometry of some associated tropicalisations is the key ingredient which allows us to tame the case analysis.

§1.2 Double branched covers of rational and ruled surfaces furnish us with a wealth of examples of surfaces of general type. In particular, all of the surfaces on the Noether line $2p_g = K^2 + 4$ arise in this way: the double branched cover is simply the canonical morphism $\kappa: X \rightarrow \kappa(X) \subset \mathbb{P}(H^0(K_X)^\vee)$. These Noether-line surfaces are called *Horikawa surfaces* after the exhaustive study by Horikawa in his seminal sequence of papers [25, 26, 27, 28, 29].

§1.3 The moduli space of smooth surfaces of general type with fixed Chern numbers is not compact, but it admits a compactification suggested by Kollár and Shepherd-Barron [34]. This compactified moduli space was shown to be separated by Kollár and Shepherd-Barron in their original paper, and was shown to be compact by Alexeev [3], so it is usually called the *Kollár–Shepherd-Barron–Alexeev (KSBA) moduli space*. See the recent comprehensive monograph by Kollár [33] for the state of the art. The boundary points of the KSBA moduli space correspond to certain singular surfaces called *KSBA-stable surfaces*. In this paper we are interested in KSBA-stable surfaces which arise as degenerations of smooth

Horikawa surfaces. For other work on this problem, see the recent papers by Rana and Rollenske [41] and Anthes [5]. An explicit understanding of KSBA limits for other choices of Chern numbers have also been the object of intense study in the last decade; progress has been made for $K^2 = 5$, $p_g = 4$ (quintics) [40] and for $K^2 = 1$, $p_g = 3$ [9, 15, 16, 18, 42]. We are particularly interested in KSBA-limits which are normal with at worst quotient singularities. For convenience, we will refer to a normal, projective surface with at worst quotient singularities as *NPQ* and we will refer to surface singularities which are not cyclic quotient singularities as *ugly*.

§1.4 Work-in-progress by Monreal, Negrete and Urzúa [39] gives a list of all possible combinations of cyclic quotient singularities that could conceivably occur on an KSBA-stable NPQ surface on the Noether line. They achieve this by observing that the minimal model of the minimal resolution of such a surface is an elliptic surface, and then proving restrictions on the possible Hirzebruch-Jung chains of rational curves one could find on a blow-up of an elliptic surface. They construct stable surfaces realising all these combinations of singularities, however, the sheaf cohomology group which measures local-to-global obstructions to smoothing their surfaces is not zero, and indeed most of these surfaces are not smoothable (this follows from Theorem §1.8 below). Even though these surfaces are not smoothable, one can rationally blow-down their minimal resolutions to get smooth 4-manifolds, and it would be interesting to know if these smooth 4-manifolds are diffeomorphic to smooth Horikawa surfaces with the same Chern numbers.

§1.5 Since we wish to understand the KSBA limits of smooth surfaces, we will work in the opposite direction to Monreal–Negrete–Urzúa: we start with a smooth Horikawa surface and see what singularities appear when it degenerates. One way to produce degenerations of double branched covers $X \rightarrow Y$ is to allow the branch curve to degenerate. Still more examples can be found if we also allow the space Y to degenerate as well. In this paper, we will explore this in the simplest case where $Y = \mathbb{P}^2$ and the branch curve has degree 8. The double cover is then called a *octic double plane*; it is a surface of general type with $K^2 = 2$, $p_g = 3$, which is the minimal value of K^2 for a surface on the Noether line. Indeed, these surfaces were already understood by Moishezon [44, Глава VI §3 Теорема 6] before the work of Horikawa. The KSBA-stable limits of octic double planes with Gorenstein singularities have been studied extensively by Anthes [5], who also gives the first examples of non-Gorenstein limits [5, Example 5.5]. Our approach is to organise the possible cases for degeneration of the branch curve using the integral affine geometry of the *tropicalisation* of Y . This is completely systematic, and would eventually reveal all normal KSBA-stable limits arising as branched double covers. In the interests of writing a paper of bounded length, we will focus the problem on classifying the NPQ limits (which are always branched double covers, see §3.8).

§1.6 Remark. The problem of studying KSBA limits of double planes is closely related to studying KSBA limits of pairs (\mathbb{P}^2, kB) for B a plane curve. Such KSBA moduli spaces

of pairs have been introduced by Hacking [22] and were the basis for Anthes’s approach in [5]. DeVleming and Stapleton [12] used Hacking’s ideas to study the failure or otherwise of planarity of a curve to persist under taking limits; their work is very much relevant to this paper and we will use some of their results to show our stable surfaces are smoothable. A tropical perspective on moduli of log Calabi-Yau pairs (Y, B) was recently introduced by Alexeev, Argüz and Bousseau [4].

§1.7 A lot of effort has gone into studying the degenerations of \mathbb{P}^2 , starting with the work of Bădescu [7] and Manetti [36]. The case where Y is an NPQ surface admitting a smoothing to \mathbb{P}^2 is now completely understood thanks to work of Hacking and Prokhorov [23, 24]. Such a surface is called a *Manetti surface* and must be (a partial smoothing of) a weighted projective plane $\mathbb{P}(a^2, b^2, c^2)$ where the triple (a, b, c) satisfies the *Markov equation* $a^2 + b^2 + c^2 = 3abc$. Such a triple is called a *Markov triple*. We will write $\mathbb{HPP}(a, b)$ (respectively $\mathbb{HPP}(c)$) for the Manetti surface obtained by partially smoothing one (respectively two) of the singularities of $\mathbb{P}(a^2, b^2, c^2)$ and keeping the two (respectively one) indicated by the label. Note that $\mathbb{HPP}(a, b)$ is uniquely determined up to isomorphism by a and b ; $\mathbb{HPP}(c)$ is uniquely determined up to isomorphism by (a, b, c) and c , where the dependence on the triple can be ignored assuming that it appears as the biggest number in a unique triple (which is conjectured to be the case—we live in hope and omit the triple from the notation).

§1.8 Theorem. *Let X be a normal KSBA-stable surface which admits a \mathbb{Q} -Gorenstein smoothing whose general fibre is a smooth octic double plane. Suppose that X has at worst isolated quotient singularities. Then either X is an octic double plane with at worst ADE singularities or else X is one of the following:*

- (i) *A double cover of $Y = \mathbb{P}(1, 1, 4)$ branched over a curve B defined by an equation of weighted homogeneous degree 16 and avoiding the singularity of Y . The non-Gorenstein singularities of X comprise two $\frac{1}{4}(1, 1)$ singularities living over the singularity of Y (see §11.3). These surfaces were constructed by Anthes [5, Example 5.5].*
- (ii) *A double cover of $Y = \mathbb{P}(1, 4, 25)$ branched over a curve B defined by an equation of weighted homogeneous degree 80, avoiding the $\frac{1}{4}(1, 1)$ singularity of Y but passing through the $\frac{1}{25}(1, 4)$ singularity. The non-Gorenstein singularities of X comprise two $\frac{1}{4}(1, 1)$ singularities and a $\frac{1}{50}(1, 29)$ singularity (see §11.12).*
- (iii) *A double cover of $Y = \mathbb{HPP}(5)$ branched over a curve B passing through the $\frac{1}{25}(1, 4)$ singularity. The only non-Gorenstein singularity of X is a $\frac{1}{50}(1, 29)$ singularity (see §11.16).*

§1.9 Remark. Note that X may additionally have ADE singularities coming from the singularities of B , but we ignore these and focus on the non-Gorenstein points. Interestingly, in Cases (i) and (ii), it is not possible to smooth one of the $\frac{1}{4}(1, 1)$ singularities

independently of the other. Similarly, although a $\frac{1}{50}(1, 29)$ singularity admits a partial smoothing with a $\frac{1}{25}(1, 14)$ singularity, this partial smoothing does not globalise in Cases (ii) and (iii) because no surface with a $\frac{1}{25}(1, 14)$ singularity appears on our list.

§1.10 Remark. In Section 14, we will show that all the surfaces from Theorem §1.8 are indeed smoothable: those in Cases (i) and (iii) form (open subsets of) divisors in the KSBA boundary, and those in Case (ii) form a codimension 2 stratum in the closure of these divisors.

§1.11 Remark. Note that Manetti [37, 38] studied the related problem of which *smooth* surfaces arise as limits of branched double covers of \mathbb{P}^2 as the base degenerates. By Horikawa’s classification, this gives us nothing new in the octic double case, and Manetti showed that it still gives nothing new if the degree of the branch curve is divisible by 4. However, when the degree is equal to $2 \pmod{4}$, Manetti shows there exist smooth surfaces which arise as limits of branched double covers of \mathbb{P}^2 and which are branched covers of $\mathbb{P}(1, 1, 4)$ but not of \mathbb{P}^2 .

§1.12 Our proof has the following structure.

- We first observe that a KSBA-stable limit of octic double planes must be an *octic double Manetti surface*, that is a branched double cover of a Manetti surface $\mathbb{P}(a^2, b^2, c^2)$, $\mathbb{H}\mathbb{P}(a, b)$ or $\mathbb{H}\mathbb{P}(c)$, branched over a limit curve B which we continue to refer to as an octic.
- We then prove that an octic double Manetti surface is not normal unless (a, b, c) is one of six possible triples (§9.4, Equation (9.1)).
- For the remaining Markov triples, we analyse their singularities case by case according to the equation of the octic. In three cases, a dense set of octics yield singularities that are worse than cyclic quotient singularities (we call these singularities “ugly” for brevity). Since cyclic quotient singularities cannot be adjacent to ugly singularities (Lemma §3.11), we can ignore these three cases. The only cases which remain are $(1, 1, 1)$ (which cannot give non-Gorenstein singularities), $(1, 1, 2)$ and $(1, 2, 5)$. In these cases, a dense set of octics yield the singularities described in Theorem §1.8 and of the octics which remain, a dense set yield ugly singularities, which allows us to stop our case analysis here.

§1.13 The key idea behind the case analysis is the method of tropicalisation developed by Gross, Hacking, Keel and Kontsevich in their sequence of papers [19, 20, 21]. As a consequence of their work, each Manetti surface has an associated integral affine polygon (*tropicalisation*) whose integral points form a basis for the space of sections of the sheaf $\mathcal{O}(B)$ where B is the octic (Weil) divisor. It is the integral affine geometry of this polygon (and its cousins) which helps us to structure the case analysis.

§1.14 Since we also find stable octic double Manetti surfaces with ugly singularities, we list them as examples here. Their stability is established in Theorem §13.2.

- $(\mathbb{P}(1, 1, 4)$, Case II; see §11.4). A stable, normal surface with one singularity modelled on the $\mathbb{Z}/2$ -quotient of a simple elliptic singularity. This comes from taking a double cover of $\mathbb{P}(1, 1, 4)$ branched over a curve of degree 16 which passes through the singular point (and generic amongst such curves).
- $(\mathbb{P}(1, 1, 4)$, Cases III (a) and (b); see Remark §11.8 and Figure 14). A stable normal surface with one singularity modelled on a $\mathbb{Z}/2$ -quotient of a cusp singularity: there are two possible quotient cusps which appear. These examples arise by taking the double cover of $\mathbb{P}(1, 1, 4)$ branched over a curve of degree 16 which passes through the singular point in specific non-generic ways. There are uglier singularities which can occur as the branch curve degenerates further, but these are not log canonical, and we do not know what the stable replacements of these surfaces are.
- $(\mathbb{P}(1, 4, 25)$, Case III; see §11.14) A stable, normal surface with one $\mathbb{Z}/2$ -quotient of a simple elliptic singularity and a further $\frac{1}{50}(1, 29)$ singularity. This comes from taking a double cover of $\mathbb{P}(1, 4, 25)$ branched over a curve of degree 80 generic amongst those which pass through both singular points.

The remaining cases are either non-normal or non-stable (with singularities that are not log canonical). In the non-stable case, there will exist stable replacements; we conjecture that in most cases these replacements will be non-normal even when the original non-stable surface is normal.

§1.15 Acknowledgements. JE and AS would like to thank GU and the Pontificia Universidad Católica de Chile for their hospitality during a research visit focused on this work. We would like to thank Marcos Canedo, Fabrizio Catanese, Kristin DeVleming, Jan Grabowski, Paul Hacking, Vicente Monreal, Jaime Negrete, Julie Rana, Sönke Rollenske, Jonathan Wahl, and Juan Pablo Zúñiga for helpful conversations and communications. JE and AS are supported by EPSRC Standard Grant EP/W015749/1. GU is supported by FONDECYT Regular Grant 1230065 and a Marie Curie FRIAS Fellowship.

2 Background on branched double covers

§2.1 Transforms of \mathbb{Q} -Cartier divisors. In the remainder of the paper, Y will always be a surface with at worst log terminal singularities. This implies that it is \mathbb{Q} -factorial, and hence that any curve $B \subset Y$ is \mathbb{Q} -Cartier. This means that we can define the total transform of B under a morphism $f: Y' \rightarrow Y$ to be the \mathbb{Q} -divisor $\text{tot}_f(B) := \frac{1}{n}f^{-1}(nB)$ for some (any) $n > 0$ for which nB is Cartier. If f is a contraction with exceptional locus $E = \sum E_i$ then we can write

$$\text{tot}_f(B) = \text{strict}_f(B) + \sum_i \varepsilon_i E_i$$

for some $\varepsilon_i \in \mathbb{Q}$, where the strict transform $\text{strict}_f(B)$ shares no irreducible components in common with E . We will usually omit to write strict_f and simply use the same letter to denote a curve and any of its strict transforms.

§2.2 Branched double covers. Let Y be a (possibly singular) normal projective surface with minimal resolution $\pi: \tilde{Y} \rightarrow Y$. Let $B \subset Y$ be a reduced¹ Cartier divisor, let L be a line bundle with $\mathcal{O}(B) \cong L$, and let s be a section of L such that $B = s^{-1}(0)$. A line bundle S with $S^{\otimes 2} \cong L$ is called a *square root* of L , and given a square root, we get a double cover $f: X \rightarrow Y$ of Y branched over B by defining

$$X = \{\sigma \in S : \sigma^{\otimes 2}(y) = s(y) \text{ for all } y \in Y\},$$

and f to be the restriction of the bundle projection. Provided that s vanishes transversely at a generic point of B , the double cover is again normal.

Now pull everything back to \tilde{Y} : since π^*S is a square root for π^*L , we obtain a double cover $\tilde{f}: \tilde{X} \rightarrow \tilde{Y}$ of \tilde{Y} , branched over $\text{tot}_\pi(B)$. Note that \tilde{X} need not be smooth even though \tilde{Y} is smooth. In fact, since the components of the exceptional locus may appear with multiplicity > 1 in $\text{tot}_\pi(B)$, it is possible that \tilde{X} is not even normal.

§2.3 Lemma. *Let \mathcal{E} denote the set of components of the exceptional set of π . For $E \in \mathcal{E}$, let m_E be the multiplicity of E in $\text{tot}_\pi(B)$. Write $\mathcal{E} = \mathcal{E}_0 \cup \mathcal{E}_1$ where $\mathcal{E}_k := \{E \in \mathcal{E} : m_E \equiv k \pmod{2}\}$. The normalisation of \tilde{X} is obtained by taking the branched double cover of \tilde{Y} branched over $\text{strict}_\pi(B) + \sum_{E \in \mathcal{E}_1} E$.*

Proof. Suppose that E is a component of the exceptional locus of π which appears with multiplicity $m \geq 2$ in $\text{tot}_\pi(B)$. Pick a section ς_E of $\mathcal{O}(-E)$ with a simple pole along E and consider the section $\varsigma_E^2 \otimes s$ of $\mathcal{O}(-E)^{\otimes 2} \otimes L$. This vanishes with multiplicity $m - 2$ along E , and the bundle $\mathcal{O}(-E)^{\otimes 2} \otimes L$ admits a square root (namely $\mathcal{O}(-E) \otimes S$), so we get an associated double cover branched over $\text{tot}_\pi(B) - 2E$. In this way we can reduce the multiplicity of E in the branch locus until it is either 0 (no branching) or 1 (which yields

¹We will only ever consider reduced divisors so that the branched double cover is normal.

a normal branched cover). These cases correspond to m being even or odd respectively. So the double cover of \tilde{Y} branched over $\text{strict}_\pi(B) + \sum_{E \in \mathcal{E}_1} E$ exists and is normal. The morphism $\sigma \mapsto \sigma / \bigotimes_{E \in \mathcal{E}_1} \varsigma_E$ exhibits this double cover as the normalisation of \tilde{X} . \square

§2.4 In most of our examples, B is only \mathbb{Q} -Cartier and we need to modify the above prescription. Suppose there is an odd integer n such that nB is Cartier and let L be a line bundle with $\mathcal{O}(nB) \cong L$ and which admits a square root S . The total transform $\text{tot}_\pi(nB) = n\text{strict}_\pi(B) + \sum m_E E$ is now Cartier because \tilde{Y} is smooth. We now tensor S by $\mathcal{O}(-\text{strict}_\pi(B))^{\otimes (n-1)/2}$ and suitable negative powers of $\mathcal{O}(E)$ to get a normal double cover with branch locus $\text{strict}_\pi(B) + \sum_{E \in \mathcal{E}_1} E$. The important quantity is now the parity of m_E , where m_E/n is the multiplicity of E in $\text{tot}_\pi(B)$: **we drop any exceptional curves of π from the branch locus for which m_E is even, and keep the rest.**

§2.5 In most of our examples, the number n is a product of Markov numbers; the only case which is somewhat subtle is §11.21. In this case, the group of Weil divisors of Y is \mathbb{Z} and the subgroup of Cartier divisors is $1156\mathbb{Z}$. Our branch curve B will live in the class $8 \times 34 = 272 \in \mathbb{Z}$ and $17B$ then inhabits the class $4624 = 4 \times 1156$, and is therefore Cartier (that is, we can get away with taking $n = 17$ rather than $n = 34$).

3 Octic double Manetti surfaces

§3.1 We will be interested in surfaces which are *normal and projective with at worst quotient singularities*, which we abbreviate to NPQ. The goal of this section is to show that an NPQ surface which is the KSBA-stable limit of a family of octic double planes is an octic double Manetti surface (and to define what that means).

§3.2 Lemma. *A finite quotient of an NPQ surface is itself NPQ.*

Proof. A finite quotient of a normal projective variety is again normal and projective. We need to prove that the quotient has at worst quotient singularities. It is sufficient to prove this locally analytically. In what follows, all objects (singularities, automorphisms) are germinal in nature, and \sim denotes equality of germs. Let X be the germ of an isolated quotient singularity \mathbb{C}^2/G with quotient map $f: \mathbb{C}^2 \rightarrow \mathbb{C}^2/G$ and let $H \subset \text{Aut}_{\text{germ}}(X)$ be a finite group of germs of automorphisms so that the quotient is the singularity germ $Y \sim X/H$. Define the group $\tilde{H} \subset \text{Aut}_{\text{germ}}(\mathbb{C}^2) \times H$ to be the group of pairs (g, h) of germs of automorphisms such that $h \circ f \sim f \circ g$. The group \tilde{H} has a forgetful homomorphism to H whose kernel is precisely G . If we can show that the forgetful homomorphism is surjective then we see that $Y \sim X/H \sim \mathbb{C}^2/\tilde{H}$. Given an automorphism $h \in \text{Aut}_{\text{germ}}(X)$, we will define a lift $\tilde{h} \in \tilde{H}$ by setting $\tilde{h}(0) = 0$ and observing that a punctured Euclidean neighbourhood of 0 in $\mathbb{C}^2 \setminus \{0\}$ is simply-connected, so that the germ $h|_{X \setminus \{0\}} \circ f: \mathbb{C}^2 \setminus \{0\} \rightarrow X \setminus \{0\}$ lifts to a germ of a map $\tilde{h}|_{\mathbb{C}^2 \setminus \{0\}}: \mathbb{C}^2 \setminus \{0\} \rightarrow \mathbb{C}^2 \setminus \{0\}$. This map germ is holomorphic because h is holomorphic and holomorphicity is a local condition. \square

§3.3 Lemma. *Suppose that $\pi: \mathcal{X} \rightarrow \Delta$ is a KSBA-stable degeneration over the disc with fibres $X_t := \pi^{-1}(t)$. Suppose that the general fibre X_t , $t \neq 0$, is a double branched cover of \mathbb{P}^2 and that the stable limit X_0 is an NPQ surface. Then X_0 is a double branched cover of a Manetti surface.*

Proof. By [15, Proposition 2.6], the fibre X_0 inherits an involution $i_0: X_0 \rightarrow X_0$ from the general fibres. Let $Y_0 = X_0/\langle i_0 \rangle$. Then, because it is a finite quotient of an NPQ surface, Y_0 is itself NPQ by Lemma §3.2. Since Y_0 is an NPQ degeneration of the plane, it is a Manetti surface. \square

Our next goal is to determine the branch locus of the double cover $X_0 \rightarrow Y_0$ constructed in Lemma §3.3. This will be achieved in Lemma §3.7 below, after some preparation.

§3.4 In the setting of Lemma §3.3, let $\mathcal{Y} \rightarrow \Delta$ be the smoothing of the Manetti surface Y_0 over the disc obtained by quotienting \mathcal{X} by its fibrewise involution, so that the general fibre Y_t is \mathbb{P}^2 . For each singularity² $\frac{1}{p_i}(1, p_i q_i - 1)$, $i = 1, \dots, K$, of Y_0 , we find an embedded copy of the Milnor fibre B_{p_i, q_i} inside \mathbb{P}^2 (note that $K \leq 3$). We can assume that the B_{p_i, q_i} for different singularities are pairwise disjoint since the singularities are distinct. We have $H_2(Y_0; \mathbb{Z}) \cong H_2(\mathbb{P}^2, \bigcup B_{p_i, q_i}; \mathbb{Z})$. The long exact sequence for this relative homology group yields

$$\dots \rightarrow H_2(\mathbb{P}^2; \mathbb{Z}) \rightarrow H_2(Y_0; \mathbb{Z}) \rightarrow H_1\left(\bigcup B_{p_i, q_i}; \mathbb{Z}\right) \rightarrow H_1(\mathbb{P}^2; \mathbb{Z}) = 0.$$

We have $H_1(\bigcup B_{p_i, q_i}; \mathbb{Z}) = \prod \mathbb{Z}/p_i$, and the exact sequence becomes³

$$0 \rightarrow \mathbb{Z} \rightarrow \mathbb{Z} \rightarrow \mathbb{Z}/\left(\prod p_i\right) \rightarrow 0.$$

Therefore the map $\mathbb{Z} = H_2(\mathbb{P}^2; \mathbb{Z}) \rightarrow H_2(Y_0; \mathbb{Z}) = \mathbb{Z}$ takes an octic curve $[B] = 8 \in \mathbb{Z} = H_2(\mathbb{P}^2; \mathbb{Z})$ to a curve in the class $8 \prod p_i \in \mathbb{Z} = H_2(Y_0; \mathbb{Z})$.

§3.5 Definition. We define a Weil divisor on Y_0 to be an *octic* if it lives in the homology class $8 \prod_{i=1}^K p_i \in \mathbb{Z} = H_2(Y_0; \mathbb{Z})$. For example, if $Y = \mathbb{P}(a^2, b^2, c^2)$ then we take a divisor in the linear system $|\mathcal{O}(8abc)|$, i.e. a divisor cut out by a polynomial of weighted degree $8abc$ in the weighted homogeneous coordinates.

§3.6 Let $f: X \rightarrow Y$ be the double cover of a surface Y branched along a curve B . A point $x \in X$ is smooth if $f(x)$ is a smooth point of Y and either $f(x) \notin B$ or $f(x)$ is in the smooth locus of B . The singularities of X therefore arise from

- (i) singular points of Y disjoint from B ,

²Each singularity like $\frac{1}{a^2}(b^2, c^2)$ can be put into this form with $p = a$ and $q = 3c/b \pmod{a}$ because then $c^2/b^2 = pq - 1 \pmod{a^2}$.

³Note that in a Manetti surface, the p_i form part of a Markov triple, and hence are pairwise coprime, which is why $\prod \mathbb{Z}/p_i \cong \mathbb{Z}/(\prod p_i)$.

- (ii) singular points of B on the smooth locus of Y ,
- (iii) singular points of B which lie at singularities of Y .

Type (ii) singularities are necessarily hypersurface singularities (and hence Gorenstein) because the local analytical equation for the branched double cover in local coordinates (x, y) on Y is $u^2 = \Omega(x, y)$ for some polynomial $\Omega(x, y)$. Therefore if we are interested only in non-Gorenstein singularities, we can focus on the singular locus of Y .

§3.7 Lemma. *In the context of Lemma §3.3, the branch curve of the double cover $X_0 \rightarrow Y_0$ is an octic curve in Y_0 in the sense of Definition §3.5.*

Proof. Since the degeneration is KSBA-stable the central fibre and the general fibre have the same value of the characteristic number K^2 . For $t \in \Delta$, let $f_t: X_t \rightarrow Y_t$ be the double cover with branch locus $B_t \subset Y_t$ and ramification locus $R_t \subset X_t$. Then $K_{X_t} = f_t^*(K_{Y_t} + B_t/2)$. When $t \neq 0$, we have $Y_t = \mathbb{P}^2$, $K_{Y_t} = -3h$ and $[B_t] = 8h$ where $h \in H_2(Y_t; \mathbb{Z})$ is a generator. So $K_{X_t}^2 = f_t^*(h^2) = 2$ because h^2 is a single point and f_t is a double cover. When $t = 0$ the generator $h_0 \in H_2(Y_0; \mathbb{Z})$ has self-intersection $\prod_{i=1}^K p_i^2$ and $K_{Y_0} = -3h_0 \prod_{i=1}^K p_i$. Write $B = \beta h_0$ for some $\beta \in \mathbb{Z}$. The only way to achieve $K_{X_0}^2 = 2$ is to take $\beta = 8 \prod_{i=1}^K p_i$, which implies that B is an octic in the sense of Definition §3.5. \square

§3.8 Octic double Manetti surfaces. To summarise, Lemmas §3.3 and §3.7 together imply that an NPQ surface arising as a KSBA-stable limit of octic double planes is an *octic double Manetti surface*, that is a double cover of a Manetti surface branched over an octic curve in the sense of Definition §3.5. The rest of the paper will be dedicated to classifying NPQ octic double Manetti surfaces. We finish this section by proving a lemma that will allow us to disregard vast swathes of octic double Manetti surfaces which have no hope of being NPQ because they are *adjacent to surfaces possessing ugly singularities* in the following sense.

§3.9 Adjacency. Suppose that P is a property of surfaces (e.g. $P(X)$ means that X has at worst cyclic quotient singularities). We say that a surface X_0 is *adjacent to surfaces satisfying P* if there exists a flat family $\pi: \mathcal{X} \rightarrow \Delta$ over the disc with $\pi^{-1}(0) \cong X_0$ and such that $P(X_t)$ holds for all sufficiently small $t \neq 0$, where $X_t := \pi^{-1}(t)$.

§3.10 Ugliness. Any singularity which is not a cyclic quotient singularity we will call *ugly* for brevity. The only cyclic quotient singularities which can appear on stable surfaces are T -singularities. Recall that these are the cyclic quotient singularities admitting a \mathbb{Q} -Gorenstein smoothing, or, equivalently, singularities of the form $\frac{1}{dp^2}(1, dpq - 1)$ for some positive integers d, p, q with $\gcd(p, q) = 1$. We will mostly focus on non-Gorenstein singularities, which means $p \geq 2$.

§3.11 Lemma. *A surface which is adjacent to surfaces possessing at least one ugly singularity must itself possess at least one ugly singularity.*

Proof. The versal deformations of a cyclic quotient singularity have at worst cyclic quotient singularities (see [13, Theorem 2.5] or [34, Corollary 7.15]), so, contrapositively, specialisations of ugly singularities must be ugly. \square

4 Markov triangles and their integral points

§4.1 Markov triples. A triple of positive integers a, b, c is a *Markov triple* if

$$a^2 + b^2 + c^2 = 3abc.$$

Given a Markov triple, we can *mutate* it, replacing a, b, c with $a, b, c' = 3ab - c$. Any Markov triple is related by a sequence of mutations to the triple $(1, 1, 1)$. This gives the set of Markov triples the structure of a directed tree: we connect two triples with an edge if they are related by a mutation, and we direct the edge towards the triple containing the biggest number. We can label an edge in the tree by the pair (a, b) of Markov numbers common to both vertices. We can embed the tree in the upper half-plane, dividing it into regions labelled by Markov numbers in such a way that the boundary of the region labelled a consists of vertices corresponding to triples containing a and linked by mutation. The tree has an obvious symmetry coming from permutations of the three numbers in a triple, and we quotient by this symmetry. See Figure 1. We call this diagram the *Markov topograph*, inspired by Conway [8] (though it is technically a quotient of a topograph). It is conjectured (the Frobenius unicity conjecture, see [1] for a survey) that, once we quotient away the symmetry, every Markov number appears precisely once in this labelling of the regions.

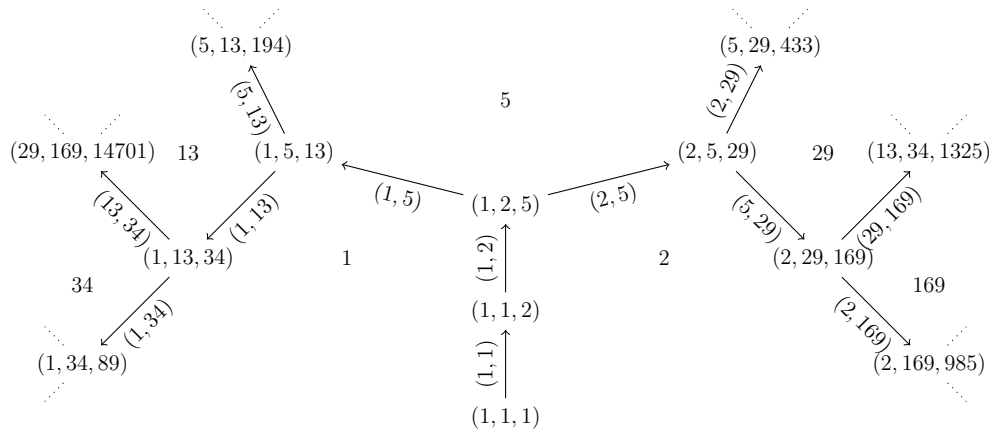


Figure 1: The Markov topograph.

§4.2 Integral affine geometry. In what follows, the details of our case analysis will be governed by the combinatorics of some convex rational polygons and their integral points. For us, the Euclidean geometry of these polygons will be less important than their *integral affine geometry*. In other words, we will consider polygons to be equivalent if and only if they are related by an integral affine transformation, i.e. an element of⁴ $GL(2, \mathbb{Z}) \times \mathbb{Z}^2$. One important quantity invariant under affine transformations is the *integral affine length* $|e|$ of an edge e whose endpoints are rational. This is defined as follows: first rescale e by some integer N to make the endpoints integral; the integral points divide the rescaled edge into some number of segments, say M ; define $|e| := M/N$.

We will be particularly interested in a family of integral affine triangles associated with Markov triples. Namely, given a Markov triple (a, b, c) there is a *Markov triangle*, unique up to the action of $GL(2, \mathbb{Z}) \times \mathbb{R}^2$, whose affine edge lengths are $a/bc, b/ca, c/ab$. Because we are focused on octic curves, we will rescale these triangles by a factor of 8. Because we are interested in integral points, we will need to specify a particular representative of this triangle: arbitrary translations will mess with the set of integral points. We will construct the Markov triangles by performing a sequence of operations called *mutations* to a fixed triangle, but we first need to recall the notion of mutation.

§4.3 Wahl vertices. Let Π be a convex rational polygon and let \mathbf{p} be a vertex of Π where two edges e_1, e_2 meet, ordered so that Π lies anticlockwise of e_1 and clockwise of e_2 . Let $\mathbf{u}_1, \mathbf{u}_2$ be the primitive integer vectors pointing along e_1, e_2 , oriented away from \mathbf{p} . We say that \mathbf{p} is a *Wahl vertex* if $\mathbf{u}_1 \wedge \mathbf{u}_2 = c^2$ and $\mathbf{u}_1 + \mathbf{u}_2 = c\mathbf{w}$ for some integer c and some primitive integer vector \mathbf{w} . Here, $\mathbf{u}_1 \wedge \mathbf{u}_2$ is the determinant of the matrix whose columns are $\mathbf{u}_1, \mathbf{u}_2$. We call c the *index* and \mathbf{w} the *eigendirection* at \mathbf{p} ; indeed, \mathbf{w} spans the unique eigenspace of the linear map $M_{\mathbf{p}}(\mathbf{u}) := \mathbf{u} - (\mathbf{u} \wedge \mathbf{w})\mathbf{w}$. The *eigenline* at \mathbf{p} is the ray emanating from \mathbf{p} in the \mathbf{w} direction.

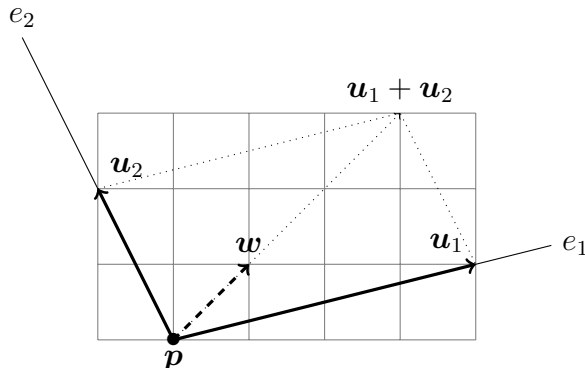


Figure 2: A Wahl vertex with index 3 and eigendirection $(1, 1)$.

⁴Caution: “Integral affine transformations” often refers to the bigger group $GL(2, \mathbb{Z}) \times \mathbb{R}^2$, but the locations of the integral points really matter for us.

§4.4 Mutations. Given a Wahl vertex \mathbf{p} of Π , the eigenline at \mathbf{p} separates Π into two pieces, Π_1 and Π_2 , such that \mathbf{u}_k points into Π_k . We define the *clockwise* (respectively *anticlockwise*) mutation⁵ $\mu_{\mathbf{p}}\Pi$ of Π to be the polygon $\widehat{\mu}_{\mathbf{p}}\Pi := \Pi_1 \cup M_{\mathbf{p}}^{-1}(\Pi_2)$ (respectively $\widehat{\mu}_{\mathbf{p}}\Pi = M_{\mathbf{p}}(\Pi_1) \cup \Pi_2$). In all the examples we will consider, Π will be a triangle contained in the upper half-plane, with a horizontal edge running along the x -axis connecting two Wahl vertices \mathbf{p}_0 on the left and \mathbf{p}_1 on the right. In this situation, for brevity, we will write $\mu_0 := \widehat{\mu}_{\mathbf{p}_0}$ and $\mu_1 := \widehat{\mu}_{\mathbf{p}_1}$. More generally, given a binary sequence $\mathbf{b} = (\mathbf{b}_1, \mathbf{b}_2, \dots, \mathbf{b}_m)$, we will write $\mu_{\mathbf{b}}\Pi := \mu_{\mathbf{b}_m}\mu_{\mathbf{b}_{m-1}} \cdots \mu_{\mathbf{b}_1}\Pi$.

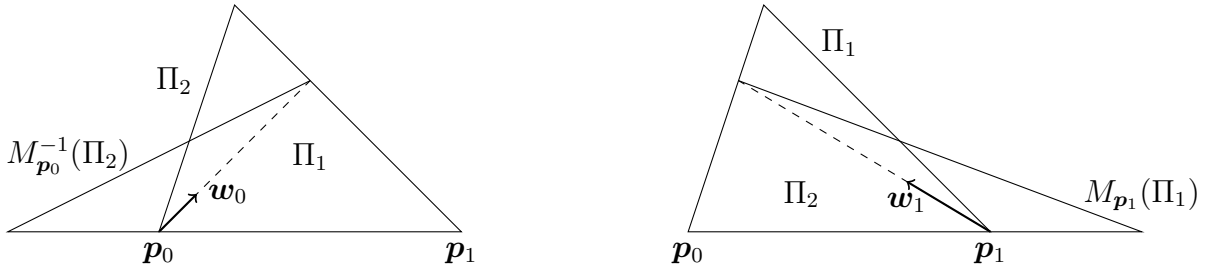


Figure 3: The mutations μ_0 (left) and μ_1 (right).

§4.5 Markov triangles. Let $\Pi(1, 1, 1)$ be the triangle with vertices at $\mathbf{p}_0 = (0, 0)$, $\mathbf{p}_1 = (8, 0)$ and $\mathbf{p}_2 = (0, 8)$. All three vertices are Wahl (with index 1). Define $\Pi(1, 1, 2) = \mu_1\Pi(1, 1, 1)$ and $\Pi(1, 2, 5) = \mu_1\Pi(1, 1, 2)$. Given a binary sequence \mathbf{b} , we obtain a polygon $\Pi(a, b, c) := \mu_{\mathbf{b}}\Pi(1, 2, 5)$. Here, the label (a, b, c) is a Markov triple constructed as follows: start with $(1, 2, 5)$ and perform a sequence of mutations to the triple: if $\mathbf{b}_i = 0$, the i th mutation replaces a by $3bc - a$; if $\mathbf{b}_i = 1$, the i th mutation replaces b by $3ac - b$. We call $\Pi(a, b, c)$ the *Markov triangle* associated with the Markov triple (a, b, c) .

Label the edges of $\Pi(a, b, c)$ as e_c (for the horizontal edge), e_b and e_a (for the edges emanating from the lefthand and righthand vertices \mathbf{p}_0 and \mathbf{p}_1). We have

$$|e_a| = \frac{8a}{bc}, \quad |e_b| = \frac{8b}{ac}, \quad |e_c| = \frac{8c}{ab}.$$

Let $I_0 = \{i : \mathbf{b}_i = 0\}$ and $I_1 = \{i : \mathbf{b}_i = 1\}$, and let $\Pi(a_i, b_i, c_i) = \mu_{(\mathbf{b}_1, \dots, \mathbf{b}_i)}\Pi(1, 2, 5)$. By construction, we have $\mathbf{p}_0 = (-\alpha, 0)$ and $\mathbf{p}_1 = (20 + \beta, 0)$, where

$$\alpha = \sum_{i \in I_0} \frac{8b_i}{a_i c_i} \quad \beta = \sum_{i \in I_1} \frac{8a_i}{b_i c_i}. \quad (4.1)$$

Note that $a, b \leq c$ but it depends on the triple as to whether $a \leq b$ or $b \leq a$.

⁵Mutations appear naturally in the context of integral affine manifolds and almost toric fibrations. The word “clockwise”/“anticlockwise” refers to the way we rotate the branch cut in an almost toric base diagram to pass between the two polygons. See [14, Section 8.4]

§4.6 Fibonacci-type triangles. If $\mathbf{b} = (1, 1, \dots, 1)$ (with length n) then we obtain the triangle $\Pi(1, F_{2n-1}, F_{2n+1}) = \mu_{\mathbf{b}}\Pi(1, 1, 1)$ where $F_1, F_2, F_3, F_4, F_5 \dots = 1, 1, 2, 3, 5 \dots$ is the Fibonacci sequence. We call these *Fibonacci-type triangles/triples*. The vertices lie at $(0, 0)$, $(8F_{2n+1}/F_{2n-1}, 0)$ and $(0, 8F_{2n-1}/F_{2n+1})$.

§4.7 Inner triangle. Let $\Pi := \Pi(a, b, c)$ be a Markov triangle as in §4.5, with edges e_a, e_b, e_c and vertices $\mathbf{p}_0, \mathbf{p}_1, \mathbf{p}_2$. We write \mathbf{w}_k for the eigendirection at \mathbf{p}_k and W_k for the corresponding eigenline. Define the *inner triangle* $\text{inn}(\Pi) \subset \Pi$ to be the subtriangle bounded by e_c, W_0 and W_1 . This has vertices at $\mathbf{p}_0 = (-\alpha, 0)$, $\mathbf{p}_1 = (20 + \beta, 0)$ and $\mathbf{c} = (8/3, 8/3)$ (see Equation (4.1) for α and β). Note that $\text{inn}(\Pi)$ is precisely the region which is fixed by both of the mutations μ_0 and μ_1 . Since the eigenlines all intersect at $(8/3, 8/3)$ in $\Pi(1, 1, 1)$, this continues to be true for all mutations, which is why the third vertex of $\text{inn}(\Pi)$ is at $(8/3, 8/3)$.

§4.8 Integral points. In Figures 4 and 5, we enumerate all the integral points of our triangles $\Pi(a, b, c)$. The \bullet s denote \mathbb{Z} -points on the boundary, the \cdot s denote interior \mathbb{Z} -points, and \circ denotes the origin. Figure 4 shows three special cases: $\Pi(1, 1, 1)$, $\Pi(1, 1, 2)$, and $\Pi(1, 2, 5)$. The remaining cases (Figure 5) fall into three types. If $\Pi = \mu_{\mathbf{b}}\Pi(1, 2, 5)$ then these types are as follows:

- Type A: Fibonacci-type with $n \geq 3$ (i.e. not one of our special cases).
- Type B: $\mathbf{b}_1 = 1$ but at least one $\mathbf{b}_i = 0$.
- Type C: $\mathbf{b}_1 = 0$.

§4.9 Lemma. *If $\Pi := \mu_{\mathbf{b}}\Pi(1, 2, 5)$ has the type described in §4.8 then its integral points are precisely those given in Figure 5.*

Proof. For $\Pi(5, 2, 29) = \mu_1\Pi(1, 2, 5)$, all integral points are contained in $\text{inn}(\Pi(5, 2, 29))$, and since $\text{inn}(\Pi)$ is unaffected by either μ_0 or μ_1 mutations, we have established the lemma for triangles of Type C, which can all be obtained by mutating $\Pi(5, 2, 29)$.

For Fibonacci-triangles starting with $\Pi(1, 5, 13)$, we find that $\text{inn}(\Pi) \cap \mathbb{Z}^2$ consists of:

$$\begin{aligned} & (2, 2), \dots, (7, 2) \\ & (1, 1), \dots, \dots, \dots, (14, 1) \\ & (0, 0), \dots, \dots, \dots, \dots, \dots, (20, 0). \end{aligned}$$

Therefore these integral points are contained in all mutations of $\Pi(1, 5, 13)$, that is all the triangles of Type A or B. If we perform only μ_1 -mutations then the integral points $(0, 1)$, $(0, 2)$, $(1, 2)$, and $(0, 3)$ stay in the polygon because they lie below the eigenline W_1 . This proves the lemma for Type A.

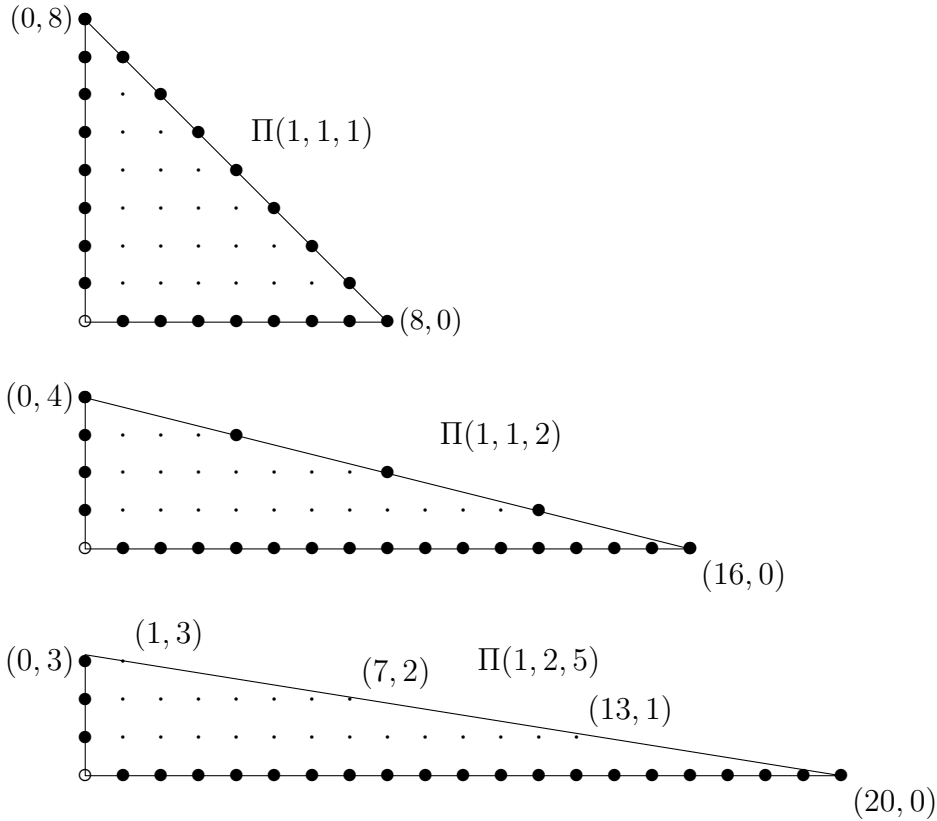


Figure 4: The polygons $\Pi(1, 1, 1)$, $\Pi(1, 1, 2)$, $\Pi(1, 2, 5)$ and their integral points. Note that the top corner of $\Pi(1, 2, 5)$ is not an integral point: it is $(0, 16/5)$.

Suppose that Π is a Type B polygon obtained from a Type A polygon $\Pi' = \Pi(1, F_{2n-1}, F_{2n+1})$ by performing a sequence of mutations starting with μ_0 . Since the eigendirection w_0 is $(1, 1)$, the mutation μ_0 sends the integral point $(1, 2)$ to $(0, 1)$ and the integral points $(0, k)$ to $(-k, 0)$. These latter points are absorbed into the bottom edge of $\mu_0\Pi'$ and are certainly contained in $\text{inn}(\mu_0\Pi')$; it remains to show that $(0, 1)$ lies in $\text{inn}(\mu_0\Pi')$.

The bottom-left vertex of $\mu_0\Pi'$ lies at $(-8F_{2n-1}/F_{2n+1}, 0)$ and the eigenline connects this to $(8/3, 8/3)$. The point $(0, 1)$ lies on or below this eigenline (and hence in $\text{inn}(\mu_0\Pi')$) provided $8F_{2n-1}/F_{2n+1} \geq 8/5$. But the sequence $8F_{2n-1}/F_{2n+1}$ converges to $12 - 4\sqrt{5} \approx 3.0557$ from above, so the inequality $8F_{2n-1}/F_{2n+1} \geq 8/5$ is certainly satisfied. \square

5 Toric and almost toric geometry

We take a moment to recap some basic toric geometry and then explain how it generalises following the work of Gross, Hacking, Keel and Kontsevich [19, 20, 21] to a wider class of varieties which we call *almost toric surfaces*.

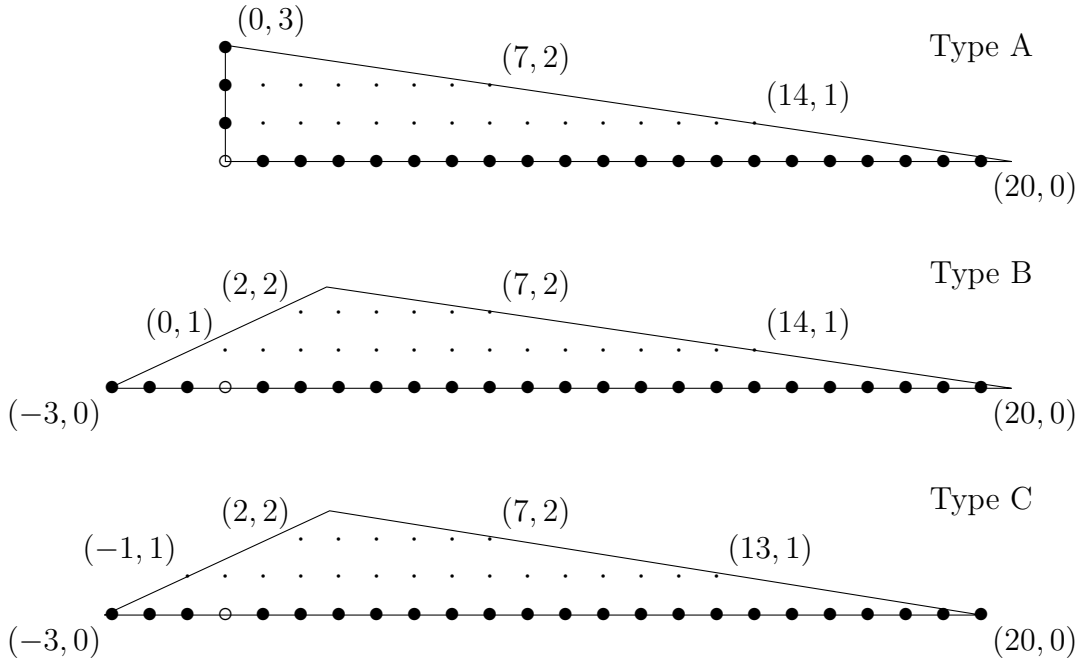


Figure 5: Representative polygons of Type A ($\Pi(1, 5, 13)$), Type B ($\Pi(13, 5, 194)$) and Type C ($\Pi(5, 2, 29)$) and their integral points, which are common to all polygons of these types. Note that none of the corners is an integral point except for $(20, 0)$ in the case $\mu_{(0, \dots, 0)}\Pi(1, 2, 5)$ (a subset of Type C). We have labelled the left- and rightmost integral points on each row.

§5.1 Toric geometry. See [10], [11] or [17] for a proper introduction. We begin by specifying a lattice $N \cong \mathbb{Z}^n$ and its dual lattice M . A toric variety Y is associated to a fan Σ in $N_{\mathbb{R}} = N \otimes_{\mathbb{Z}} \mathbb{R}$. Each cone $\sigma \in \Sigma$ has a dual cone $\sigma^{\vee} \subset M_{\mathbb{R}}$ and the monoid $\sigma^{\vee} \cap M$ of integer points in the dual cone gives us a ring $\mathbb{C}[\sigma^{\vee} \cap M]$ and hence an affine variety. The variety Y is obtained by gluing together these affine pieces using transition functions determined by the fan. The integer points of M therefore have interpretations as local functions on Y . The correct global interpretation is as follows. Each ray $\rho \in \Sigma(1)$ is associated with a torus-invariant divisor $D_{\rho} \subset Y$, and if $B \subset Y$ is a Weil \mathbb{Q} -divisor $B \in |\sum b_{\rho} D_{\rho}|$, then we get a polytope

$$P_B := \{u \in M \otimes_{\mathbb{Z}} \mathbb{R} : \langle u, \rho \rangle \geq -b_{\rho} \forall \rho \in \Sigma(1)\} \subset M_{\mathbb{R}}. \quad (5.1)$$

The integral points of P_B correspond to a basis of the space of sections of the sheaf $\mathcal{O}(B)$ (see [10, Proposition 4.3.3, Example 5.4.5]).

§5.2 Almost toric geometry. Let Y be a rational surface and $D \subset Y$ be a cycle of rational curves supporting an anticanonical divisor. If $p \in D$ is an intersection point between two components of the cycle then the *toric blow-up* of (Y, D) at p is the pair $(\text{Bl}_p(Y), \text{tot}_{\pi}(D))$. If $p \in D$ is any other point then the *non-toric blow-up* of (Y, D) at

p is the pair $(\text{Bl}_p(Y), \text{strict}_\pi(D))$. In both cases, $\pi: \text{Bl}_p(Y) \rightarrow Y$ denotes the blow-up map. We will call a surface Y an *almost toric surface* with *almost toric boundary* D if there exists a toric surface \tilde{Y} with toric boundary \tilde{D} and a sequence of toric and non-toric blow-ups yielding a pair (\tilde{Y}, \tilde{D}) dominating (Y, D) , so that the map $\tilde{Y} \rightarrow Y$ contracts some subchains of the cycle \tilde{D} . Gross, Hacking, Keel and Kontsevich show that the geometry of almost toric surfaces is governed by *tropical manifolds* in a way very similar to how toric varieties are governed by polytopes. A concise exposition of their work which highlights the parallels with toric geometry can be found in the work of Mandel [35]; we now summarise the important points.

§5.3 Tropicalisation. The almost toric analogue of the lattices N and M are the *tropicalisations* $V^{\text{trop}}(\mathbb{Z})$ and $U^{\text{trop}}(\mathbb{Z})$ of the log Calabi-Yau surface $V = Y \setminus D$ and of its mirror U ; each of these is a constellation of integer points in an integral affine manifold⁶ (respectively V^{trop} and U^{trop}) and there is a canonical “pairing” $\langle \cdot, \cdot \rangle: U^{\text{trop}} \times V^{\text{trop}} \rightarrow \mathbb{R}$ which is integral when restricted to the integer points. Despite the forbidding terminology, these integral affine manifolds are constructed in an elementary way from the cycle D , see [20, Section 1.1] or [35, Sections 2.2, 4.1]. The manifold V^{trop} contains a fan Σ consisting of rays ρ_1, \dots, ρ_n corresponding to the curves D_i in the almost toric boundary. Given a Weil \mathbb{Q} -divisor $B \subset Y$ with $B \in |\sum b_i D_i|$, we get a *strongly convex polygon* $\text{Trop}(Y, B) \subset U^{\text{trop}}$ defined by

$$\text{Trop}(Y, B) := \{u \in U^{\text{trop}} : \langle u, \rho_i \rangle \geq -b_i \forall i\} \subset U^{\text{trop}}, \quad (5.2)$$

see [35, Definition 5.14]. We will call $\text{Trop}(Y, B)$ the *tropicalisation of the pair* (Y, B) and will also adopt this notation for the polygon P_B from Equation (5.1). The integral points $\text{Trop}(Y, B) \cap U^{\text{trop}}(\mathbb{Z})$ correspond with a basis for the space of sections of $\mathcal{O}(B)$ [35, Proposition 5.15]. The basis elements are the canonical GHK theta functions.

§5.4 Remark. For symplectically-oriented readers, who are used to Symington’s almost toric geometry [43], there is a close connection. If B is Poincaré-dual to the cohomology class of a symplectic form on Y then the integral affine polygon $\text{Trop}(Y, B)$ is simply the almost toric base diagram for an almost toric fibration on Y , except with all the nodes slid along their eigenlines to the barycentre⁷. The rays in Σ are the eigenrays. We will not use any symplectic almost toric geometry in this paper, but we will use the terminology of branch cuts, nodal trades/slides and mutations for manipulating integral affine manifolds, see for example [14, Chapter 8].

⁶Technically this is not a manifold: the origin is a singular point.

⁷One cannot, in practice, realise this as an almost toric base diagram if the nodes collide in this way, but it still makes sense as an integral affine manifold. If you want a precise statement, you should think of $U^{\text{trop}} \setminus \{(0, 0)\}$ as the almost toric base diagram for an almost toric fibration on the symplectisation of the ideal contact boundary of $Y \setminus D$.

6 Manetti surfaces

§6.1 Manetti surfaces. A *Manetti surface* is a normal projective variety with at worst quotient singularities which arises as a singular limit of a degeneration of \mathbb{P}^2 . The Manetti surfaces have been classified by Hacking and Prokhorov (see [24, Corollary 1.2] or [23, Theorem 1.1]), building on work of Manetti [36]. Some of the Manetti surfaces are toric: they are weighted projective planes $Y = \mathbb{P}(a^2, b^2, c^2)$ associated to Markov triples (a, b, c) . The remaining Manetti surfaces are partial smoothings of the toric Manetti surfaces. They are not toric, but they are almost toric, in the sense of §5.2.

§6.2 Toric Manetti surfaces. Let Y be the toric Manetti surface $\mathbb{P}(a^2, b^2, c^2)$ and $B \subset Y$ be an octic Weil divisor, that is $\mathcal{O}(B) \cong \mathcal{O}(8abc)$, where $\mathcal{O}(8abc)$ is the sheaf whose sections are weighted homogeneous polynomials of total degree $8abc$. Then $\text{Trop}(Y, B)$ is the Markov triangle $\Pi(a, b, c)$ constructed in §4.5. The three vertices $\mathbf{p}_0, \mathbf{p}_1, \mathbf{p}_2$ of $\Pi(a, b, c)$ correspond under the moment map to the three toric fixed points⁸ p_a, p_b, p_c of Y , which are respectively cyclic quotient points modelled on

$$\frac{1}{a^2}(b^2, c^2), \quad \frac{1}{b^2}(c^2, a^2), \quad \frac{1}{c^2}(a^2, b^2).$$

§6.3 Partial smoothings. Fix a toric Manetti surface $Y = \mathbb{P}(a^2, b^2, c^2)$. Pick a proper⁹ subset $S \subset \{a, b, c\}$ of the Markov triple. If you look carefully at the proofs in [24, Section 8] or [23, Section 6], you will see that Hacking and Prokhorov establish more than is stated in their main result: they show that if Y_1 and Y_2 are Manetti surfaces obtained from Y by smoothing precisely the subset $\{p_m, m \notin S\}$ of singularities, then $Y_1 \cong Y_2$. We may therefore unambiguously write $\mathbb{H}\mathbb{P}(S)$ for this partially-smoothed surface. Moreover, they give an explicit description of $\mathbb{H}\mathbb{P}(S)$: it is obtained by taking a (toric) Hirzebruch surface, performing some toric blow-ups, performing one or two non-toric blow-ups (blowing up points on the interior of the toric boundary), and then contracting $|S|$ Wahl chains in the strict transform of the toric boundary. In other words, $\mathbb{H}\mathbb{P}(S)$ is almost toric. In Section 7 we include an example to aid the unversed reader in figuring out exactly how to carry this procedure out in a non-trivial example, and connect this with Symington's almost toric geometry. The number of non-toric blow-ups required is equal to $3 - |S|$, and they occur on different components of the toric boundary. In particular, since all the T -singularities of $\mathbb{P}(a^2, b^2, c^2)$ have Milnor number zero, we never need to non-torically blow-up multiple times on the same boundary component.

§6.4 Topograph revisited. As a result of this refined Hacking–Prokhorov result, the Manetti surfaces can be organised according to the Markov topograph:

- the vertex (a, b, c) corresponds to the toric Manetti surface $\mathbb{H}\mathbb{P}(a, b, c) := \mathbb{P}(a^2, b^2, c^2)$;

⁸The notation p_a, p_b, p_c is ambiguous in the cases of $\mathbb{P}(1, 1, 1)$ and $\mathbb{P}(1, 1, 4)$, but hopefully this will lead to no confusion.

⁹For completeness we can also write $\mathbb{H}\mathbb{P}(\emptyset)$ for \mathbb{P}^2 and $\mathbb{H}\mathbb{P}(a, b, c)$ for $\mathbb{P}(a^2, b^2, c^2)$.

- the edge¹⁰ $\{a, b, c\} \rightsquigarrow \{a, b, c'\}$ corresponds to the Manetti surface we will call $\mathbb{H}\mathbb{P}(a, b)$, obtained from $\mathbb{P}(a^2, b^2, c^2)$ by smoothing the $\frac{1}{c^2}(a^2, b^2)$ singularity and keeping the other two singularities;
- the region labelled c containing the vertex (a, b, c) corresponds to the Manetti surface we will call $\mathbb{H}\mathbb{P}(c)$, obtained from $\mathbb{P}(a^2, b^2, c^2)$ by smoothing everything except the $\frac{1}{c^2}(a^2, b^2)$ singularity.

There is some minor redundancy in this description when the triple contains a 1, for example $\mathbb{H}\mathbb{P}(2) = \mathbb{H}\mathbb{P}(1, 2) = \mathbb{H}\mathbb{P}(1, 1, 2) = \mathbb{P}(1, 1, 4)$.

§6.5 Iten's deformation. If P_1 and P_2 are polygons related by a mutation then Iten [30] constructed a deformation connecting the associated toric surfaces (see also [2]). If $(a, b, c) \rightsquigarrow (a, b, c' = 3ab - c)$ is a mutation of Markov triples, we can write the deformation connecting $\mathbb{H}\mathbb{P}(a, b, c)$ to $\mathbb{H}\mathbb{P}(a, b, c')$ (corresponding to an edge of the topograph) explicitly. Consider weighted homogeneous coordinates $[\xi_1 : \xi_2 : \xi_3 : \xi_4]$ on $\mathbb{P}(a^2, b^2, c, c')$ and consider the pencil of surfaces

$$S_{[t_1:t_2]} := \{\xi_1 \xi_2 = t_1 \xi_3^{c'} + t_2 \xi_4^c\} \subset \mathbb{P}(a^2, b^2, c, c').$$

The surface $S_{[0:1]}$ is isomorphic to $\mathbb{P}(a^2, b^2, c^2)$: it is the image of the embedding

$$\begin{aligned} \mathbb{P}(a^2, b^2, c^2) &\cong \mathbb{P}(a^2 c', b^2 c', c^2 c') \rightarrow \mathbb{P}(a^2 c c', b^2 c c', c^2 c', c(c')^2) \cong \mathbb{P}(a^2, b^2, c, c'), \\ [x : y : z] &\mapsto [x^c : y^c : z : xy]. \end{aligned}$$

The surface $S_{[1:0]}$ is isomorphic to $\mathbb{P}(a^2, b^2, (c')^2)$: it is the image of the embedding

$$\begin{aligned} \mathbb{P}(a^2 c, b^2 c, (c')^2 c) &\rightarrow \mathbb{P}(a^2 c c', b^2 c c', c^2 c', c(c')^2), \\ [x : y : z] &\mapsto [x^{c'} : y^{c'} : xy : z]. \end{aligned}$$

The general fibre $S_{[t_1:t_2]}$ is $\mathbb{H}\mathbb{P}(a, b)$.

§6.6 Note that a divisor on $\mathbb{P}(a^2, b^2, c, c')$ of degree $8ab$ intersects each fibre of the deformation in an octic curve: it has degree $8ab$ on the general fibre $\mathbb{H}\mathbb{P}(a, b)$, degree $8abc$ on $\mathbb{P}(a^2, b^2, c^2)$ and degree $8abc'$ on $\mathbb{P}(a^2, b^2, (c')^2)$. This allows us to give explicit models for the octic double $\mathbb{P}(a^2, b^2, c^2)$ or $\mathbb{H}\mathbb{P}(a, b)$ surfaces:

- In $\mathbb{P}(a^2, b^2, c^2)$, an octic is defined by a weighted homogeneous polynomial $\Omega(x, y, z)$ of weighted degree $8abc$, and an explicit model for the branched double cover is

$$\{[u : x : y : z] \in \mathbb{P}(4abc, a^2, b^2, c^2) : u^2 = \Omega(x, y, z)\}.$$

¹⁰We write curly brackets here to indicate that the triple is unordered: there is a canonical way to order an unordered triple.

- If $\Omega(\xi_1, \xi_2, \xi_3, \xi_4)$ is a polynomial in $[\xi_1 : \xi_2 : \xi_3 : \xi_4] \in \mathbb{P}(a^2, b^2, c, c')$ of weighted degree $8ab$ then an explicit model of the branched double cover of $\mathbb{H}\mathbb{P}(a, b)$ is

$$\left\{ [u : \xi_1 : \xi_2 : \xi_3 : \xi_4] \in \mathbb{P}(4ab, a^2, b^2, c, c') : u^2 = \Omega(\xi_1, \xi_2, \xi_3, \xi_4), \xi_1 \xi_2 = \xi_3^{c'} + \xi_4^c \right\}.$$

The double covers of $\mathbb{H}\mathbb{P}(c)$ are harder to construct explicitly: we will build them instead by taking a double cover of a resolution and then contracting.

7 Example: Manetti surfaces as almost toric surfaces

To help the reader, we include a detailed example of the first really nontrivial almost toric Manetti surface, $\mathbb{H}\mathbb{P}(5)$.

§7.1 Take $\mathbb{P}(1, 4, 25)$, and smooth the $\frac{1}{4}(1, 1)$ singularity. This gives the Manetti surface $\mathbb{H}\mathbb{P}(5)$ with a single $\frac{1}{25}(1, 4)$ singularity. We obtain $\mathbb{H}\mathbb{P}(5)$ as follows. Take the Hirzebruch surface \mathbb{F}_7 and let $A+B+C+D$ be its toric boundary divisor, where $A^2 = -7$, $B^2 = D^2 = 0$ and $C^2 = 7$. Blow up at $B \cap C$, label the exceptional curve E and label all strict transforms with the names of their blown-down selves. Blow up at $B \cap E$ and call the new -1 -curve F . Finally blow up an interior point¹¹ of F and call the final -1 -curve G . We get the configuration of curves shown in Figure 6.

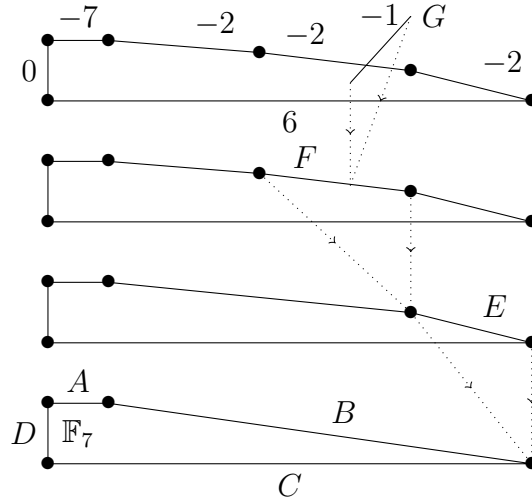


Figure 6: The minimal resolution of $\mathbb{H}\mathbb{P}(5)$ built from \mathbb{F}_7 by two toric blow-ups and one non-toric blow-up. Curves and their self-intersections are labelled.

The surface $\mathbb{H}\mathbb{P}(5)$ is obtained by contracting the divisor $A + B + F + E$ (a Wahl chain with self-intersections $-7, -2, -2, -2$). Note that $\mathbb{H}\mathbb{P}(5)$ is uniquely determined up to

¹¹i.e. a point of F which is not a toric fixed point.

isomorphism by this recipe: although we had to choose the interior point of F for the final, non-toric, blow-up, any two choices are related by the torus action.

§7.2 There is a (Symington-style) almost toric picture of $\mathbb{H}\mathbb{P}(5)$ (Figures 7 and 8). Start with the moment polygon of $\mathbb{P}(1, 4, 25)$: a triangle with vertices at $(0, 0)$, $(25, 0)$ and $(0, 4)$. Make a generalised nodal trade at the corner $(25, 0)$ by introducing a focus-focus singularity connected to this corner along a branch cut pointing in the $(-13, 2)$ direction (you find this direction by adding the two primitive edge vectors $(-1, 0)$ and $(-25, 4)$ emanating from this vertex: $(-1, 0) + (-25, 4) = 2(-13, 2)$). This is an almost toric base diagram for the orbifold $\mathbb{H}\mathbb{P}(5)$ (Figure 7(f))—it can be obtained by a sequence of mutations from the standard moment triangle for \mathbb{P}^2 (Figure 7 (a-f)).

If we take the minimal resolution then the base diagram changes (Figure 8(b)): we make the top corner Delzant by chopping off pieces, introducing new edges pointing in the directions:

$$(1, 0), \quad (7, -1), \quad (13, -2), \quad (19, -3).$$

These correspond to the $-7, -2, -2, -2$ curves A, B, F, E . Note that the edge F is parallel to the branch cut. If we perform a suitable change of branch cut (Figure 8(c)) and a non-toric blow-down (Figure 8(d)), the result is a toric surface which can be blown-down to \mathbb{F}_7 (Figure 8(e)).

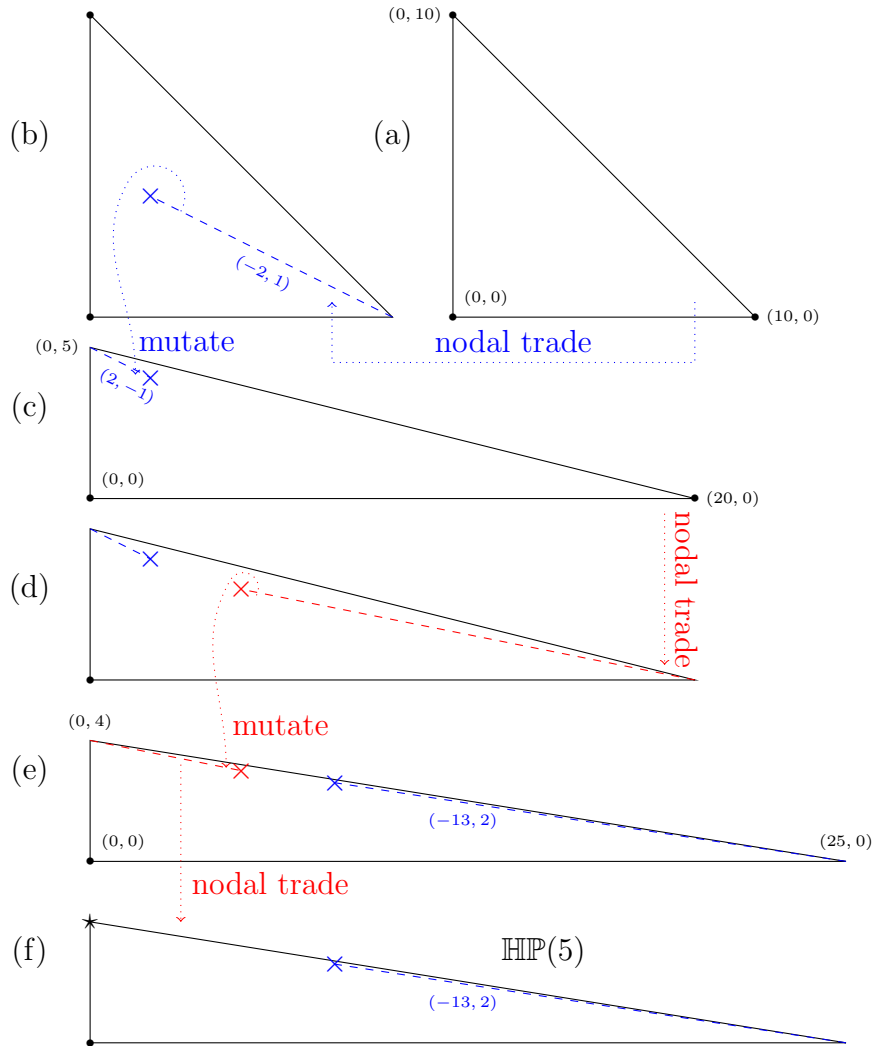


Figure 7: A sequence of mutations to get the almost toric base diagram for $\mathbb{H}\mathbb{P}(5)$. The point marked \star is a $\frac{1}{25}(1, 4)$ singularity. The points marked \bullet are Delzant vertices. The points marked \times are focus-focus fibres.

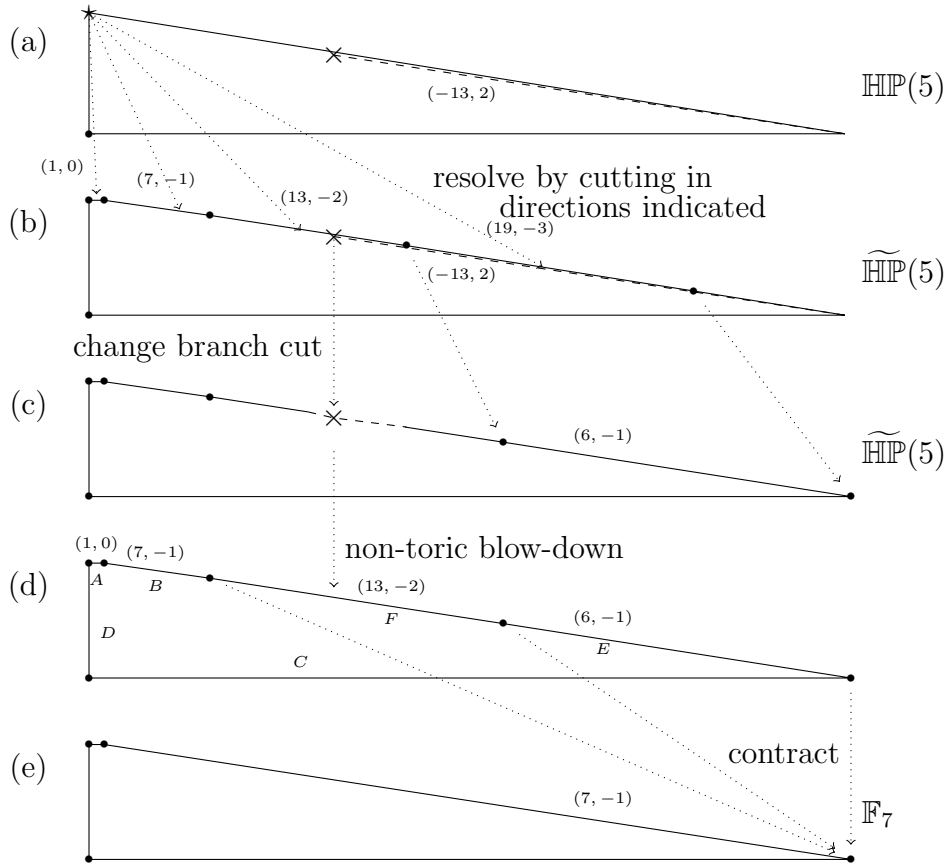


Figure 8: The almost toric base diagram for the minimal resolution $\widetilde{\mathbb{H}\mathbb{P}(5)}$ and its blow-down to \mathbb{F}_7 . Since this is drawn to scale, the branch cuts are hard to see. In (c), there are two branch cuts related by the affine monodromy around the focus-focus singularity. These form two legs of a triangular “hole” whose base is parallel to $(13, -2)$. Non-toric blow-down means filling in this hole. The labels in (d) refer to Figure 6 (with G blown-down).

8 Octic tropicalisations of Manetti surfaces

§8.1 Octic tropicalisations. Let Y be a Manetti surface and $B \subset Y$ be an octic curve. We refer to tropicalisation $\text{Trop}(Y, B)$ as an *octic tropicalisation*. Octic tropicalisations of Manetti surfaces can be described in the following way.

- For the toric case $\mathbb{P}(a^2, b^2, c^2)$, the polygon $\text{Trop}(Y, B)$ is the Markov triangle $\Pi(a, b, c)$ constructed in §4.5.
- For $\mathbb{H}\mathbb{P}(a, b)$, we start with the triangle $\Pi(a, b, c)$ perform a single *nodal trade* at the corner \mathbf{p}_2 corresponding to the $\frac{1}{c^2}(a^2, b^2)$ singularity, and slide the node to the barycentre. In other words, we make a branch cut along the eigenline W_2 connecting \mathbf{p}_2 to $(8/3, 8/3)$ and twist the integral affine structure by the monodromy $M_{\mathbf{p}_2}$ when we cross this branch cut in a clockwise direction.
- For $\mathbb{H}\mathbb{P}(c)$, we start with the moment triangle of $\mathbb{P}(a^2, b^2, c^2)$, perform two nodal trades at the corners \mathbf{p}_0 and \mathbf{p}_1 corresponding to the $\frac{1}{a^2}(b^2, c^2)$ and $\frac{1}{b^2}(c^2, a^2)$ singularities, and slide both nodes to the barycentre. In other words, we make branch cuts connecting \mathbf{p}_0 and \mathbf{p}_1 to $(8/3, 8/3)$ and twist the integral affine structure by the monodromy $M_{\mathbf{p}_0}$ or $M_{\mathbf{p}_1}$ when we cross the corresponding branch cut clockwise.

Note that if any of the “singularities” in S are actually smooth points (e.g. $a = 1$), we omit to perform these nodal trades.

In each of the last two cases, the full tropicalisation U^{trop} is obtained from the resulting picture by erasing the edges of $\text{Trop}(Y, B)$ and extending the branch-cuts out to infinity.

§8.2 We write $\Pi(S)$ for the octic tropicalisation of $\mathbb{H}\mathbb{P}(S)$. Figures 4 and 5 show the octic tropicalisations (i.e. moment polygons) for some of the toric Manetti surfaces. Figure 9 shows the octic tropicalisations for two of the simplest almost toric Manetti surfaces $\Pi(5)$ and $\Pi(29)$.

§8.3 Tropicalisations of the minimal resolution. Let Y be a(n almost) toric Manetti surface $\mathbb{H}\mathbb{P}(S)$ and $B \subset Y$ be an octic curve. The minimal resolution $\pi: \tilde{Y} \rightarrow Y$ is again (almost) toric and the tropicalisation $\text{Trop}(\tilde{Y}, \text{tot}_\pi(B))$ is again $\Pi(S)$: all of the components E_i of the exceptional locus gives us a new edge e_i with inward normal ρ_i but having zero length, residing at the one of the vertices of $\Pi(S)$ (whichever vertex corresponds to the singularity being resolved). We will now compute $\text{Trop}(\tilde{Y}, \text{strict}_\pi(B))$, but first a definition is in order.

§8.4 Definition. (See Figure 10). Let

- $\Pi_5^{\mathbb{Z}}$ be the quadrilateral with vertices at $(0, 0)$, $(0, 3)$, $(1, 3)$, $(20, 0)$,
- $\Pi_A^{\mathbb{Z}}$ be the quadrilateral with vertices at $(0, 0)$, $(0, 3)$, $(14, 1)$, and $(20, 0)$,

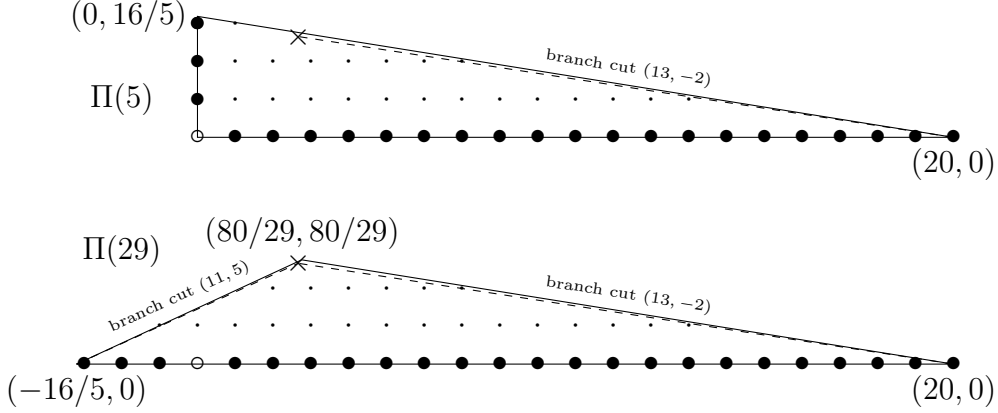


Figure 9: The integral affine manifolds $\Pi(5)$ and $\Pi(29)$. The branch cuts always meet at the point $(8/3, 8/3)$ (marked \times) since this point is invariant under mutation. The origin is marked \circ .

- $\Pi_B^{\mathbb{Z}}$ be the pentagon with vertices at $(-3, 0)$, $(2, 2)$, $(7, 2)$, $(14, 1)$, and $(20, 0)$,
- $\Pi_C^{\mathbb{Z}}$ be the pentagon with vertices at $(-3, 0)$, $(-1, 1)$, $(2, 2)$, $(7, 2)$, $(20, 0)$.

§8.5 Lemma. *Let $B \subset Y$ be an octic curve in a Manetti surface and let $\pi: \tilde{Y} \rightarrow Y$ be the minimal resolution of Y . Recall that we defined Types A, B and C for Markov triangles in §4.8.*

- If $Y = \mathbb{P}(1, 2, 5)$ or $\mathbb{HIP}(5)$ then $\text{Trop}(\tilde{Y}, \text{strict}_{\pi}(B))$ is contained in $\Pi_5^{\mathbb{Z}}$.
- If $\text{Trop}(Y, B)$ is of Type K (for some $K \in \{A, B, C\}$) then $\text{Trop}(\tilde{Y}, \text{strict}_{\pi}(B)) \subset \Pi_K^{\mathbb{Z}}$.

Proof. By Equation (5.2), to find $\text{Trop}(\tilde{Y}, \text{strict}_{\pi}(B))$, we simply move each of these new edges e_i parallelly inwards by $\varepsilon_i \rho_i$ where ε_i is defined in §2.1. Since $\text{strict}_{\pi}(B)$ is an integral Cartier divisor on a smooth variety, [35, Proposition 5.15] implies that $\text{Trop}(\tilde{Y}, \text{strict}_{\pi}(B))$ has vertices at integral points. By Lemma §4.9, this means that $\text{Trop}(\tilde{Y}, \text{strict}_{\pi}(B))$ is contained in one of the three triangles from Definition §8.4 according to its type. \square

9 $\mathbb{HIP}(c)$

§9.1 We will need a particularly good understanding of the surfaces $\mathbb{HIP}(c)$ where two of three singularities have been smoothed, so we now explain their geometry in a little more detail. Fix a Markov triangle $\Pi := \Pi(a, b, c)$ of Type¹² B or C in the sense of §4.8, let $Y = \mathbb{HIP}(c)$, and let \tilde{Y} be its minimal resolution. Recall that Y has a cyclic quotient singularity of type $\frac{1}{c^2}(a^2, b^2)$, or equivalently $\frac{1}{c^2}(1, cq - 1)$ for some $1 \leq q \leq c$ coprime to

¹²Type A surfaces have only two singularities to begin with, so we ignore them for the purposes of this discussion.

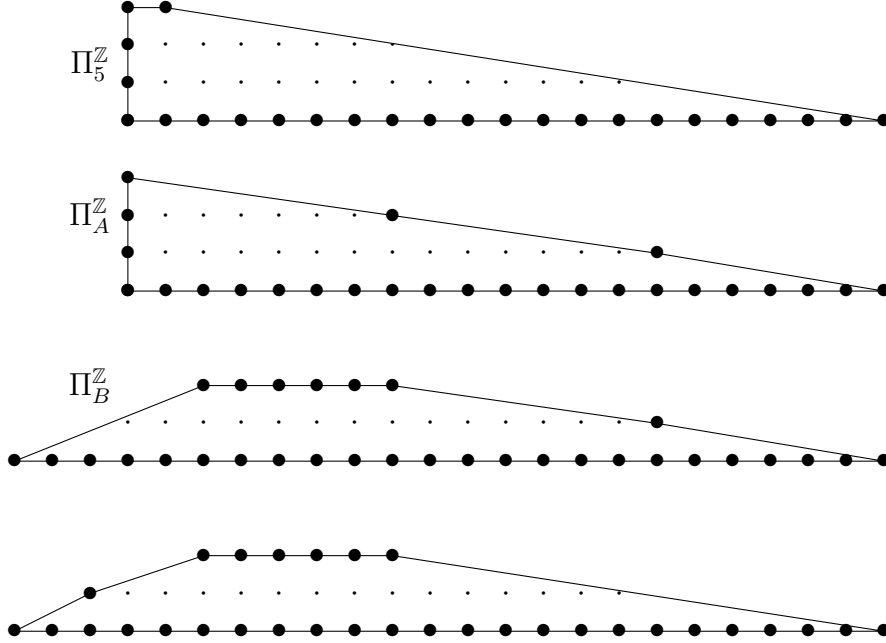


Figure 10: The integral polygons $\Pi_A^{\mathbb{Z}}$, $\Pi_B^{\mathbb{Z}}$, and $\Pi_C^{\mathbb{Z}}$.

c , where $b^2 = (cq - 1)a^2 \pmod{c^2}$. The exceptional locus of the minimal resolution of this singularity is a chain of curves D_1, \dots, D_n with self-intersections given by $D_i^2 = -d_i$ where $[d_1, \dots, d_n]$ is the continued fraction expansion of $\frac{c^2}{cq-1}$. The almost toric boundary is the cycle $D = \sum_{i=0}^n D_i$ of rational curves where D_1, \dots, D_n are the exceptional curves of the minimal resolution and D_0 is the strict transform of the almost toric boundary of Y .

§9.2 As noted in §6.3, the almost toric surface \tilde{Y} involves precisely two non-toric blow-ups. Let us write \mathcal{E}_0 and \mathcal{E}_1 for the exceptional -1 -curves. Define i_0 and i_1 to be the indices such that

$$\mathcal{E}_0 \cdot D_i = \delta_{ii_0}, \quad \mathcal{E}_1 \cdot D_i = \delta_{ii_1}.$$

One can read off these indices from the tropical picture as follows. Recall that the full tropicalisation U^{trop} of \tilde{Y} has two branch cuts parallel to \mathbf{w}_0 and \mathbf{w}_1 (emanating from the point $(8/3, 8/3)$). There are $n + 1$ edges e_i (possibly of length zero) in any tropicalisation, with inward normals ρ_i corresponding to the irreducible components of D . By construction, the edge e_{i_0} is parallel to \mathbf{w}_0 and the edge e_{i_1} is parallel to \mathbf{w}_1 .

§9.3 Since (a, b, c) has Type B (or C), Lemma §8.5 means that $\text{Trop}(\tilde{Y}, \text{strict}_{\pi}(B))$ is contained in the pentagon $\Pi_B^{\mathbb{Z}}$ (or $\Pi_C^{\mathbb{Z}}$). Let us write $\text{strict}_{\pi}(B) \in |\sum_{i=0}^n \tilde{b}_i D_i|$ so that $\text{Trop}(\tilde{Y}, \text{strict}_{\pi}(B))$ is defined by the inequalities (5.2): $\langle u, \rho_i \rangle \geq -\tilde{b}_i$. Here we are expressing u as a vector with respect to an origin at the barycentre $(8/3, 8/3)$. Since $\Pi_B^{\mathbb{Z}} \subset \text{inn}(\Pi)$, and since the edges e_{i_0} and e_{i_1} of $\text{inn}(\Pi)$ run through the barycentre, we must have $\tilde{b}_{i_0} \leq 0$ and $\tilde{b}_{i_1} \leq 0$. In fact, we have the following stronger inequalities:

§9.4 Proposition. *If (a, b, c) is not any of the following triples:*

$$\begin{aligned} (1, 1, 1), \quad (1, 1, 2), \quad (1, 2, 5), \\ (1, 5, 13), \quad (1, 13, 34), \quad (2, 5, 29), \end{aligned} \tag{9.1}$$

then either $\tilde{b}_{i_0} \leq -2$ or $\tilde{b}_{i_1} \leq -2$.

Proof. We defer the proof (which is a pleasant exercise in integral affine geometry) until Section 10. \square

§9.5 Corollary. *Unless (a, b, c) is listed in Equation (9.1), we have $\text{strict}_\pi(B) \cdot \mathcal{E}_0 \leq -2$ or $\text{strict}_\pi(B) \cdot \mathcal{E}_1 \leq -2$.*

Proof. The divisor $\text{strict}_\pi(B)$ is homologous to $\sum_{i=0}^n \tilde{b}_i D_i$ and $\mathcal{E}_k \cdot \sum_{i=0}^n \tilde{b}_i D_i = \tilde{b}_{i_k}$ for $k = 0, 1$, so this follows immediately from Proposition §9.4. \square

§9.6 Corollary. *Unless (a, b, c) is listed in Equation (9.1), the curve B contains either $\pi(\mathcal{E}_0)$ or $\pi(\mathcal{E}_1)$ with multiplicity at least 2.*

Proof. Let $k \in \{0, 1\}$ be such that $\text{strict}_\pi(B) \cdot \mathcal{E}_k \leq -2$. Since this is negative, $\text{strict}_\pi(B)$ must contain \mathcal{E}_k as an irreducible component. Since $(\text{strict}_\pi(B) - \mathcal{E}_k) \cdot \mathcal{E}_k \leq -1$ is still negative, $\text{strict}_\pi(B) - \mathcal{E}_k$ still contains \mathcal{E}_k as an irreducible component, so \mathcal{E}_k appears in $\text{strict}_\pi(B)$ as an irreducible component with multiplicity at least 2. Since \mathcal{E}_k is not contracted by π , this implies that $\pi(\mathcal{E}_k)$ is a component of B with multiplicity at least 2. \square

§9.7 Corollary. *Unless (a, b, c) is listed in Equation (9.1), the double cover of $\mathbb{H}\mathbb{P}(c)$ branched over any octic curve fails to be normal.*

Proof. By Corollary §9.6, we know that any octic curve contains some component $E := \pi(\mathcal{E}_k)$ with multiplicity at least 2. Pick a smooth point of E and choose local analytic coordinates (x, y) centred at this point in such a way that $E = \{y = 0\}$. The equation of B in these coordinates is $y^n f(x, y) = 0$ for some $n \geq 2$ and some analytic function f . The (local analytic) equation of the branched double cover is then $u^2 = y^n f(x, y)$. This is singular along the line $u = y = 0$, that is along the ramification locus. Since this is not an isolated singularity of the surface, it is not normal. \square

§9.8 Remark. Let (a, b, c) be a Markov triple and let B be an octic in $\mathbb{P}(a^2, b^2, c^2)$ (or in $\mathbb{H}\mathbb{P}(b, c)$). If c is not one of 1, 2, 5, 13, 29, 34 then when we partially smooth the singularities p_a and p_b , any deformation of B must contain an irreducible component with multiplicity ≥ 2 by Corollary §9.6. This means that B itself must contain such a multiple component already, so any octic double cover of $\mathbb{P}(a^2, b^2, c^2)$ (or $\mathbb{H}\mathbb{P}(b, c)$) must also be

non-normal. This means that to classify normal octic double Manetti surfaces, it suffices to consider the following finite list of possibilities:

$$\mathbb{P}(1, 1, 2^2), \quad \mathbb{P}(1, 2^2, 5^2), \quad \mathbb{P}(1, 5^2, 13^2), \quad \mathbb{P}(5^2, 2^2, 29^2), \quad \mathbb{P}(1, 13^2, 34^2), \\ \mathbb{HIP}(5, 29), \quad \mathbb{HIP}(2, 29), \quad \mathbb{HIP}(5), \quad \mathbb{HIP}(13), \quad \mathbb{HIP}(29), \quad \mathbb{HIP}(34).$$

10 Proof of Proposition §9.4

§10.1 Lemma. *For a Markov triangle $\Pi(a, b, c)$, we have*

$$\mathbf{w}_1 \wedge \mathbf{w}_2 = 3a, \quad \mathbf{w}_2 \wedge \mathbf{w}_0 = 3b, \quad \mathbf{w}_0 \wedge \mathbf{w}_1 = 3c$$

Proof. One can construct a quiver from a Markov triangle whose vertices correspond to vertices of the triangle and where the number of edges between vertices i and j is $\mathbf{w}_i \wedge \mathbf{w}_j$. Mutation of the polygon induces mutation of this quiver (see [31, Proposition 3.17]). For $\Pi(1, 1, 1)$ we get $3, 3, 3$ and the quiver mutation rule for these arrows is the same as the mutation rule for trebled Markov triples $(3a, 3b, 3c)$. \square

§10.2 Definition. Let $\Pi := \Pi(a, b, c)$ be a Markov triangle with vertices $\mathbf{p}_0, \mathbf{p}_1, \mathbf{p}_2$ and let $\mathbf{n} \in \Pi$ be an integral point. Let J be a clockwise 90° rotation, and let $\mathbf{w}_k^\perp = J\mathbf{w}_k$ for $k = 0, 1, 2$. Define

$$n_k := (\mathbf{n} - \mathbf{p}_k) \cdot \mathbf{w}_k^\perp.$$

Note that if $\mathbf{n} \in \text{inn}(\Pi)$ then

$$n_0 \geq 0, \quad n_1 \leq 0.$$

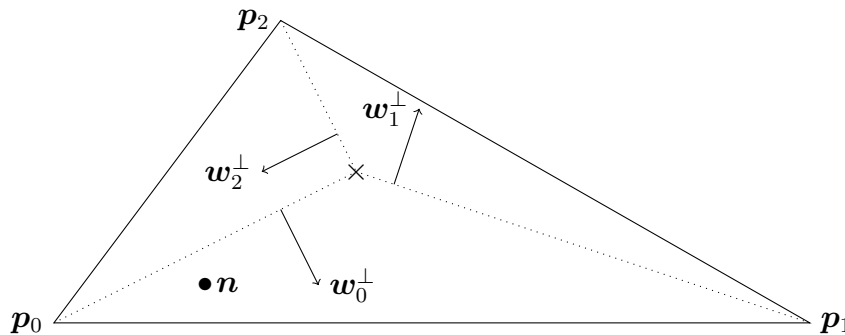


Figure 11: The points \mathbf{n} , \mathbf{p}_i and vectors \mathbf{w}_i^\perp from Definition §10.2. (Not to scale for any Markov triple.)

§10.3 Lemma. *If $\Pi' = \mu_0\Pi$ (and all the quantities/vectors for Π' are just written as for Π but with primes) then*

$$n'_0 = n_2 + 3bn_0, \quad n'_1 = n_1, \quad n'_2 = -n_0.$$

Similarly, if $\Pi'' = \mu_1\Pi$ then

$$n''_0 = n_0, \quad n''_1 = n_2 + 3an_1, \quad n''_2 = -n_1.$$

Proof. We will just prove the formula for μ_0 : the one for μ_1 is similar. We work in coordinates where the origin is at \mathbf{p}_0 . In particular, we have $n_0 = \mathbf{n} \cdot \mathbf{w}_0^\perp$. We have

$$\begin{aligned} \mathbf{p}'_0 &:= \mu_0\mathbf{p}_2 = \mathbf{p}_2 + (\mathbf{p}_2 \wedge \mathbf{w}_0)\mathbf{w}_0 \\ \mathbf{w}'_0 &:= \mu_0\mathbf{w}_2 = \mathbf{w}_2 + (\mathbf{w}_2 \wedge \mathbf{w}_0)\mathbf{w}_0 \\ &= \mathbf{w}_2 + 3b\mathbf{w}_0 \\ (\mathbf{w}'_0)^\perp &= J\mathbf{w}'_0 = \mathbf{w}_2^\perp + 3b\mathbf{w}_0^\perp \end{aligned}$$

Then we have

$$\begin{aligned} n'_0 &= (\mathbf{n} - \mathbf{p}'_0) \cdot (\mathbf{w}'_0)^\perp \\ &= (\mathbf{n} - \mathbf{p}_2 - (\mathbf{p}_2 \wedge \mathbf{w}_0)\mathbf{w}_0) \cdot (\mathbf{w}_2^\perp + 3b\mathbf{w}_0^\perp) \\ &= n_2 + 3b(\mathbf{n} - \mathbf{p}_2) \cdot \mathbf{w}_0^\perp - (\mathbf{p}_2 \wedge \mathbf{w}_0)\mathbf{w}_0 \cdot \mathbf{w}_2^\perp. \end{aligned}$$

We also have $\mathbf{u} \cdot \mathbf{v}^\perp = \mathbf{v} \wedge \mathbf{u}$, so $(\mathbf{p}_2 \wedge \mathbf{w}_0)\mathbf{w}_0 \cdot \mathbf{w}_2^\perp = (\mathbf{w}_0 \wedge \mathbf{w}_2)\mathbf{p}_2 \cdot \mathbf{w}_0^\perp = -3b\mathbf{p}_2 \cdot \mathbf{w}_0^\perp$. Therefore

$$n'_0 = n_2 + 3b\mathbf{n} \cdot \mathbf{w}_0^\perp = n_2 + 3bn_0. \quad \square$$

§10.4 Lemma. *Suppose that Π is a Markov triangle and that \mathbf{n} is a point in $\text{inn}(\Pi)$. Suppose that $n_2 \geq (1 - 3b)n_0$ (respectively $n_2 \leq (1 - 3a)n_1$). Then the same inequality holds for any $\mu_b\Pi$.*

Proof. We will focus on the first inequality; the proof of the second is similar. By induction, it is sufficient to prove the claim for $\Pi' = \Pi(a', b', c') = \mu_0\Pi$ and $\Pi'' = \Pi(a'', b'', c'') = \mu_1\Pi$. For Π'' , the quantity n''_2 is positive and hence automatically satisfies $n''_2 \geq (1 - 3b'')n''_0$. For Π' , we have

$$n'_0 = n_2 + 3bn_0, \quad n'_2 = -n_0.$$

Since $b' \geq 1$, we have $1 - 3b' \leq -2$. Therefore the assumption $n_2 \geq (1 - 3b)n_0$ implies

$$(1 - 3b')(n_2 + 3bn_0) \leq (1 - 3b')n_0. \quad (10.1)$$

Therefore

$$\begin{aligned} n'_2 &= -n_0 \\ &\geq (1 - 3b')n_0 && \text{since } 1 - 3b' < -1 \\ &\geq (1 - 3b')(n_2 + 3bn_0) && \text{by Equation (10.1)} \\ &= (1 - 3b')n'_0 && \text{as required.} \end{aligned} \quad \square$$

§10.5 Corollary. *Suppose that Π is a Markov triangle and that \mathbf{n} is a point in $\text{inn}(\Pi)$. Suppose that*

- $n_2 \geq (1 - 3b)n_0$ and $n_0 \geq 2$, or
- $n_2 \leq (1 - 3a)n_1$ and $n_1 \leq -2$.

Then these inequalities persist for any mutation $\mu_{\mathbf{b}}\Pi$.

Proof. By Lemma §10.4, the inequality $n_2 \geq (1 - 3b)n_0$ persists for any mutation. This means that under a μ_0 mutation, $n'_0 = n_2 + 3bn_0 \geq n_0$, so n_0 cannot decrease. Under a μ_1 mutation, n_0 is unchanged. Therefore $n_0 \geq 2$ for any combination of mutations. The proof for $n_1 \leq -2$ is similar. \square

§10.6 We can now prove Proposition §9.4. Let $\Pi = \Pi(a, b, c)$ be a Markov triangle. As the edge e_{i_0} moves inwards along its normal direction, it first encounters the eigenline W_0 (to which it is parallel) and then it moves over $\text{inn}(\Pi)$ until it reaches the closest integral point, \mathbf{n} . During this final stage of its motion, the affine displacement it suffers is n_0 . On the other side of the polygon, the edge e_{i_1} similarly undergoes a displacement of at least n_1 where \mathbf{n} is a different closest integral point.

If $(a, b, c) = (29, 2, 169)$ (corresponding to the Type C triangle $\mu_{(0,0)}\Pi(1, 2, 5)$) and $\mathbf{n} = (-1, 1)$ then $n_0 = 2$ and $n_2 = 0$. By Lemma §8.5, the same integral point is the closest to e_{i_0} for this (Type C) triple and all its mutations. Corollary §10.5, the inequality $n_0 \geq 2$ persists for all subsequent mutations, so we deduce that $\tilde{b}_{i_0} \leq -2$ for such triples.

Similar arguments work with the triples shown in Table 1. Any triple which is not listed in the statement of Proposition §9.4 is either on Table 1 or is obtained from such a triple by mutation, and hence satisfies either $\tilde{b}_{i_0} \leq -n_0 \leq -2$ or $\tilde{b}_{i_1} \leq n_1 \leq -2$. This completes the proof of Proposition §9.4.

\mathbf{b}	(a, b, c)	Type	\mathbf{n}		
(1, 1, 1)	(1, 34, 89)	A	(14, 1)	$n_1 = -3$	$n_2 = 1$
(1, 1, 0)	(34, 13, 1325)	B	(0, 1)	$n_0 = 31$	$n_2 = 1$
(1, 0)	(13, 5, 194)	B	(0, 1)	$n_0 = 12$	$n_2 = 1$
(0, 1)	(5, 29, 433)	C	(13, 1)	$n_1 = -27$	$n_2 = 1$
(0, 0)	(29, 2, 169)	C	(-1, 1)	$n_0 = 2$	$n_2 = 0$

Table 1: Cases for the proof of Proposition §9.4. Each row refers to the triangle $\mu_{\mathbf{b}}\Pi(1, 2, 5)$.

11 Classification

§11.1 We now proceed case by case with the list of Manetti surfaces given in Remark §9.8. In fact, we will be able to ignore $\mathbb{P}(5^2, 2^2, 29^2)$, $\mathbb{HIP}(5, 29)$, $\mathbb{HIP}(2, 29)$, $\mathbb{P}(1, 5^2, 13^2)$, and $\mathbb{P}(1, 13^2, 34^2)$ because they are adjacent to $\mathbb{HIP}(29)$, $\mathbb{HIP}(13)$ and $\mathbb{HIP}(34)$, all of which

will be seen to give ugly singularities. This leaves us with the following six possibilities to analyse:

$$\mathbb{P}(1, 1, 4), \quad \mathbb{P}(1, 4, 25), \quad \mathbb{HIP}(5), \quad \mathbb{HIP}(13), \quad \mathbb{HIP}(29), \quad \mathbb{HIP}(34).$$

We will do the case of $\mathbb{P}(1, 1, 4)$ in a lot of detail because it illustrates the techniques nicely in a toric situation. In the other cases, we will only outline the answers.

$\mathbb{P}(1, 1, 4)$

§11.2 Let $Y = \mathbb{P}(1, 1, 4)$ with weighted homogeneous coordinates $[x : y : z]$. Our octic curve is a Weil divisor $B \subset Y$ defined by the vanishing of a section Ω of the \mathbb{Q} -line bundle $\mathcal{O}(16)$, that is $\Omega(x, y, z)$ is a polynomial in $[x : y : z] \in \mathbb{P}(1, 1, 4)$ of weighted degree 16. We will write $\Omega(x, y, z) = \sum_{k=0}^4 z^k \Omega_k(x, y)$. Our tropicalisation (moment polygon) is $\Pi(1, 1, 2)$ shown in Figure 12. In this figure, we have also labelled a selection of the integer points with monomials $\mathcal{O}(16)$ according to their affine distances to the three edges (see e.g. [10, Example 5.4.5]). Let $\text{Newt}(\Omega)$ be the set of integral points of $\Pi(1, 1, 2)$ corresponding to monomials appearing with nonzero coefficient in Ω . The branched double cover is

$$X = \{[u : x : y : z] \in \mathbb{P}(8, 1, 1, 4) : u^2 = \Omega(x, y, z)\}.$$

We consider three cases:

- Case I: The $\frac{1}{4}(1, 1)$ singularity of Y at $[0 : 0 : 1]$ does not belong to B . Equivalently, $\Omega_4 \neq 0$. Equivalently, $(0, 4) \in \text{Newt}(\Omega)$.
- Case II: $(0, 4) \notin \text{Newt}(\Omega)$ (i.e. $\Omega_4 = 0$) but the quartic polynomial $\Omega_3(x, y)$ has four distinct roots.
- Case III: Anything else.

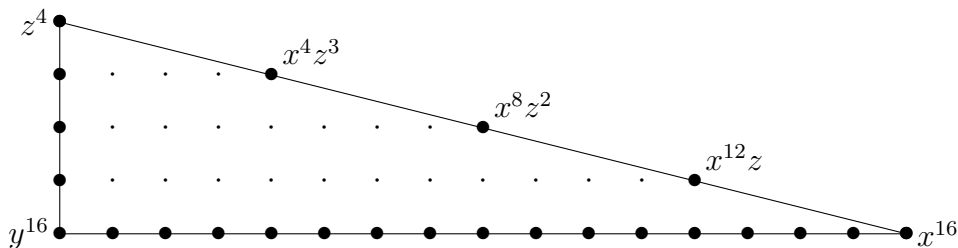


Figure 12: The octic tropicalisation $\Pi(1, 1, 2)$ of $\mathbb{P}(1, 1, 4)$ with some integral points labelled by monomial sections from $\mathcal{O}(16)$.

§11.3 $\mathbb{P}(1, 1, 4)$, **Case I:** $(0, 4) \in \text{Newt}(\Omega)$. If $[0 : 0 : 1] \notin B$ then our branched double cover has precisely two¹³ non-Gorenstein singularities, $[\pm \sqrt{\Omega(0, 0, 1)} : 0 : 0 : 1]$ each of type $\frac{1}{4}(1, 1)$. This case was already observed by Anthes [5, Example 5.5].

¹³These are distinct because they are not related by the projective rescaling. This can happen if the weight of u were congruent to 2 modulo 4, which yields *degenerate covers* in the terminology of [38].

§11.4 $\mathbb{P}(1, 1, 4)$, **Case II:** $(0, 4) \notin \text{Newt}(\Omega)$ and Ω_3 has four distinct roots. Let $\tilde{Y} \rightarrow Y$ be the minimal resolution, so that \tilde{Y} is the fourth Hirzebruch surface \mathbb{F}_4 with a -4 -curve C_1 that is contracted to $[0 : 0 : 1]$. This resolution is toric: we introduce a new ray $(0, -1)$ into our fan and take the associated toric variety. We can think of the polygon $\Pi(1, 1, 4)$ as $\text{Trop}(\tilde{Y}, \text{tot}_{\tilde{Y}}(B))$. This is because B is linearly equivalent to something disjoint from the singularity, so $\text{tot}_{\tilde{Y}}(B) \cdot C_1 = 0$, which means that the edge of the polygon corresponding to the curve C_1 has length zero: it is hiding at the point $(0, 4)$. We introduce a new Cox variable w associated to the new ray: the points of \tilde{Y} can be represented as $[x : y : z : w]$ with

$$[x : y : z : w] = [\lambda x : \lambda y : \lambda^4 \mu z : \mu w], \quad (\lambda, \mu) \in (\mathbb{C}^\times)^2, \quad (x, y) \neq (0, 0), \quad (z, w) \neq (0, 0),$$

and the curve C_1 is defined by $\{w = 0\}$. The integer points of the polygon $\text{Trop}(\tilde{Y}, \text{tot}_{\tilde{Y}}(B))$ now correspond to Cox monomials which transform like $\lambda^{16} \mu^4$, namely (i, j) corresponds to $x^i y^{16-i-4j} z^j w^{4-j}$ and we can write $\text{tot}_{\tilde{Y}}(B) = \{[x : y : z : w] \in \tilde{Y} : \text{tot}_{\tilde{Y}}(\Omega)(x, y, z, w) = 0\}$ with

$$\begin{aligned} \text{tot}_{\tilde{Y}}(\Omega)(x, y, z, w) &= \sum_{k=0}^3 z^k w^{4-k} \Omega_k(x, y) \\ &= w \tilde{\Omega}(x, y, z, w). \end{aligned}$$

Therefore $\text{tot}_{\tilde{Y}}(B) = C_1 + \text{strict}_{\tilde{Y}}(B)$ where $\text{strict}_{\tilde{Y}}(B)$ is the strict transform of B . By our genericity assumption on Ω_3 , the curves $\text{strict}_{\tilde{Y}}(B)$ and C_1 intersect transversely at the four points $\{[x : y : 1 : 0] : \Omega_3(x, y) = 0\}$.

§11.5 The double cover \tilde{X} of \tilde{Y} branched over $\text{tot}_{\tilde{Y}}(B)$ is a partial resolution of X , but although \tilde{Y} is smooth, \tilde{X} still has singularities coming from the singularities of $\text{tot}_{\tilde{Y}}(B)$, that is from the intersections $C_1 \cap \text{strict}_{\tilde{Y}}(B)$. The easiest way to resolve these is simply blow up \tilde{Y} at these four points to get a surface $\tilde{\tilde{Y}}$ and take the double cover $\tilde{\tilde{X}}$ of $\tilde{\tilde{Y}}$ branched over the total transform of $\text{tot}_{\tilde{Y}}(B)$. Note that

$$\text{tot}_{\tilde{\tilde{Y}}}(\text{tot}_{\tilde{Y}}(B)) = \text{strict}_{\tilde{\tilde{Y}}}(C_1 + \text{strict}_{\tilde{Y}}(B)) + 2(E_1 + E_2 + E_3 + E_4)$$

where the E_i are the -1 -curves contracted by $\tilde{\tilde{Y}} \rightarrow \tilde{Y}$. This means that $\tilde{\tilde{X}}$ is not normal: the curves E_i become double curves. So we replace $\tilde{\tilde{X}}$ by its normalisation $\tilde{\tilde{\tilde{X}}}$. Equivalently, we can obtain $\tilde{\tilde{\tilde{X}}}$ as the double cover of $\tilde{\tilde{Y}}$ branched along the *strict* transform of $\text{tot}_{\tilde{Y}}(B)$.

§11.6 To avoid clutter, we drop strict_* from the notation; for example, the surface $\tilde{\tilde{\tilde{X}}}$ is obtained from $\tilde{\tilde{Y}}$ as a double cover $\tilde{f}: \tilde{\tilde{\tilde{X}}} \rightarrow \tilde{\tilde{Y}}$ branched over $B + C_1$. We also write $\overline{G} := \tilde{f}^{-1}(G)$ for a curve $G \subset \tilde{\tilde{Y}}$. Note that $C_1 \subset \tilde{\tilde{Y}}$ has self-intersection -8 and the curves $E_i, i = 1, \dots, 4$, have self-intersection -1 . In $\tilde{\tilde{Y}}$, the curve C_1 has $C_1^2 = -8$; in $\tilde{\tilde{\tilde{X}}}$, the curve \overline{C}_1 has self-intersection -4 because C_1 was part of the branch locus, so the normal bundle

of \overline{C}_1 is the square root of the normal bundle of C_1 . Each curve $E_i \subset \tilde{Y}$ has $E_i^2 = -1$ and meets the branch locus at two points transversely, so each \overline{E}_i is a connected, embedded, rational curve of self-intersection -2 : its normal bundle is pulled back from the normal bundle of E_i along a map $\mathbb{P}^1 \rightarrow \mathbb{P}^1$ of degree 2. The contraction $\tilde{X} \rightarrow X$ contracts precisely $\overline{C}_1 + \sum_{i=1}^4 \overline{E}_i$. See Figure 13 for a pictorial summary of the argument.

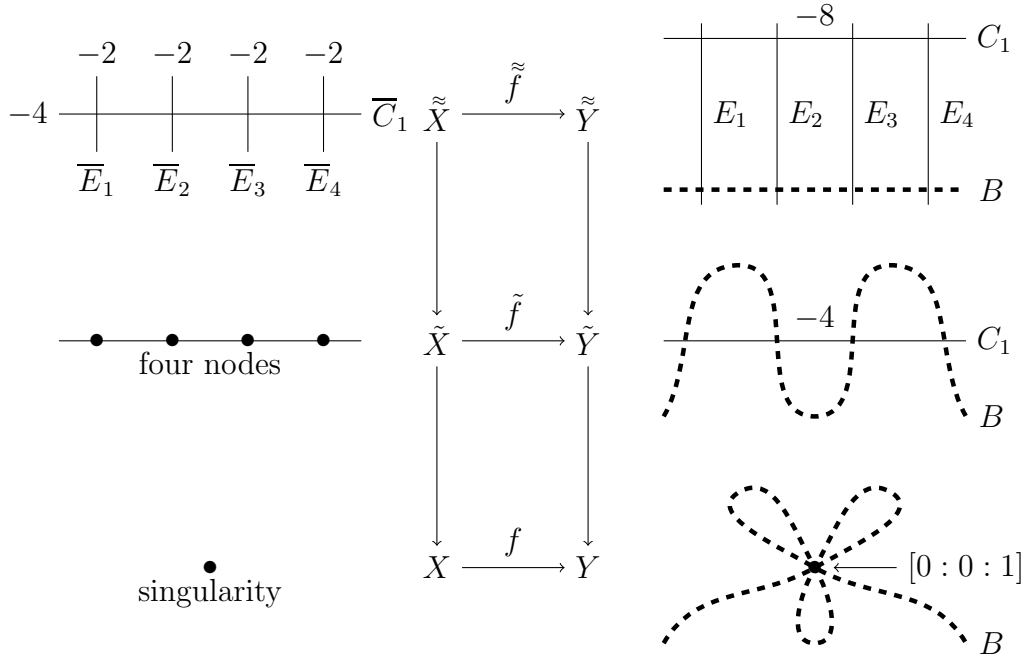
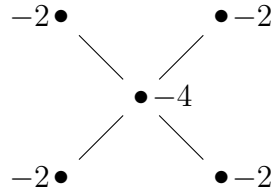


Figure 13: The process for finding the minimal resolution of the double cover of $Y = \mathbb{P}(1, 1, 4)$ branched along a curve B in Case II.

This means that the surface X has a singularity locally analytically modelled on a rational singularity whose minimal resolution has dual graph



This is a quotient of a simple elliptic singularity by an involution; this is an ugly singularity (in the sense of §3.10).

§11.7 Case III: Any of the octics Ω which do not fall into Cases I and II are adjacent to octics from Case II: we simply pick a one-parameter perturbation of the coefficients of Ω_3 so that Ω_3 has four distinct zeros for all non-zero values of the parameter in a small

disc. Therefore any octic double $\mathbb{P}(1, 1, 4)$ we have not already analysed must possess an ugly singularity, by Lemma §3.11.

§11.8 Remarks. The reader may well be interested in KSBA stable surfaces with quotient elliptic singularities or worse. The surfaces obtained in Case II are stable (see Theorem §13.2). We remark that in Case III, by allowing the roots of Ω_3 to collide, one can obtain some further interesting singularities. Figure 14 shows the singularities obtained when the branch curve meets C_1 with:

- (a) two points with multiplicity 1 and one with multiplicity 2: this gives a $\mathbb{Z}/2$ -quotient of a cusp singularity, and the generic surface of this type is stable.
- (b) two points with multiplicity 2: this gives a $\mathbb{Z}/2$ -quotient of a (different) cusp singularity, and the generic surface of this type is stable.
- (c) one point with multiplicity 1 and one with multiplicity 3: this yields a singularity which is not log-canonical (so these surfaces are not stable).
- (d) one point with multiplicity 4: this also yields a singularity which is not log-canonical (so these surfaces are not stable).

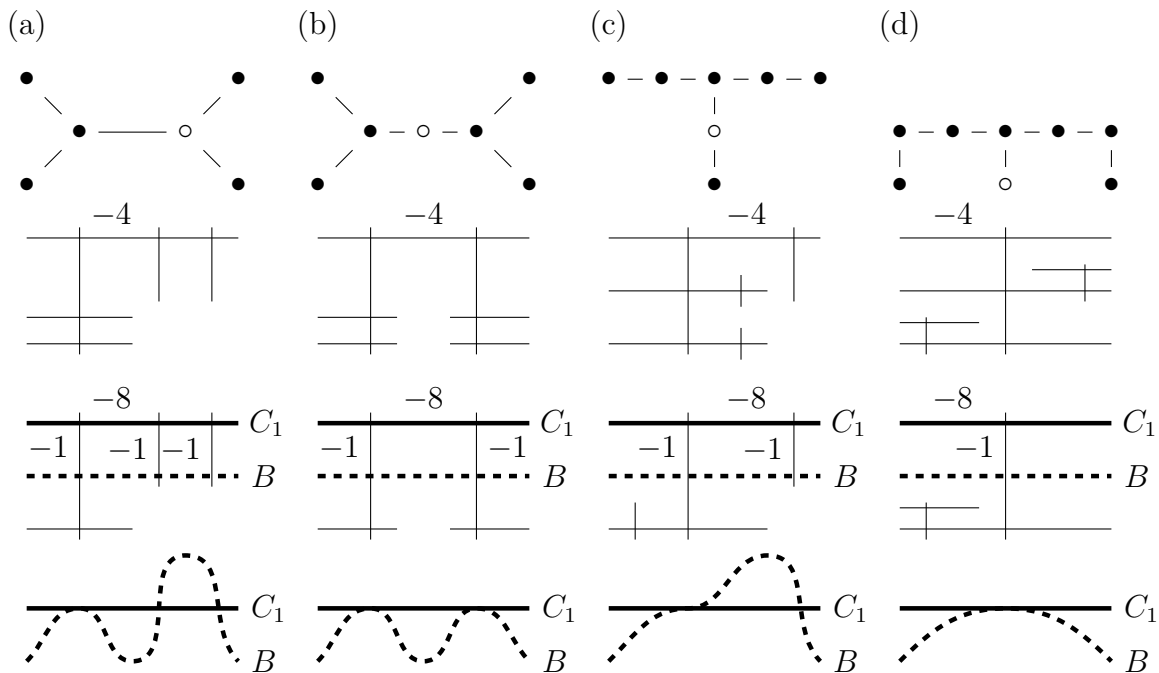


Figure 14: Some singularities obtained when the roots of Ω_3 collide. Any unmarked curves other than B have square -2 . In the resolution graphs, \bullet indicates a -2 -curve whilst \circ indicates a -4 -curve. The two singularities on the left are log canonical ($\mathbb{Z}/2$ -quotients of a cusp singularity) whilst the two on the right are not (they are, however, quasi-homogeneous).

§11.9 Summary. We now summarise the results. Having fixed a Manetti surface $Y = \mathbb{P}(1, 1, 4)$, we considered various cases according to the Newton polygon of the octic Ω :

- Case I: $(0, 4) \in \text{Newt}(\Omega)$. In this case, we found two $\frac{1}{4}(1, 1)$ singularities.
- Case II: $(0, 4) \notin \text{Newt}(\Omega)$ and Ω_3 has distinct roots. In this case, we found an ugly singularity (a $\mathbb{Z}/2$ -quotient of an elliptic singularity).
- Case III: Anything else. Such a surface is adjacent to something from Case II. In this case, we will necessarily find at least one ugly singularity.

§11.10 We also pause to record a useful observation that speeds up calculations. In Case II, we were able to factor out C_1 from $\text{tot}_{\tilde{Y}}(B)$. In other words, the coefficient of C_1 in the strict transform was one less than in the total transform, so by Equation (5.1), the polygon $\text{Trop}(\tilde{Y}, \text{strict}_{\tilde{Y}}(B))$ is obtained from $\text{Trop}(\tilde{Y}, \text{tot}_{\tilde{Y}}(B))$ by moving the edge associated to C_1 inwards along its normal ρ_{C_1} by an affine distance 1, or more generally, until it hits an integer point (i, j) . If C_1 is part of the exceptional locus of $\tilde{Y} \rightarrow Y$ living over a vertex $p \in \text{Trop}(\tilde{Y}, \text{tot}_{\tilde{Y}}(B))$ then this affine distance is $\langle ((i, j) - p), \rho_{C_1} \rangle$, which then gives the multiplicity in $\text{tot}_{\tilde{Y}}(B)$ of a curve $C_1 \subset \text{Exc}(\tilde{Y} \rightarrow Y)$.

The number of intersection points $B \cap C_1$ was given by the degree of $\mathcal{O}(B)$ restricted to C_1 , which in turn is equal to the affine length of the edge corresponding to C_1 : in Case I ($(0, 4) \in \text{Newt}(\Omega)$) this affine length is zero because B and C_1 are disjoint, whilst in Case II ($(0, 4) \notin \text{Newt}(\Omega)$) this affine length is 4.

These two pieces of information were essentially all we needed to carry out our calculations, so everything can be read off directly from the polygon. In fact, this remains true in the almost toric case: see [35, Propositions 5.15 and 5.18].

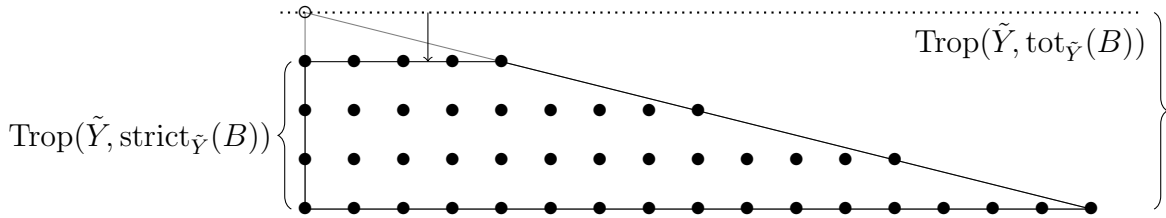


Figure 15: Graphical summary of $\mathbb{P}(1, 1, 4)$, Case II. When the integer point $(0, 4)$ is missing from $\text{Newt}(\Omega)$, we move the edge corresponding to the exceptional divisor of the minimal resolution $\mathbb{F}_4 \rightarrow \mathbb{P}(1, 1, 4)$ normally inwards until it reaches an integer point. The new edge has affine length 4, which implies that the strict transform of the branch curve intersects the contracted -4 -curve C_1 with total multiplicity 4. The affine distance from the missing point to the new edge is 1, so the curve C_1 appears in $\text{tot}_{\tilde{Y}}(B)$ with multiplicity 1.

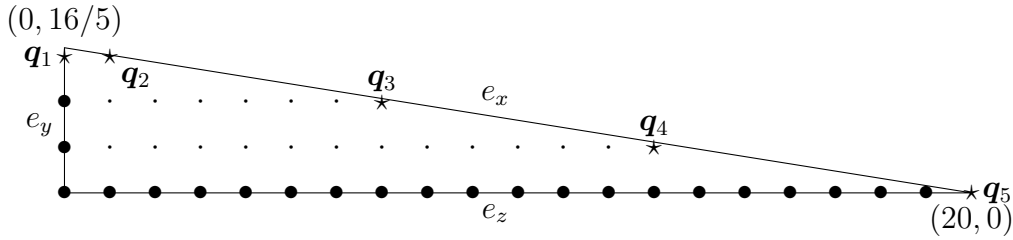
We now give the details for the remaining cases, following the strategy followed in the case of $\mathbb{P}(1, 1, 4)$ and the graphical method for calculations explained in §11.10 and Figure 15.

$\mathbb{P}(1, 4, 25)$

§11.11 In this case, B is a curve of weighted degree 80 in $[x : y : z] \in \mathbb{P}(1, 4, 25)$. The polygon $\text{Trop}(Y, B)$ is $\Pi(1, 2, 5)$ and its integer points correspond to “octic” monomials, i.e. weighted degree $80 = 8abc$. We have marked with a \star the most important integer points

$$\mathbf{q}_1 = (0, 3), \quad \mathbf{q}_2 = (1, 3), \quad \mathbf{q}_3 = (7, 1), \quad \mathbf{q}_4 = (13, 2), \quad \mathbf{q}_5 = (20, 0);$$

the rest we have drawn with a \bullet if they lie on the boundary of the polygon and a \cdot if they are on the interior (otherwise it can be hard to tell: for example, \mathbf{q}_1 and \mathbf{q}_5 are on the boundary but $\mathbf{q}_2, \mathbf{q}_3$ and \mathbf{q}_4 are not).



The inward normal rays to the edges e_x, e_y and e_z are $\rho_x = (-4, -25), \rho_y = (1, 0)$ and $\rho_z = (0, 1)$ corresponding to the Cox variables x, y, z of weights 1, 4, 25 respectively. We write D_x, D_y and D_z for the corresponding divisors. In our tables below, we will keep track of the edge e_x with normal ρ_x but e_y and e_z will play no role.

The singularities of $\mathbb{P}(1, 4, 25)$ comprise:

- a $\frac{1}{4}(1, 1)$ singularity living over $(20, 0)$,
- a $\frac{1}{25}(1, 4)$ singularity living over $(0, 16/5)$.

Let $\pi: \tilde{Y} \rightarrow Y$ be the minimal resolution of $Y = \mathbb{P}(1, 4, 25)$. The exceptional locus $\text{Exc}(\pi)$ comprises Wahl chain C_1, C_2, C_3, C_4 with self-intersections $-7, -2, -2, -2$ and a -4 -curve C_5 . This is still a toric variety: the fan acquires new rays

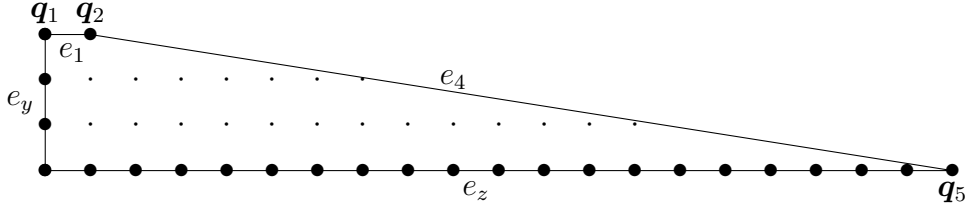
$$\rho_1 = (0, -1), \quad \rho_2 = (-1, -7), \quad \rho_3 = (-2, -13), \quad \rho_4 = (-3, -19), \quad \rho_5 = (-1, -6)$$

which we think of as the normals to zero-length edges e_1, \dots, e_4 at the vertex $(0, 16/5)$ and e_5 at $(20, 0)$. Since $(0, 16/5)$ is not an integer point, all of our octics must pass through the $\frac{1}{25}(1, 4)$ singularity. Note that $\mathbf{q}_5 \in \text{Newt}(\Omega)$ if and only if B does not pass through the $\frac{1}{4}(1, 1)$ singularity. We consider the following cases:

- Case I: $\mathbf{q}_2, \mathbf{q}_5 \in \text{Newt}(\Omega)$. We will find that X has a $\frac{1}{50}(1, 29)$ singularity and two $\frac{1}{4}(1, 1)$ singularities.
- Case II: $\mathbf{q}_2 \notin \text{Newt}(\Omega)$ but $\mathbf{q}_1, \mathbf{q}_3, \mathbf{q}_5 \in \text{Newt}(\Omega)$. We will find an ugly singularity.
- Case III: $\mathbf{q}_5 \notin \text{Newt}(\Omega)$ plus a genericity assumption on the other coefficients which we state later. We will find an ugly singularity.

- Case IV: Anything else is adjacent to either Case II or Case III, and must therefore have an ugly singularity by Lemma §3.11.

§11.12 $\mathbb{P}(1, 4, 25)$, **Case I:** $\mathbf{q}_2, \mathbf{q}_5 \in \text{Newt}(\Omega)$. In this case, the coefficients of xyz^3 and y^{20} are nonzero in our octic Ω . Moving the new edges e_i inwards along their normals ρ_i , we find the following polygon:



We label only those edges whose affine length is nonzero; e_2 and e_3 are concentrated at the point \mathbf{q}_2 and e_4 and e_5 are concentrated at the point \mathbf{q}_5 . We also adopt the convention that points on the boundary of the polygon are marked \bullet and points in the interior are marked \cdot (otherwise it can be hard to distinguish).

The following table summarises the affine lengths of the new edges together with how far (in affine distance) the edges were displaced.

Edge	e_1	e_2	e_3	e_4	e_5	e_6
Affine length	1	0	0	1	0	0
Affine displacement	1/5	2/5	3/5	4/5	0	0

This means that the strict transform of B intersects each of C_1 and C_4 transversely at one point and is disjoint from C_2, C_3, D_x and C_5 . The branch curve will be $B + C_1 + C_3$: by §2.4, the components of $\text{Exc}(\pi)$ which we retain in the branch locus is determined by the parity (odd/even) of their multiplicity in the total transform, i.e. of the affine displacement they have suffered. We blow \tilde{Y} up at the intersection point $B \cap C_1$ to get a surface $\tilde{\tilde{Y}}$ with an embedded branch curve and then take $\tilde{f}: \tilde{X} \rightarrow \tilde{\tilde{Y}}$ to be the double cover branched along¹⁴ $B + C_1 + C_3$. Write E_1 for the exceptional curve of $\tilde{\tilde{Y}} \rightarrow \tilde{Y}$ and, for any $G \subset \tilde{\tilde{Y}}$, write $\tilde{G} \subset \tilde{X} := \tilde{f}^{-1}(G)$. Then $\tilde{E}_1 + \sum_{i=1}^4 \tilde{C}_i$ and \tilde{C}_5 are the curves in \tilde{X} we need to contract to recover X . The former yields a singularity of type $\frac{1}{50}(1, 29)$; the latter yields two $\frac{1}{4}(1, 1)$ singularities. See Figure 16.

¹⁴Recall that we do not distinguish notationally between a curve and its strict transform.

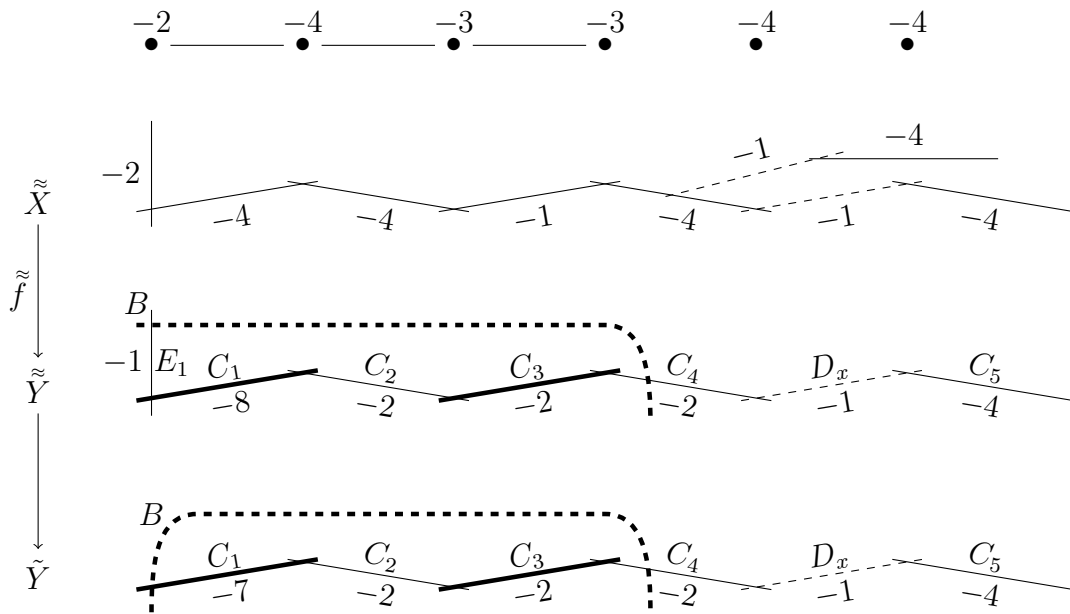
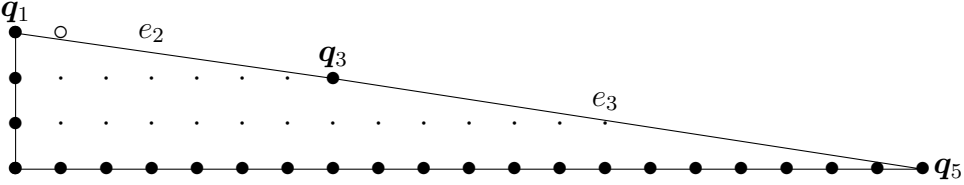


Figure 16: $\mathbb{P}(1, 4, 25)$, Case I. The minimal resolution \tilde{Y} , its blow-up $\tilde{\tilde{Y}}$, and the double cover $\tilde{\tilde{X}}$ of $\tilde{\tilde{Y}}$. Thick curves are the branch locus. Any non-dashed curves in $\tilde{\tilde{X}}$ are contracted to get X . The top row shows the Wahl chains associated to the three singularities of X .

§11.13 $\mathbb{P}(1, 4, 25)$, **Case II:** $q_2 \notin \text{Newt}(\Omega)$ but $q_1, q_3, q_5 \in \text{Newt}(\Omega)$. The polygon becomes



The following table summarises the affine lengths of the new edges together with how far (in affine distance) the edges were displaced.

Edge	e_1	e_2	e_3	e_4	e_x	e_5
Affine length	0	1	1	0	0	0
Affine displacement	1/5	7/5	8/5	4/5	0	0

This means that the strict transform of B intersects each of C_2 and C_3 transversely at one point and is disjoint from C_1 , C_4 and C_5 . Since $q_1, q_3, q_5 \in \text{Newt}(\Omega)$, the intersection points $B \cap C_2$ and $B \cap C_3$ will be at interior points of C_2 and C_3 (i.e. not at $C_1 \cap C_2$, $C_2 \cap C_3$ or $C_3 \cap C_4$). According to the prescription in §2.4, the branch curve will be $B + C_1 + C_2$: blow this up at $C_1 \cap C_2$ and $B \cap C_2$ (introducing exceptional curves E_1 and E_2 respectively) to get \tilde{Y} and let $\tilde{f}: \tilde{X} \rightarrow \tilde{Y}$ be the branched double cover. Writing $\bar{G} := \tilde{f}^{-1}(G)$, we need to contract $\bar{E}_1 + \bar{E}_2 + \sum_{i=1}^4 \bar{C}_i$ and \bar{C}_4 to recover X ; see Figure 17. The latter gives two $\frac{1}{4}(1, 1)$ singularities, but the former gives an ugly singularity. Indeed, this singularity is not even log canonical, so \tilde{X} is not KSBA-stable; it is not yet clear to us what the stable replacement of this surface is.

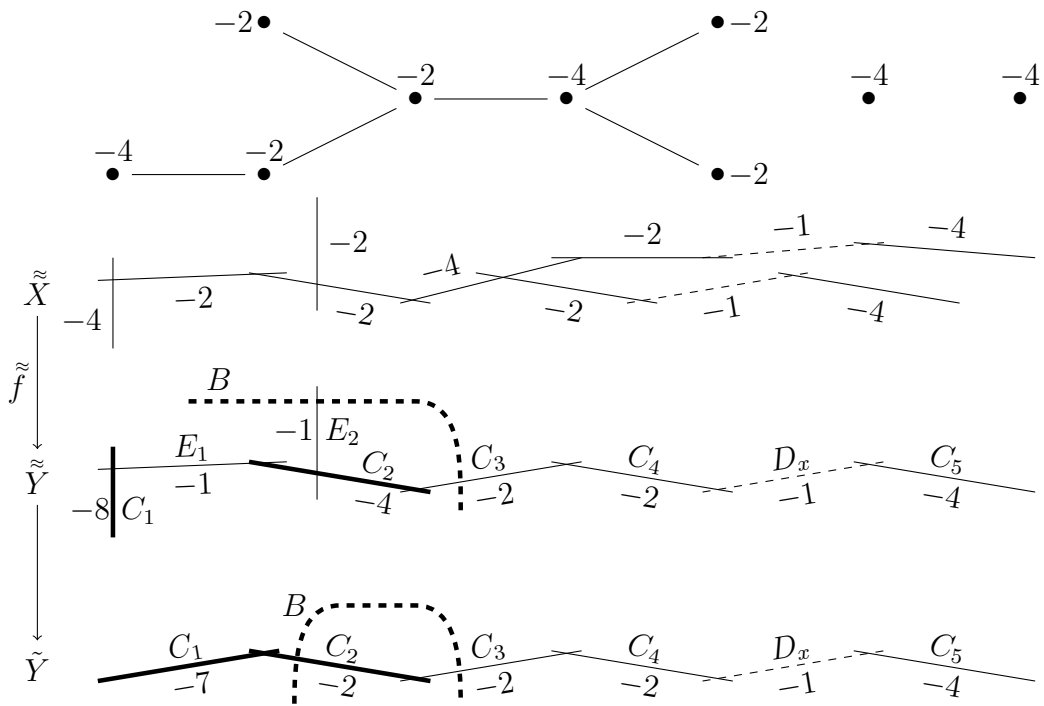
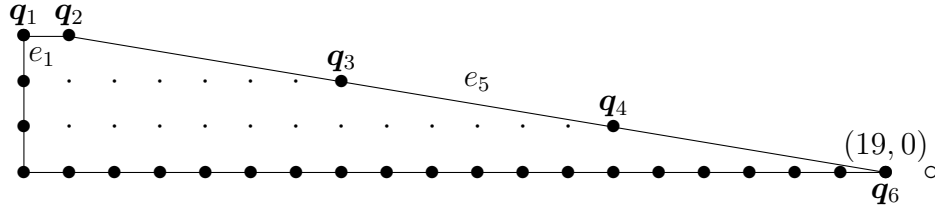


Figure 17: $\mathbb{P}(1, 4, 25)$, Case II. The minimal resolution \tilde{Y} , its blow-up \tilde{Y} , and the double cover \tilde{X} of \tilde{Y} . Thick curves are the branch locus. Any non-dashed curves in \tilde{X} are contracted to get X . The top row shows the dual graphs of the minimal resolutions of the singularities of X .

§11.14 $\mathbb{P}(1, 4, 25)$, Case III: $\mathbf{q}_5 \notin \text{Newt}(\Omega)$. The polygon and table become:



Edge	e_1	e_2	e_3	e_4	e_x	e_5
Affine length	1	0	0	0	0	3
Affine displacement	$1/5$	$2/5$	$3/5$	$4/5$	1	1

Note: here, we have additionally moved the edge e_x with normal $(-25, -4)$ inwards by an affine distance 1 and it now resides (with length zero) at \mathbf{q}_2 . This is because now all monomials are divisible by the variable x of weight 1 and we pull out this factor.

We now impose the following genericity assumptions on the coefficients of the monomials; anything not satisfying these assumptions is considered to be in Case IV. Let x, y, z, w_1, \dots, w_5 be the Cox variables associated to the polygon and let ω_p be the monomial associated with the integer point p . Write $\Omega = \sum_p a_p \omega_p$.

(†) Let $\mathbf{q}_6 := (19, 0)$ and take the sum of the four terms

$$a_{\mathbf{q}_2} \omega_{\mathbf{q}_2} + a_{\mathbf{q}_3} \omega_{\mathbf{q}_3} + a_{\mathbf{q}_4} \omega_{\mathbf{q}_4} + a_{\mathbf{q}_6} \omega_{\mathbf{q}_6}$$

in Ω along the slanted edge. Substitute $y = z = w_1 = w_2 = w_5 = 1$ and $w_4 = 0$ to obtain a homogeneous cubic in x and w_5 . We assume that this cubic has three distinct roots, none of which is at $x = 0$.

Anything which does not satisfy this assumption is adjacent to octics which do. Under this assumption, we find that B transversely intersects C_1 once, C_5 three times and avoids C_2 , C_3 , and C_4 . According to the prescription in §2.4, the branch curve is $B + D_x + C_1 + C_3 + C_5$. Let \tilde{Y} be the blow-up of \tilde{Y} at the five points $B \cap C_1$, $D_x \cap C_5$ and $B \cap C_5$, and write E_1, \dots, E_5 for the exceptional curves. Let \tilde{X} be the double cover of \tilde{Y} branched over the (now embedded) curve $B + D_x + C_1 + C_3 + C_5$. The surface X is obtained by contracting both $\overline{E}_1 + \sum_{i=1}^4 \overline{C}_i$ and $\overline{C}_5 + \sum_{i=2}^5 \overline{E}_i$ which then yields a $\frac{1}{50}(1, 29)$ singularity and a $\mathbb{Z}/2$ -quotient of a simple elliptic singularity (see Figure 18). This last is an ugly singularity.

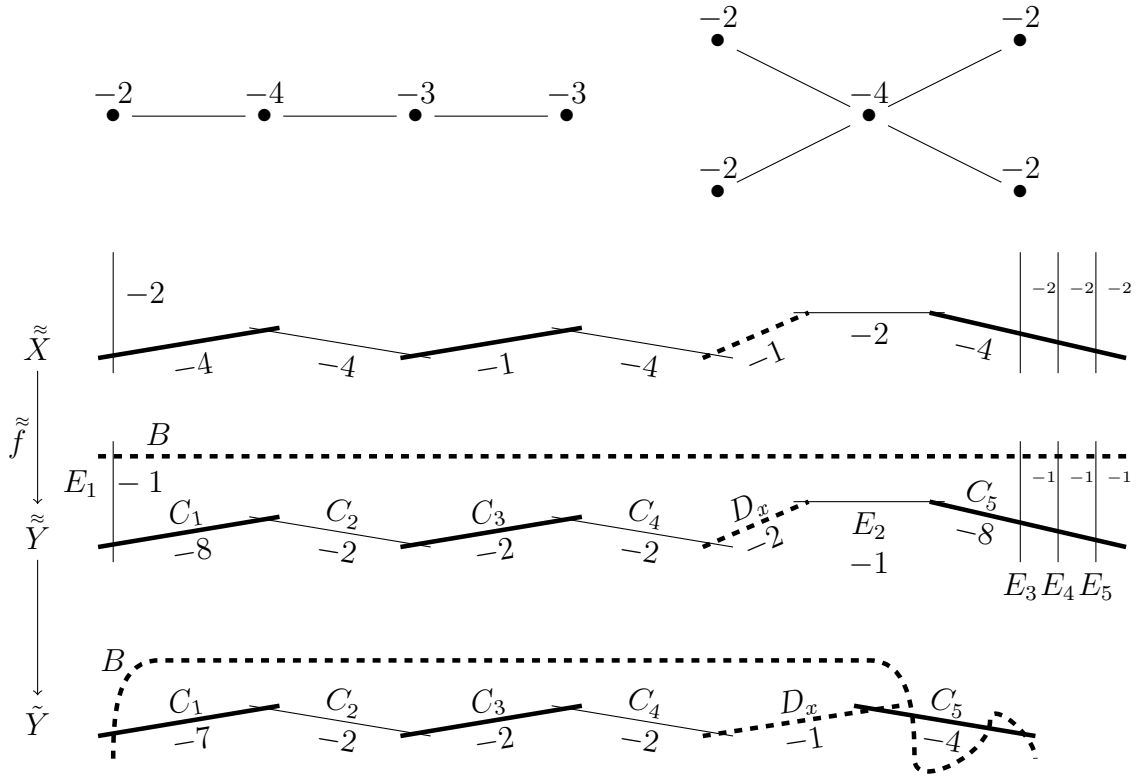
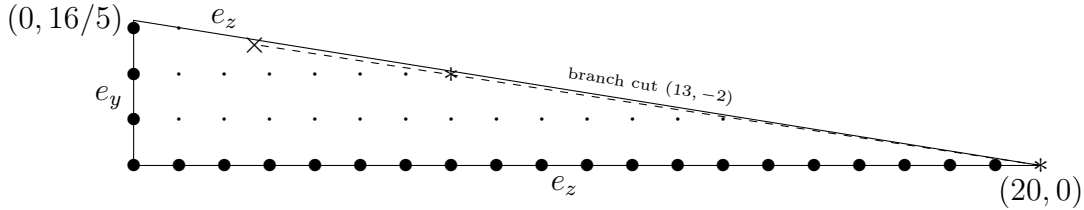


Figure 18: $\mathbb{P}(1, 4, 25)$, Case III. The minimal resolution \tilde{Y} , its blow-up $\tilde{\tilde{Y}}$, and the double cover $\tilde{\tilde{X}}$ of $\tilde{\tilde{Y}}$. Thick curves are the branch locus. Any non-dashed curves in $\tilde{\tilde{X}}$ are contracted to get X . The top row shows the dual graphs of the minimal resolutions of the singularities of X .

$\mathbb{HP}(5)$

§11.15 We now proceed to the next Manetti surface, where we smooth the $\frac{1}{4}(1, 1)$ singularity of $\mathbb{P}(1, 4, 25)$ and keep the $\frac{1}{25}(1, 4)$ singularity. This is almost toric, with associated integral affine polygon:



For convenience, we will consider the integral affine manifold as obtained from this polygon by gluing either sides of the branch cut using $\begin{pmatrix} -25 & -169 \\ 4 & 27 \end{pmatrix}$. The integer points in this polygon then become integer points of the integral affine manifold; we draw them as $*$ if they lie on our chosen branch cut. The end of the branch cut (denoted \times) is not an integer point, and the edge e_z crosses the branch cut so appears broken (we have labelled both pieces). Note that there are now no curves C_5, D_x : instead, D_x has merged with D_z to become a single curve which we will continue to denote by D_z .

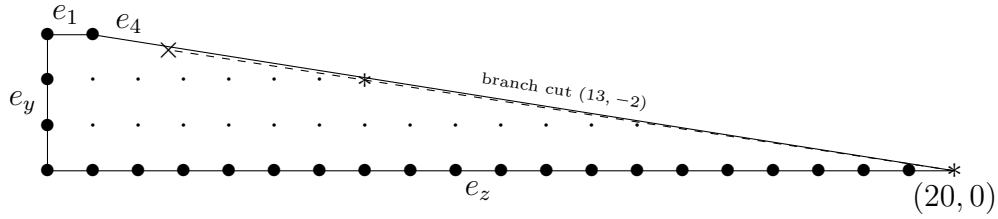
As before, the key integer points are

$$\mathbf{q}_1 = (0, 3), \quad \mathbf{q}_2 = (1, 3), \quad \mathbf{q}_3 = (7, 1), \quad \mathbf{q}_4 = (13, 2), \quad \mathbf{q}_5 = (20, 0).$$

Our cases are as follows:

- Case I: $\mathbf{q}_2 \in \text{Newt}(\Omega)$, $q \in \text{Newt}(\Omega)$ for some q in the bottom two rows. We will find that X has a $\frac{1}{50}(1, 29)$ singularity.
- Case II: $\mathbf{q}_2 \notin \text{Newt}(\Omega)$, $\mathbf{q}_1, \mathbf{q}_3, \mathbf{q}_5 \in \text{Newt}(\Omega)$. We will find that X has an ugly singularity.
- Case III: $\mathbf{q}_2 \in \text{Newt}(\Omega)$, $q \notin \text{Newt}(\Omega)$ for all q in the bottom two rows. We will find that X is not normal.
- Case IV: Anything else is adjacent to Case II or III, and must therefore have an ugly singularity by Lemma §3.11.

§11.16 $\mathbb{HP}(5)$, **Case I.** $\mathbf{q}_2 \in \text{Newt}(\Omega)$, $q \in \text{Newt}(\Omega)$ for some q from the bottom two rows. Assuming for a moment that $\mathbf{q}_5 \in \text{Newt}(\Omega)$, the polygon and the table become:



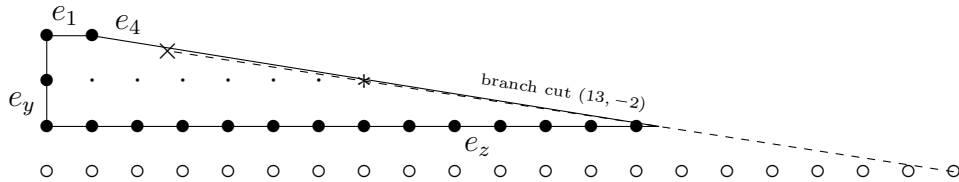
Edge	e_1	e_2	e_3	e_4
Affine length	1	0	0	1
Affine displacement	$1/5$	$2/5$	$3/5$	$4/5$

Note: the edge e_z now terminates at \mathbf{q}_5 . Just as in $\mathbb{P}(1, 4, 25)$, Case I, B hits C_1 and C_4 once transversely and is disjoint from C_2 and C_3 , so the same argument as in that case yields a $\frac{1}{50}(1, 29)$ singularity on X . See Figure 19.

According to the prescription in §2.4, the branch curve in \tilde{Y} is $B + C_1 + C_3$. We introduce a -1 -curve E_1 when we blow-up the point $B \cap C_1$ to resolve the branch curve in \tilde{Y} . Note that there is also a -1 -curve \mathcal{E}_1 in the minimal resolution of $\mathbb{H}\mathbb{P}(5)$ that is not part of the almost toric boundary, coming from a non-toric blow-up. This curve \mathcal{E}_1 intersects C_3 and none of the other exceptional curves. The intersection number $B \cdot \mathcal{E}_1$ can therefore be computed from the coefficient of C_3 in the expression $B = b_z D_z + \sum b_i C_i$, which can be computed by taking the affine displacement between $(1, 3)$ (where e_3 is concentrated) and $(8/3, 8/3)$ (the barycentre) in the $\rho_3 = (-2, -13)$ direction, which gives

$$B \cdot \mathcal{E}_1 = \begin{pmatrix} 8/3 - 1 \\ 8/3 - 3 \end{pmatrix} \cdot \begin{pmatrix} -2 \\ -13 \end{pmatrix} = 1.$$

The same picture applies as long as some q on the bottom row appears in $\text{Newt}(\Omega)$. If the lowest $q \in \text{Newt}(\Omega)$ is on the next row up then the polygon looks as follows, and the conclusions are the same:



Indeed, the same conclusion would hold if q sat on the second row up, but in that case we would also have non-normal singularities along D_z .

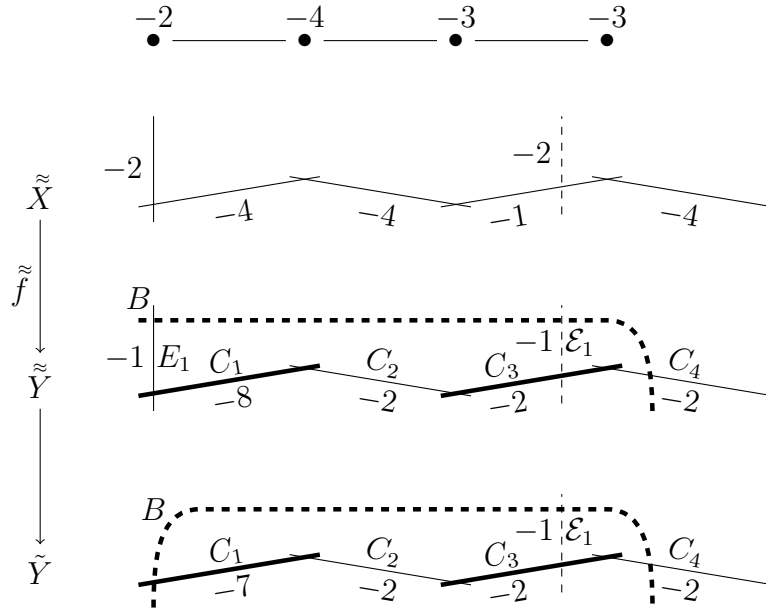
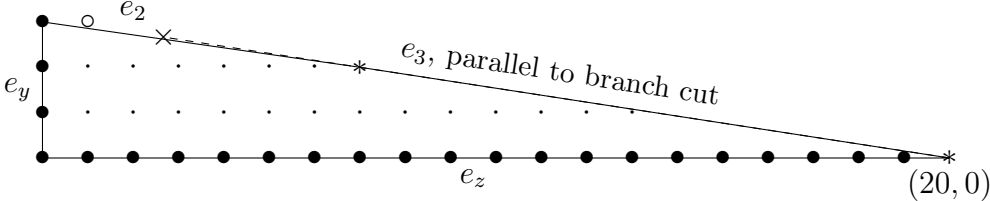


Figure 19: $\mathbb{H}\mathbb{P}(5)$, Case I. The minimal resolution \tilde{Y} , its blow-up $\tilde{\tilde{Y}}$, and the double cover $\tilde{\tilde{X}}$ of $\tilde{\tilde{Y}}$. Thick curves are the branch locus. Any non-dashed curves in $\tilde{\tilde{X}}$ are contracted to get X . The top row shows the Wahl chains associated to the three singularities of X .

§11.17 $\mathbb{HP}(5)$, **Case II.** $q_2 \notin \text{Newt}(\Omega)$, $q_1, q_3, q_5 \in \text{Newt}(\Omega)$. The polygon and the table become



Edge	e_1	e_2	e_3	e_4
Affine length	0	1	1	0
Affine displacement	1/5	7/5	8/5	4/5

Here we encounter some new phenomena in the picture: the singular point of our integral affine manifold \times lies outside the positive polygon and the edge e_3 runs along the branch cut. The branch curve hits C_2 and C_3 each once transversely and is disjoint from C_1 and C_4 , and we obtain the same non-log canonical singularity as in $\mathbb{P}(1, 4, 25)$, Case II; see Figure 20. Note that in this case (by §2.4) the branch locus is $B + C_1 + C_2$ and we need to make two blow-ups (exceptional curves E_1 and E_2) to resolve the singularities of the branch curve and there is a further -1 -curve \mathcal{E}_1 coming from the non-toric blow-up satisfying $B \cdot \mathcal{E}_1 = 0$.

§11.18 $\mathbb{HP}(5)$, **Case III.** $q_2 \in \text{Newt}(\Omega)$, $q \notin \text{Newt}(\Omega)$ for all q in the bottom two rows. In this case, the edge e_z moves through an affine displacement of 2, so D_z appears with multiplicity 2 in the branch curve B . As in the proof of Corollary §9.7, this implies that the double cover $f: X \rightarrow Y$ branched over B is not normal.

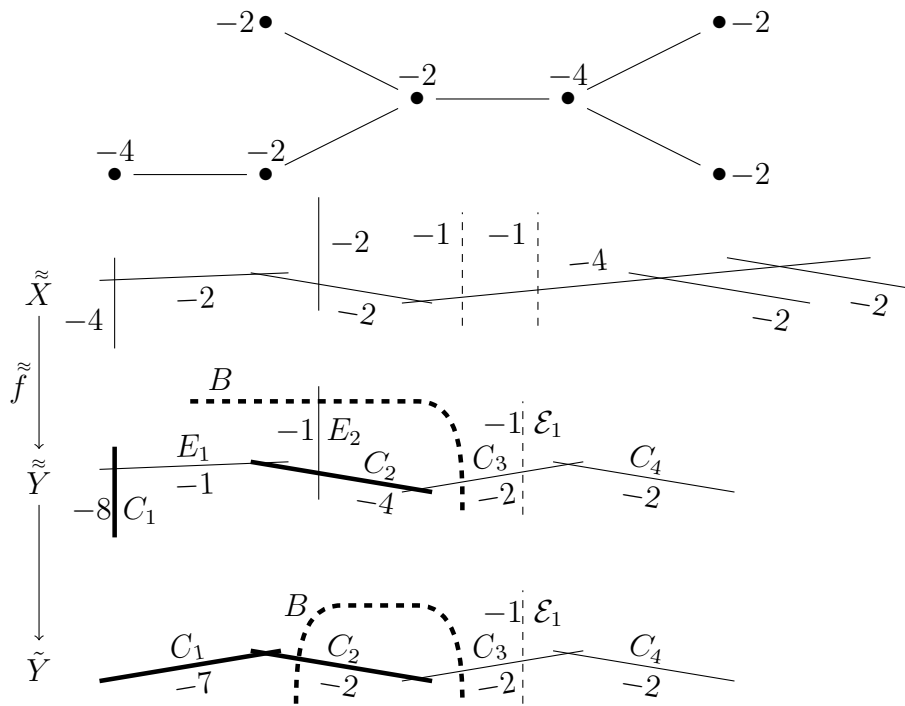
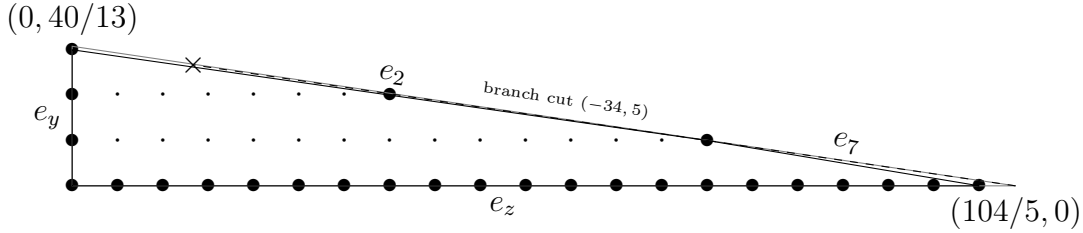


Figure 20: $\mathbb{H}\mathbb{P}(5)$, Case II. The minimal resolution \tilde{Y} , its blow-up \tilde{Y} , and the double cover \tilde{X} of \tilde{Y} . Thick curves are the branch locus. Any non-dashed curves in \tilde{X} are contracted to get X . The top row shows the dual graphs of the minimal resolutions of the singularities of X .

$\mathbb{H}\mathbb{P}(13)$

§11.19 The Manetti surface $\mathbb{H}\mathbb{P}(13)$ is obtained from $\mathbb{P}(1, 25, 169)$ by smoothing the $\frac{1}{25}(1, 4)$ singularity and keeping the $\frac{1}{169}(1, 25)$ singularity. The octic tropicalisation of $\mathbb{H}\mathbb{P}(13)$ has vertices at $\mathbf{p}_0 = (0, 0)$, $\mathbf{p}_1 = (104/5, 0)$ and $\mathbf{p}_2 = (0, 40/13)$, and a branch cut emanating from \mathbf{p}_1 in the $(-34, 5)$ -direction with monodromy matrix $M_{\mathbf{p}_1} = \begin{pmatrix} -169 & -1156 \\ 25 & 171 \end{pmatrix}$.

Below we show the convex hull $\Pi_A^{\mathbb{Z}}$ of the integral points (vertices at $(0, 3)$, $(14, 1)$ and $(20, 0)$) together with the ambient Markov triangle in grey. Note that, even if it is not immediately clear from the picture, the branch cut lies above the convex hull of the integer points, and intersects it only at $(14, 1)$.



We resolve the $\frac{1}{169}(1, 25)$ singularity by adding edges e_1, \dots, e_7 with inward normals

$$\begin{aligned} \rho_1 &= (0, -1), \rho_2 = (-1, -7), \rho_3 = (-5, -34), \rho_4 = (-9, -61), \\ \rho_5 &= (-13, -88), \rho_6 = (-17, -115), \rho_7 = (-21, -142) \end{aligned}$$

corresponding to curves C_i with

$$C_1^2 = -7, \quad C_2^2 = -5, \quad C_3^2 = \dots = C_7^2 = -2.$$

Note that the edge corresponding to C_3 is parallel to the branch cut: this means that, as they move inwards, the edges e_4, \dots, e_7 cross the branch cut, and appear as $M_{\mathbf{p}_1}^{-1}e_i$. The zero-length edges are e_1 (concentrated at $(0, 3)$), and e_3, \dots, e_6 concentrated at $(14, 1)$. The table of affine lengths and displacements becomes:

Edge	e_1	e_2	e_3	e_4	e_5	e_6	e_7
Affine length	0	2	0	0	0	0	1
Affine displacement	1/13	7/13	8/13	9/13	10/13	11/13	12/13

Write our octic as $\Omega = \sum_p a_p \theta_p$ where θ_p is the GHK theta-function corresponding to the integral point p . If we pick $a_{(0,3)}$, $a_{(7,1)}$, $a_{(14,1)}$ and $a_{(20,0)}$ generically, we find that the strict transform of B intersects C_2 transversely at two points, C_7 once transversely, and is disjoint from the other curves C_i . According to the prescription in §2.4, the branch locus is $B + C_1 + \sum_{i=1}^3 C_{2i}$. Let \tilde{Y} be the blow-up of \tilde{Y} at $C_1 \cap C_2$ and $C_2 \cap B$ with exceptional divisors E_1 , E_2 , and E_3 , and let \tilde{X} be the double cover of \tilde{Y} branched over $B + C_1 + \sum_{i=1}^3 C_{2i}$. We obtain X by contracting $\sum_{i=1}^7 \bar{C}_i + \sum_{i=1}^3 \bar{E}_i$. This contains an ugly singularity (see Figure 21). Note that there is also a -1 -curve \mathcal{E}_1 in $\mathbb{H}\mathbb{P}(13)$ coming

from the non-toric blow-up; this intersects C_3 once transversely and is disjoint from B , so yields two -1 curves in \tilde{X} both hitting $\overline{C_3}$.

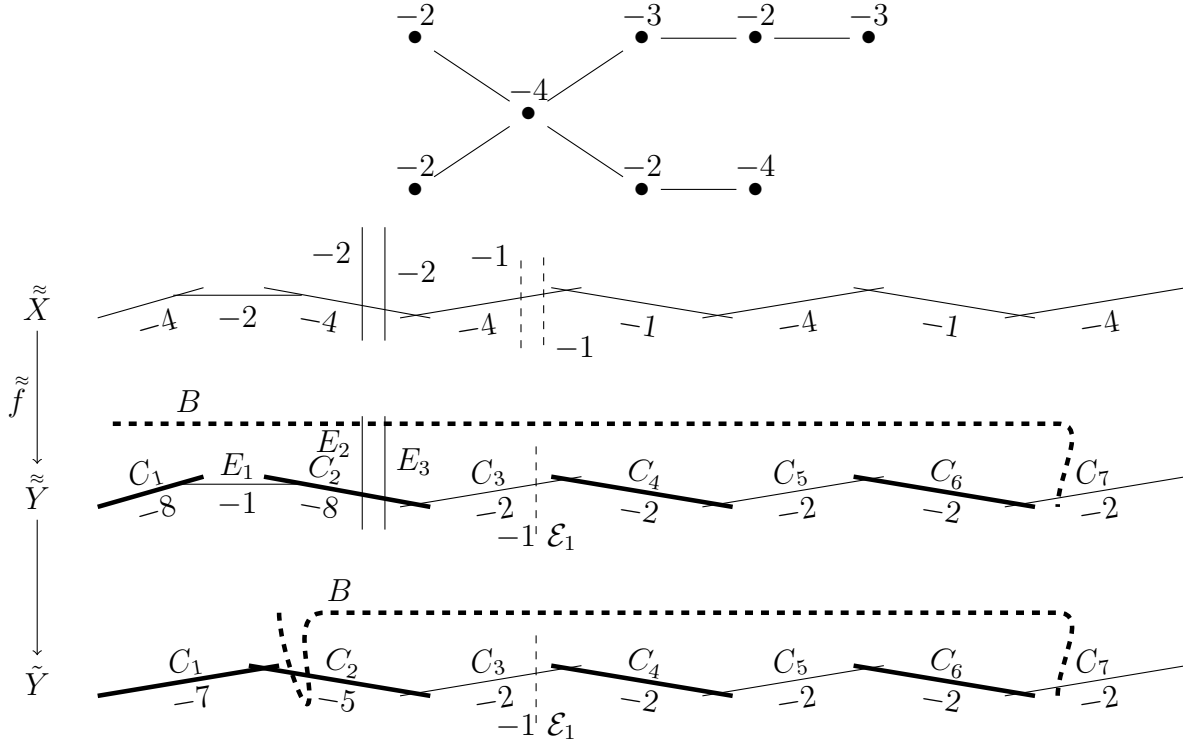
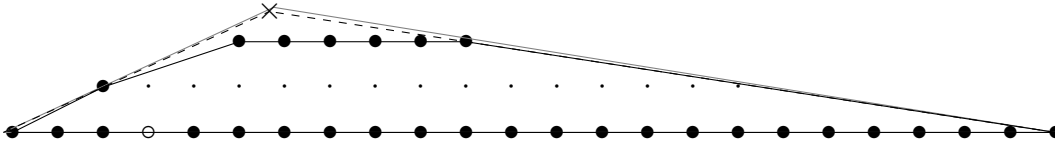


Figure 21: HYP(13). The minimal resolution \tilde{Y} , its blow-up $\tilde{\tilde{Y}}$, and the double cover $\tilde{\tilde{X}}$ of $\tilde{\tilde{Y}}$. Thick curves are the branch locus. Any non-dashed curves in $\tilde{\tilde{X}}$ are contracted to get X . The top row shows the dual graph of the minimal resolution of the singularity of X .

$\mathbb{H}\mathbb{P}(29)$

§11.20 The Manetti surface $\mathbb{H}\mathbb{P}(29)$ has as its octic tropicalisation the polygon with vertices at $\mathbf{p}_0 = (-16/5, 0)$, $\mathbf{p}_1 = (20, 0)$ and $\mathbf{p}_2 = (80/29, 80/29)$ and branch cuts emanating from \mathbf{p}_0 in the $(11, 5)$ -direction and from \mathbf{p}_1 in the $(-13, 2)$ -direction with monodromy matrices $M_{\mathbf{p}_0} = \begin{pmatrix} 56 & -121 \\ 25 & -54 \end{pmatrix}$ and $M_{\mathbf{p}_1} = \begin{pmatrix} -25 & -169 \\ 4 & 27 \end{pmatrix}$. All the integral points are contained in the polygon $\Pi_C^{\mathbb{Z}}$, whose vertices are at $(-3, 0)$, $(-1, 1)$, $(2, 2)$, $(7, 2)$ and $(20, 0)$.



The resolution of the $\frac{1}{841}(1, 637)$ singularity introduces exceptional curves, C_i , $i = 1, \dots, 10$ with

$$C_1^2 = -5, \quad C_2^2 = \dots = C_6^2 = -2, \quad C_7^2 = -10, \quad C_8^2 = C_9^2 = C_{10}^2 = -2.$$

The correspond to zero-length edges e_1, \dots, e_{10} in the tropicalisation sitting at \mathbf{p}_2 , with inward normal vectors:

$$\begin{aligned} \rho_1 &= (6, -13), & \rho_2 &= (5, -11), & \rho_3 &= (4, -9), & \rho_4 &= (3, -7), & \rho_5 &= (2, -5), \\ \rho_6 &= (1, -3), & \rho_7 &= (0, -1), & \rho_8 &= (-1, -7), & \rho_9 &= (-2, -13), & \rho_{10} &= (-3, -19). \end{aligned}$$

The edge e_2 is parallel to the branch cut through \mathbf{p}_0 and the edge e_9 is parallel to the branch cut through \mathbf{p}_1 . By the time it has reached the inner triangle, the edge e_1 has passed through the branch cut so appears as $M_{\mathbf{p}_0}e_1$, i.e. parallel to $(2, 1)$, having affine length 1 in the picture (note that if an edge transforms according to M then its normal transforms according to $(M^{-1})^T$). Similarly, the edge e_{10} appears as $M_{\mathbf{p}_1}^{-1}e_{10}$, parallel to $(6, -1)$, having affine length zero in the picture. The table of affine lengths and displacements becomes:

Edge	e_1	e_2	e_3	e_4	e_5
Affine length	1	0	0	0	0
Affine displacement	9/29	16/29	23/29	30/29	37/29
Edge	e_6	e_7	e_8	e_9	e_{10}
Affine length	1	5	0	1	0
Affine displacement	44/29	22/29	31/29	40/29	20/29

Write Ω as $\sum_p a_p \theta_p$ where θ_p is the GHK theta-function corresponding to the integral point p . If we pick the coefficients $a_{(2,2)}, a_{(3,2)}, \dots, a_{(7,2)}$ generically then we can ensure that the five intersection points $B \cap C_7$ are distinct and different from $C_7 \cap (C_6 \cup C_8)$. We will find that in this generic situation (and hence in any specialisation) there is an ugly singularity.

In this generic situation, the strict transform B intersects each of C_1, C_6, C_9 once transversely, C_7 at five points transversely, and is disjoint from all other C_i . According to the prescription in §2.4, the branch curve is $B + C_1 + C_3 + C_5 + C_8$. We blow up $B \cap C_1$ to

get a surface \tilde{Y} and write E_1 for the exceptional curve. Let \tilde{X} be the double cover of \tilde{Y} branched over $B+C_1+C_3+C_5+C_8$ and let $\bar{G} = \tilde{f}^{-1}(G)$ for any curve $G \subset \tilde{Y}$. We need to contract $\bar{E}_1 + \sum_{i=1}^{10} \bar{C}_i$ to recover X . This yields an irrational (and hence ugly) singularity whose minimal resolution includes a genus 2 curve \bar{C}_7 . See Figure 22 for an illustration of this. Note that \bar{C}_6 and \bar{C}_7 intersect twice because the intersection point $C_6 \cap C_7$ is not on the branch locus. We have also depicted (dashed) the -1 -curves \mathcal{E}_0 and \mathcal{E}_1 present in $\mathbb{H}\mathbb{P}(29)$ coming from the non-toric blow-ups in its presentation as an almost toric surface.

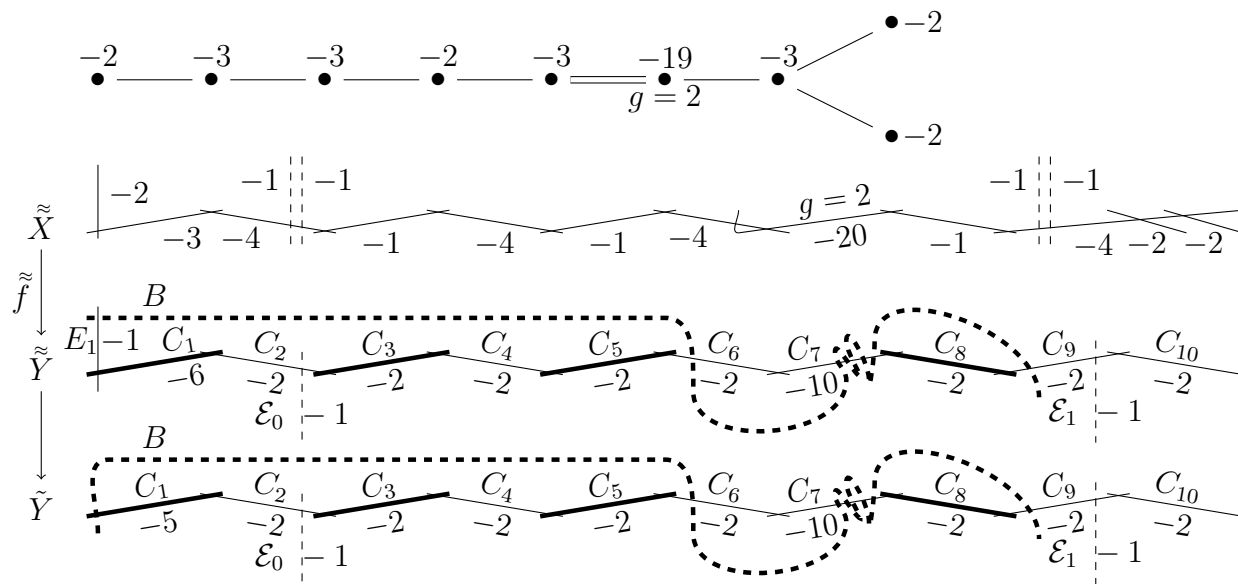
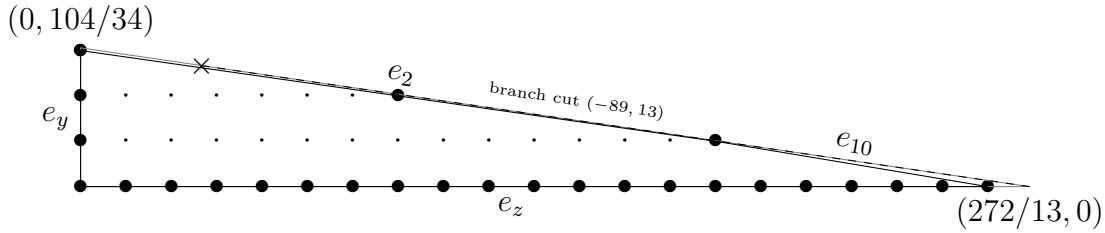


Figure 22: $\mathbb{H}\mathbb{P}(29)$. The minimal resolution \tilde{Y} , its blow-up $\tilde{\tilde{Y}}$, and the double cover \tilde{X} of \tilde{Y} . Thick curves are the branch locus. Any non-dashed curves in \tilde{X} are contracted to get X . The top row shows the dual graph of the minimal resolution of the singularity of X .

$\mathbb{H}\mathbb{P}(34)$

§11.21 The Manetti surface $\mathbb{H}\mathbb{P}(34)$ is obtained from $\mathbb{P}(1, 169, 1156)$ by smoothing the $\frac{1}{169}(1, 25)$ singularity and keeping the $\frac{1}{1156}(1, 169)$ singularity. The octic tropicalisation of $\mathbb{H}\mathbb{P}(34)$ has vertices at $\mathbf{p}_0 = (0, 0)$, $\mathbf{p}_1 = (272/13, 0)$ and $\mathbf{p}_2 = (0, 104/34)$, and a branch cut emanating from \mathbf{p}_1 in the $(-89, 13)$ -direction with monodromy matrix $M_{\mathbf{p}_1} = \begin{pmatrix} -1156 & -7921 \\ 169 & 1158 \end{pmatrix}$. Below we show the convex hull $\Pi_A^{\mathbb{Z}}$ of the integral points (vertices at $(0, 3)$, $(14, 1)$ and $(20, 0)$) together with the ambient Markov triangle in grey. Note that the branch cut lies strictly above the convex hull of the integer points, and never intersects it.



The resolution of the $\frac{1}{1156}(1, 169)$ singularity introduces edges e_1, \dots, e_{10} with inward normals

$$\begin{aligned} \rho_1 &= (0, -1), & \rho_2 &= (-1, -7), & \rho_3 &= (-7, -48), & \rho_4 &= (-13, -89), \\ \rho_5 &= (-19, -130), & \rho_6 &= (-44, -301), & \rho_7 &= (-69, -472), \\ \rho_8 &= (-94, -643), & \rho_9 &= (-119, -814), & \rho_{10} &= (-144, -985). \end{aligned}$$

corresponding to exceptional curves, C_i , $i = 1, \dots, 10$ with

$$C_1^2 = -7, \quad C_2^2 = -7, \quad C_3^2 = C_4^2 = -2, \quad C_5^2 = -3, \quad C_6^2 = \dots = C_{10}^2 = -2$$

Note that the edge e_4 is parallel to the branch cut: this means that, as they move inwards, the edges e_5, \dots, e_{10} cross the branch cut, and appear as $M_{\mathbf{p}_1}^{-1}e_i$. Moving the edges normally inwards to $\Pi_A^{\mathbb{Z}}$, edge e_1 ends up with zero-length concentrated at $(0, 3)$, and e_3, \dots, e_9 end up with zero-length concentrated at $(20, 0)$. The table of affine lengths and displacements becomes:

Edge	e_1	e_2	e_3	e_4	e_5	e_6
Affine length	0	2	0	0	0	0
Affine displacement	1/17	7/17	14/17	21/17	11/17	12/17
Edge	e_7	e_8	e_9	e_{10}		
Affine length	1	0	0	1		
Affine displacement	13/17	14/17	15/17	16/17		

There is an important feature in this example which did not appear in the other examples. Namely, the curve \mathcal{E}_1 from the non-toric blow-up in the construction of \tilde{Y} appears as a

part of the branch locus, with multiplicity 1. This follows from the discussion in §9.3: the polygon $\Pi_A^{\mathbb{Z}}$ has a zero-length edge concentrated at $(14, 1)$ defined by

$$\tilde{b}_1 := \langle u, \rho_4 \rangle = \left(\begin{pmatrix} 8/3 \\ 8/3 \end{pmatrix} - \begin{pmatrix} 14 \\ 1 \end{pmatrix} \right) \cdot \begin{pmatrix} -13 \\ -89 \end{pmatrix} = -1.$$

Write our octic as $\Omega = \sum_p a_p \theta_p$ where θ_p is the GHK theta-function corresponding to the integral point p . If we pick $a_{(0,3)}$, $a_{(7,1)}$, $a_{(14,1)}$ and $a_{(20,0)}$ generically, we find that the strict transform of B intersects C_2 transversely at two points, C_{10} once transversely, and is disjoint from the other curves C_i . According to the prescription in §2.4, the branch locus is $B + C_1 + C_2 + C_4 + C_5 + C_7 + C_9 + \mathcal{E}_1$. Let \tilde{Y} be the blow up of Y at $C_1 \cap C_2$, $C_2 \cap B$, $C_4 \cap C_5$ and $C_4 \cap \mathcal{E}_1$ with exceptional divisors E_1, E_2, E_3, E_4, E_5 and let \tilde{X} be the double cover of \tilde{Y} over the curve. We obtain the surface X by contracting $\sum_{i=1}^{10} \bar{C}_i + \sum_{i=1}^5 \bar{E}_i$. Thus X contains an ugly singularity (see Figure 23).

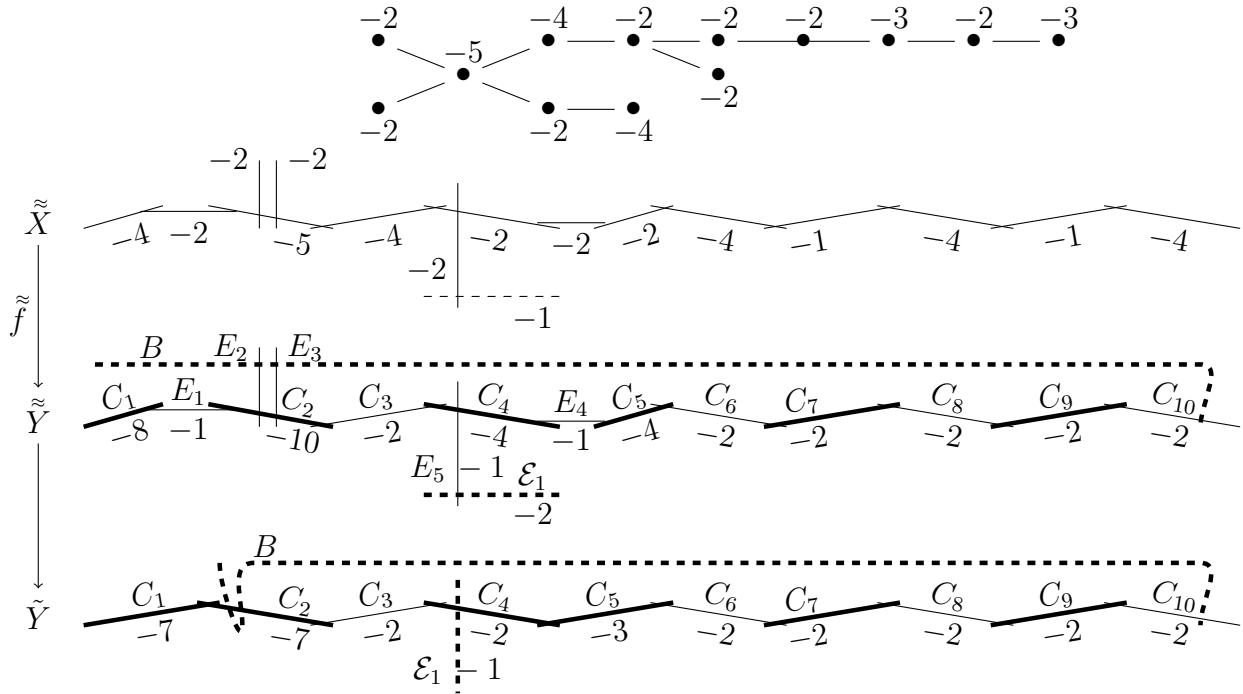


Figure 23: HIP(34). The minimal resolution \tilde{Y} , its blow-up $\tilde{\tilde{Y}}$, and the double cover $\tilde{\tilde{\tilde{X}}}$ of \tilde{Y} . Thick curves are the branch locus. Any non-dashed curves in $\tilde{\tilde{X}}$ are contracted to get X . The top row shows the dual graph of the minimal resolution of the singularity of X .

12 Elliptic fibrations

§12.1 If X is a normal octic double Manetti surface with at worst rational singularities then its geometric genus is the same as an octic double plane, namely $p_g = 3$. The minimal

model of X is then an elliptic surface with $p_g = 3$. To see where the elliptic fibration comes from, observe that the minimal resolutions of Manetti surfaces are blow-ups of rational ruled (Hirzebruch) surfaces: when the branch curve intersects the rulings with total multiplicity 4, the ruling lifts to an elliptic fibration on the branched double cover. Note that the singularities for the octic double $\mathbb{H}\mathbb{P}(29)$ surfaces are irrational, and indeed the minimal model in that case is a ruled surface rather than an elliptic surface.

This point of view can be helpful for studying stable surfaces, so in this section we give a description of the elliptic surfaces which contract down to give our octic double Manetti surfaces in all the cases where it exists. These descriptions can be read off easily from the tropical pictures.

§12.2 Let \mathcal{F} be a singular fibre of the elliptic fibration on the minimal resolution X' of X .

- We call \mathcal{F} an *S-fibre* if it contains an exceptional curve of $X' \rightarrow X$.
- Otherwise, we call \mathcal{F} a *B-fibre*. The *B-fibres* arise from taking double covers of rulings which happen to intersect the branch curve B non-transversely.

We will first describe the *S-fibres* in our examples, then discuss the possibilities for *B-fibres*. To relate this with what we did earlier, recall that we constructed a (not necessarily minimal) resolution $\tilde{X} \rightarrow X$ which was a double cover $\tilde{f}: \tilde{X} \rightarrow \tilde{Y}$. Our figures below show X' , and in each case we will record which curves (if any) in \tilde{X} need to be contracted to get X' . The curves C_i and E_i in \tilde{Y} make reference to the notation and figures from Section 11 and the curves $\mathcal{E}_i \subset \tilde{Y}$ are curves coming from the non-toric blow-ups (defined in §9.2). Recall that \bar{G} denotes $\tilde{f}^{-1}(G)$; we will continue to write \bar{G} for the projection of this curve to X' . Whenever we write F_i we will mean the -1 -curve given by the strict transform of the ruling through the point whose blow-up created the curve E_i (whenever that makes sense). We use standard notation for the Kodaira types of the fibres, see [32] or [6] for an explanation of this notation.

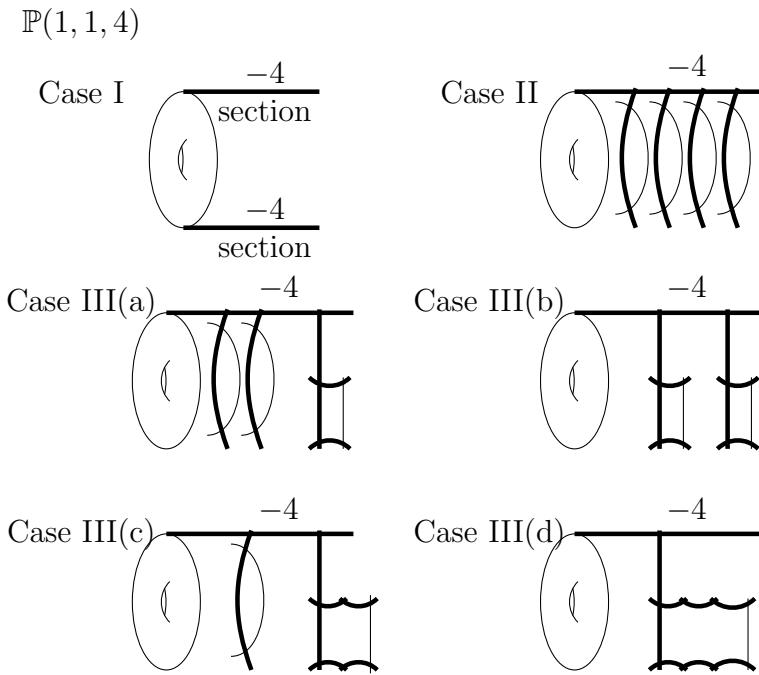


Figure 24: Minimal resolutions for octic double $\mathbb{P}(1, 1, 4)$ surfaces as elliptic fibrations. The exceptional locus is drawn thickly. Any unlabelled curves have self-intersection -2 . Any flat horizontal lines are sections.

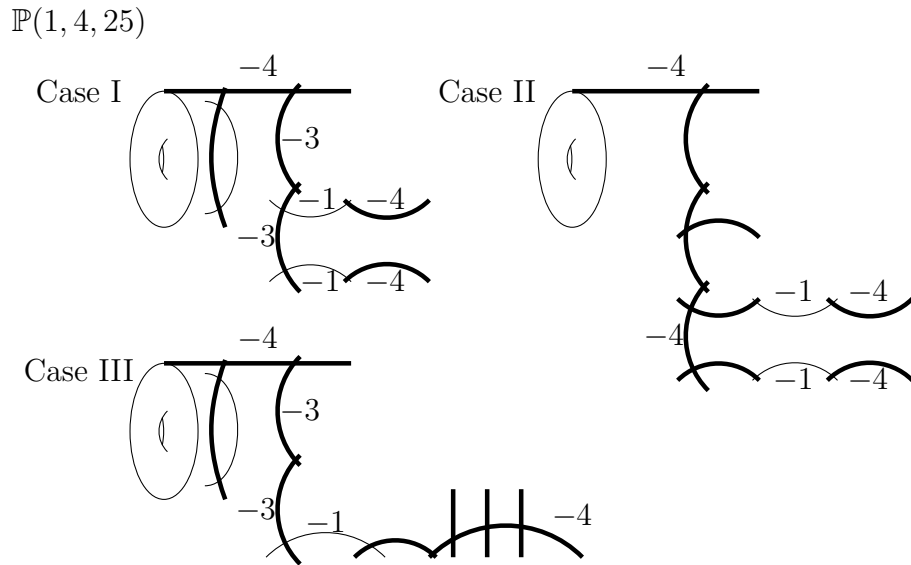


Figure 25: Minimal resolutions for octic double $\mathbb{P}(1, 4, 25)$ surfaces as elliptic fibrations. The exceptional locus is drawn thickly. Any unlabelled curves have self-intersection -2 . Any flat horizontal lines are sections.

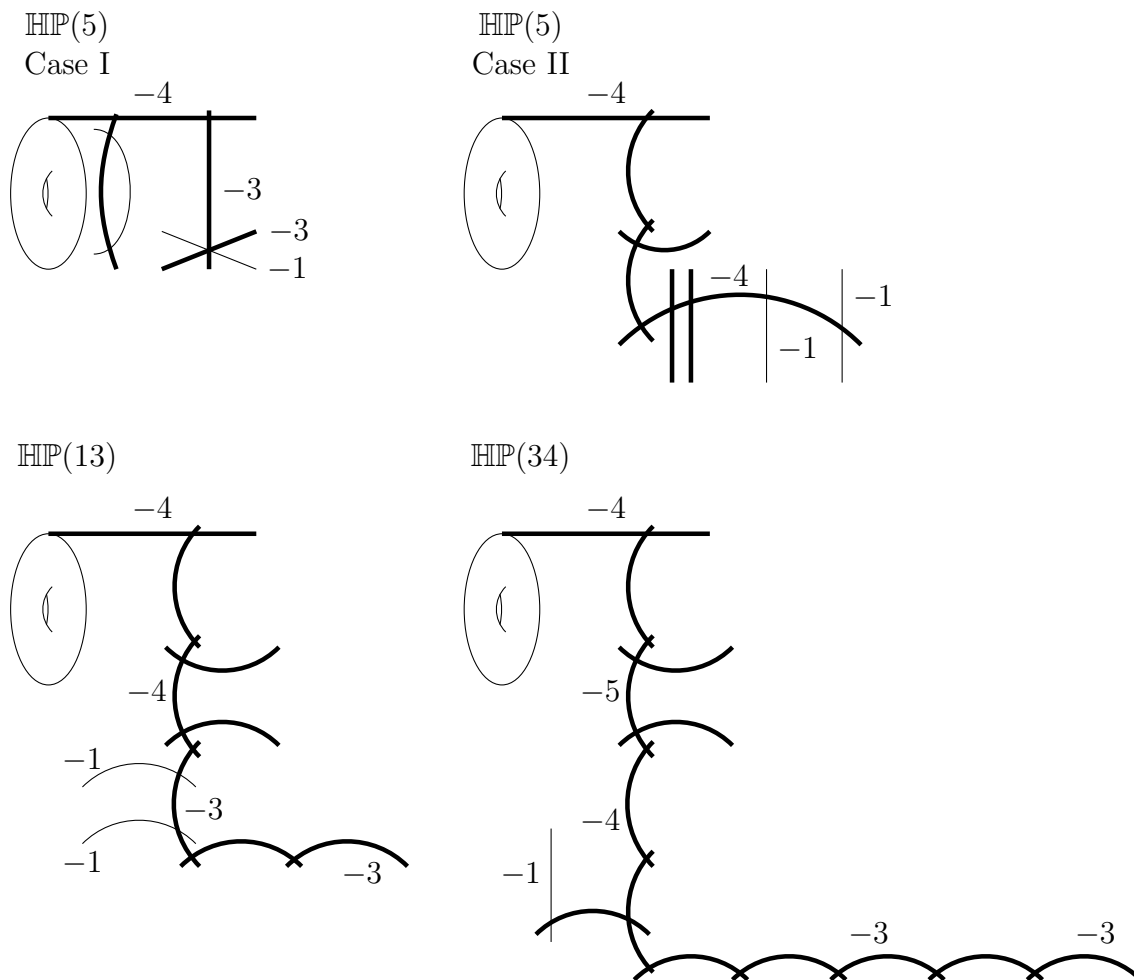


Figure 26: Minimal resolutions for octic double $\mathbb{H}\mathbb{P}(5)$, $\mathbb{H}\mathbb{P}(13)$, and $\mathbb{H}\mathbb{P}(34)$ surfaces as elliptic fibrations. The exceptional locus is drawn thickly. Any unlabelled curves have self-intersection -2 . Any perfectly horizontal lines are sections. The -1 -curves come from non-toric blow-ups.

§12.3 $\mathbb{P}(1, 1, 4)$. See Figure 24. In these cases, $\tilde{X} = X'$. The possible S -fibres are as follows.

- In Case I the curve \overline{C}_1 comprises two disjoint sections of square -4 . There are no S -fibres.
- In Case II (compare with Figure 13), the curve \overline{C}_1 is a single section of square -4 ; the curves $\overline{E}_i + \overline{F}_i$ form four I_2 fibres.
- In Case III we include the subcases (a)–(d) shown in Figure 14: III(a) has two I_2 and one I_4 fibre; III(b) has two I_4 fibres; III(c) has one I_2 and one I_6 fibre; III(d) has one I_8 fibre. In all these cases, \overline{C}_1 is the section of square -4 and the \overline{E}_i and \overline{F}_i assemble themselves into I_n fibres (the curves \overline{F}_i are precisely those which are not drawn thickly in Figure 24).

§12.4 $\mathbb{P}(1, 4, 25)$. See Figure 25. The possible S -fibres are as follows.

- In Case I (compare with Figure 16), \overline{C}_1 is a section of square -4 , $\overline{E}_1 + \overline{F}$ forms an I_2 fibre and $\overline{D}_x + \sum_{i=2}^5 \overline{C}_i$ is a (blown-up) IV fibre. Note that in X' is obtained from \tilde{X} by contracting \overline{C}_3 .
- In Case II (compare with Figure 17), the curve \overline{C}_1 is a section of square -4 , and the curves $\overline{E}_1 + \overline{E}_2 + \sum_{i=2}^5 \overline{C}_i + \overline{D}_x$ is a (blown-up) I_1^* fibre. In this case, $\tilde{X} = X'$.
- In Case III (compare with Figure 18), the curve \overline{C}_1 is a section of square -4 , $\overline{E}_1 + \overline{F}_1$ is an I_2 fibre, and $\overline{D}_x + \sum_{i=2}^5 \overline{E}_i + \sum_{i=2}^5 \overline{C}_i$ is a (blown-up) I_0^* fibre. In this case, X' is obtained from \tilde{X} by contracting \overline{C}_3 .

§12.5 $\mathbb{H}\mathbb{P}(5)$. See Figure 26. The possible S -fibres are as follows.

- In Case I (compare with Figure 19), \overline{C}_1 is a section of square -4 , $\overline{E}_1 + \overline{F}_1$ is an I_2 fibre and $\overline{E}_1 + \sum_{i=2}^4 \overline{C}_2$ is a (blown-up) III fibre. In this case, X' is obtained from \tilde{X} by contracting \overline{C}_3 .
- In Case II (compare with Figure 20), the curve \overline{C}_1 is a section of square -4 and $\overline{E}_1 + \sum_{i=1}^2 \overline{E}_i + \sum_{i=2}^4 \overline{C}_i$ is a (blown-up) I_1^* fibre. In this case, $\tilde{X} = X'$.

§12.6 $\mathbb{H}\mathbb{P}(13)$ (**generic situation**). See Figure 26. In this case (compare with Figure 21), the curve \overline{C}_1 is a section of square -4 and $\overline{E}_1 + \sum_{i=1}^3 \overline{E}_i + \sum_{i=2}^7 \overline{C}_i$ is a (blown-up) I_0^* fibre. This is the only S -fibre. In this case, X' is obtained from \tilde{X} by contracting \overline{C}_4 and \overline{C}_6 .

§12.7 $\mathbb{H}\mathbb{P}(29)$ (**generic situation**). The minimal model is ruled rather than elliptic. The genus 2 curve \overline{C}_7 is a bi-section and the curves $\overline{E}_1 + \overline{E}_0 + \overline{C}_1 + \cdots + \overline{C}_6$ and $\overline{C}_8 + \overline{C}_9 + \overline{C}_{10} + \overline{E}_1$ are each fibres.

§12.8 $\mathbb{H}\mathbb{P}(34)$ (**generic situation**). See Figure 26. For this surface (compare with Figure 23), the curve \overline{C}_1 is a section of square -4 and $\overline{\mathcal{E}}_1 + \sum_{i=1}^5 \overline{E}_i + \sum_{i=2}^{10} \overline{C}_i$ is a (blown-up) I_0^* fibre. This is the only S -fibre. In this case, X' is obtained from \tilde{X} by contracting \overline{C}_7 and \overline{C}_9 .

§12.9 B -fibres for $\mathbb{P}(1, 1, 4)$, **Case I**. The B -fibres appear when the branch locus $B \subset \tilde{Y}$ intersects the branch locus non-transversely. In $\mathbb{P}(1, 1, 4)$, Case I, B intersects each ruling F with total multiplicity four. If we assume that B is smooth away from the singularities of Y , the following possibilities can occur for the remaining singular elliptic fibres:

- B intersects F at two points transversely and one with multiplicity 2. This yields a B -fibre of Type I_1 in the double cover.
- B intersects F at two points with multiplicity 2. This yields a B -fibre of Type I_2 in the double cover.
- B intersects F at one point transversely and at one point with multiplicity 3. This yields a B -fibre of Type II (cuspidal) in the double cover.
- B intersects F at one point with multiplicity 4. This yields a B -fibre of Type III in the double cover.

The B -fibres of Type I_1 and II are irreducible, and hence intersect both components of \overline{C}_1 . The B -fibres of Types I_2 and III are reducible, but each component necessarily intersects one of the irreducible components of \overline{C}_1 .

§12.10 B -fibres in other cases. For all the other cases except $\mathbb{H}\mathbb{P}(29)$, the branch curve B intersects each ruling F at three points: the the fourth branch point of each elliptic fibre over a ruling comes from where the ruling intersects the section C_1 . If we assume that B is smooth away from the singularities of Y , the following possibilities can occur for the remaining B -fibres:

- B intersects F at one point transversely and one point with multiplicity 2. All three points are distinct from $F \cap C_1$, so we get a B -fibre of Type I_1 in the double cover.
- B intersects F at one point with multiplicity 3, distinct from $F \cap C_1$. This yields a B -fibre of Type II in the double cover.

This implies that all of the B -fibres are irreducible, and hence intersect \overline{C}_1 . We will use this fact when we study stability of these surfaces.

13 Stability

§13.1 In this section, we will discuss the stability of the surfaces we have found. The surfaces not covered by Theorem §13.2 below are not log canonical, and hence not stable.

We expect that their stable replacements are non-normal; it would be interesting to know what you get.

§13.2 Theorem. *We call an octic curve $B \subset Y$ generic if it is smooth away from the singularities of Y . Assuming genericity of the branch curve, the following octic double Manetti surfaces are KSBA-stable: $\mathbb{P}(1, 1, 4)$, Cases I, II; $\mathbb{P}(1, 4, 25)$, Cases I, III; $\mathbb{H}\mathbb{P}(5)$, Case I.*

§13.3 Proof of Theorem §13.2. The proof of this theorem will occupy the rest of this section. Certainly the singularities are log canonical, so it remains only to show that K_X is positive on all curves. We will suppose there is an irreducible curve $D \subset X$ with $K_X \cdot D \leq 0$ and derive a contradiction. Let $\rho: X' \rightarrow X$ be the minimal resolution and write A_1, \dots, A_m for the irreducible components of the exceptional locus. In these cases, the minimal model of X' is an elliptic surface, as discussed in Section 12. We write S for this elliptic surface, $\varphi: X' \rightarrow S$ for the contraction, and B_1, \dots, B_n for the exceptional curves of φ .

§13.4 We have $\rho^*K_X = K_{X'} + \sum \alpha_i A_i$ (where $-\alpha_i$ are the discrepancies of ρ) and $K_{X'} = \varphi^*K_S + \sum \beta_i B_i$. Here α_i and β_i are all positive numbers and K_S is homologous to a positive multiple of an elliptic fibre. Therefore ρ^*K_X is an effective sum of curves. Write Σ for the support of ρ^*K_X . Let D be a curve in X and $D' = \text{strict}_\rho(D)$. We have $K_X \cdot D = \rho^*K_X \cdot D'$. If this quantity is non-positive then either D' is one of the curves in Σ or else $D' \cap \Sigma = \emptyset$.

§13.5 Lemma. *If $K_X \cdot D \leq 0$ then D' is an irreducible component of an elliptic fibre.*

Proof. There are two possible cases: either D' is disjoint from Σ or it is a component of Σ . In the first case, since Σ contains an elliptic fibre, D' must be contained in a (different) fibre. In the second case, D' is either contained in a fibre or else it is one of the curves A_i or B_i . It cannot be one of the A_i , since these project to points in X , and the B_i are contained in elliptic fibres. Therefore D' is contained in an elliptic fibre. \square

§13.6 If D' is contained in a B -fibre then it is a -2 -curve which intersects one of the A_i (one of the components of \overline{C}_1). This implies that $\rho^*K_X \cdot D' > 0$. Therefore such a D' cannot satisfy $K_X \cdot D \leq 0$.

§13.7 If D' is contained in an S -fibre then it is one of the uncontracted (thinly-drawn) curves in Figures 24–26. For each of these curves in the cases of interest, we can check (by calculating discrepancies) that $\rho^*K_X \cdot D' > 0$, so again, it is impossible to find such a D with $K_X \cdot D \leq 0$. This completes the proof of Theorem §13.2. \square

14 Smoothability

§14.1 We now address the question of smoothability of octic double Manetti surfaces, and how the various strata of the moduli space we have found fit together. We have seen that an NPQ limit of octic double planes is an octic double Manetti surface; it turns out that *every* octic double Manetti surface is the limit of a degeneration of octic double planes:

§14.2 Theorem. *Any octic double Manetti surface is smoothable.*

Proof. Suppose that Y is a Manetti surface and let n be the product of the Markov numbers associated to the singularities of Y , that is:

$$n = \begin{cases} abc & \text{if } Y = \mathbb{P}(a^2, b^2, c^2) \\ ab & \text{if } Y = \mathbb{HP}(a, b) \\ c & \text{if } Y = \mathbb{HP}(c). \end{cases}$$

Let $B \subset Y$ an octic curve and $f: X \rightarrow Y$ the double cover of Y branched over B . Let $\mathcal{Y} \rightarrow \Delta$ be a \mathbb{Q} -Gorenstein smoothing of Y with general fibre \mathbb{P}^2 . By [12, Theorem 1.6(4)], after possibly making a base change, we can find a divisor $\mathcal{B} \subset \mathcal{Y}$ extending $B \subset Y$ if and only if the Weil divisor class $[B]$ is divisible by n . Since B is an octic curve, $[B] = 8n$, so \mathcal{B} exists, and we can take the double cover of \mathcal{Y} branched over \mathcal{B} to get a smoothing of X . \square

§14.3 The moduli space of smooth octic double planes is 36-dimensional: the projective space of octics is the 44-dimensional space $\mathbb{P}(\text{Sym}^8(V^*))$ where V is the standard representation of the 9-dimensional group $GL(3)$ (whose projectivisation is the 8-dimensional $PGL(3)$), so $\dim \mathbb{P}(\text{Sym}^8(V^*)) // PGL(3) = 36$. We have the following boundary strata comprising NPQ surfaces:

D_A : Surfaces with two $\frac{1}{4}(1, 1)$ singularities (§1.8(i)).

D_B : Surfaces with one $\frac{1}{25}(1, 4)$ singularity (§1.8(iii)).

D_{AB} : Surfaces with two $\frac{1}{4}(1, 1)$ singularities and one $\frac{1}{25}(1, 4)$ singularity (§1.8(ii)).

This enumeration of NPQ strata is only scratching the surface of the KSBA boundary: there are also strata corresponding to the surfaces mentioned in §1.14, which can also be understood similarly, and many deeper strata which we left untouched. There are also degenerations corresponding to double covers of singular limits of \mathbb{P}^2 with irrational singularities, which are not amenable to the (almost) toric methods from this paper.

§14.4 Proposition. *These strata have dimensions:*

$$\dim(D_A) = \dim(D_B) = 35, \quad \dim(D_{AB}) = 34$$

and D_{AB} is in the intersection of the closures of D_A and D_B .

Proof. For any Manetti surface, the space of generic “octics” is 45-dimensional, which becomes 44 after projectivising. This is because a (GHK)-basis is in bijection with the integral points of the corresponding Markov triangle; this is easily seen to be 45 for $\Pi(1, 1, 1)$, and the number of integral points is invariant under mutation.

The cases A , B and AB respectively correspond to general octic double covers of $\mathbb{P}(1, 1, 4)$, $\mathbb{H}\mathbb{P}(5)$ and $\mathbb{P}(1, 4, 25)$. Since $\mathbb{P}(1, 4, 25)$ is a common degeneration of both $\mathbb{H}\mathbb{P}(5)$ and $\mathbb{P}(1, 1, 4)$, we find that D_{AB} is in the closure of both D_A and D_B . It remains to compute the dimensions, and for that it is sufficient to show:

$$\dim(\text{Aut}(\mathbb{P}(1, 1, 4))) = \dim(\text{Aut}(\mathbb{H}\mathbb{P}(5))) = 9, \quad \dim(\text{Aut}(\mathbb{P}(1, 4, 25))) = 10.$$

The general automorphism of $\mathbb{P}(1, 1, 4)$ is:

$$[x : y : z] \mapsto [a_1x + a_2y : a_3x + a_4y : a_5z + a_6x^4 + a_7x^3y + \cdots + a_{10}y^5]$$

(we thank Sönke Rollenske for pointing the five terms we originally missed) which has 9 free parameters up to an overall scale factor.

The general automorphism of $\mathbb{P}(1, 4, 25)$ is:

$$[x : y : z] \mapsto [a_1x : a_2y + a_3x^4 : a_4z + a_5x^{25} + a_6x^{21}y + \cdots + a_{11}xy^6]$$

which has 10 free parameters up to scale.

To understand the automorphism group of $\mathbb{H}\mathbb{P}(5)$, recall that its minimal resolution is obtained from \mathbb{F}_7 by a sequence of two toric and one non-toric blow-ups (see §7.1—we use the notation from that paragraph). Let Y denote the result of performing the two toric blow-ups to \mathbb{F}_7 . An automorphism of Y which fixes the -1 -curve denoted F in Figure 6 lifts to a unique automorphism of $\mathbb{H}\mathbb{P}(5)$ and every automorphism of $\mathbb{H}\mathbb{P}(5)$ arises this way, because the three points $F \cap B$, $F \cap E$ and $F \cap G$ must be fixed, so any automorphism of $\mathbb{H}\mathbb{P}(5)$ fixes F pointwise and can be blown-down.

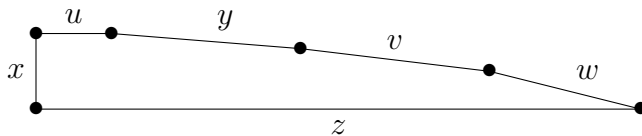


Figure 27: The moment polygon of Y .

It therefore suffices to find the group of automorphisms of Y fixing F pointwise. Since Y is toric, with hexagonal moment polygon, there is a GIT model for Y as $\mathbb{C}^6 // \mathbb{G}_m^4$. Let x, y, z, u, v, w be the Cox variables associated to the edges of the moment hexagon as shown in Figure 27. The inward normals associated to these edges are

$$\rho_x = (0, 1), \rho_y = (-1, -7), \rho_z = (0, 1), \rho_u = (0, -1), \rho_v = (-2, -13), \rho_w = (-1, -6),$$

from which we can read off the weights of the Cox variables under the \mathbb{G}_m^4 -action:

$$\begin{array}{cccccc}
x & y & z & u & v & w \\
1 & 1 & 7 & 0 & 0 & 0 \\
0 & 0 & 1 & 1 & 0 & 0 \\
2 & 0 & 13 & 0 & 1 & 0 \\
1 & 0 & 6 & 0 & 0 & 1
\end{array}$$

The unstable locus is

$$vwyz = vwzx = uwxz = uxyz = uvxy = uvwy = 0.$$

An automorphism has the form

$$[x : y : z : u : v : w] \mapsto \left[ax + byv^2w : cy : dz + \sum_{i=0}^6 e_i uv^{13-2i} w^{6-i} x^i y^{7-i} : fu : gv : hw \right]$$

for some $a, b, c, d, e_0, \dots, e_6, f, g, h$. Invertibility implies that c, f, g, h are all nonzero, and using the \mathbb{G}_m^4 -action we can assume they are all equal to 1. This leaves 10 free parameters a, b, d, e_0, \dots, e_6 . The points $F \cap B = [1 : 0 : 1 : 1 : 0 : 1]$ and $F \cap E = [1 : 1 : 1 : 1 : 0 : 0]$ are automatically fixed, so it suffices to fix another point on F , say $[1 : 1 : 1 : 1 : 0 : 1]$. This reduces to the condition that

$$[a : 1 : d : 1 : 0 : 1] = [1 : 1 : 1 : 1 : 0 : 1].$$

If we pick a square root of a then act using $(1, 1, 1/\sqrt{a}, 1) \in \mathbb{G}_m^4$ we get

$$[1 : 1 : d/\sqrt{a} : 1 : 0 : 1] = [1 : 1 : 1 : 1 : 0 : 1]$$

and have used up all of the freedom in the group action, so the relevant subgroup is defined by the condition that $d^2 = a$. This leaves 9 free parameters, as required. \square

References

- [1] M. Aigner. *Markov's theorem and 100 years of the uniqueness conjecture*. Springer, Cham, 2013. A mathematical journey from irrational numbers to perfect matchings.
- [2] M. Akhtar, T. Coates, A. Corti, L. Heuberger, A. Kasprzyk, A. Oneto, A. Petracci, T. Prince, and K. Tveiten. Mirror symmetry and the classification of orbifold del Pezzo surfaces. *Proc. Amer. Math. Soc.*, 144(2):513–527, 2016.
- [3] V. Alexeev. Boundedness and K^2 for log surfaces. *Internat. J. Math.*, 5(6):779–810, 1994.
- [4] V. Alexeev, H. Argüz, and P. Bousseau. The KSBA moduli space of stable log Calabi-Yau surfaces. *arXiv:2402.15117*, 2024.
- [5] B. Anthes. Gorenstein stable surfaces with $K_X^2 = 2$ and $\chi(\mathcal{O}_X) = 4$. *Ann. Sc. Norm. Super. Pisa Cl. Sci. (5)*, 21:1137–1186, 2020.

- [6] W. P. Barth, K. Hulek, C. A. M. Peters, and A. Van de Ven. *Compact complex surfaces*, volume 4 of *Ergebnisse der Mathematik und ihrer Grenzgebiete. 3. Folge. A Series of Modern Surveys in Mathematics*. Springer-Verlag, Berlin, second edition, 2004.
- [7] L. Bădescu. Normal projective degenerations of rational and ruled surfaces. *J. Reine Angew. Math.*, 367:76–89, 1986.
- [8] J. H. Conway. *The sensual (quadratic) form*, volume 26 of *Carus Mathematical Monographs*. Mathematical Association of America, Washington, DC, 1997. With the assistance of Francis Y. C. Fung.
- [9] S. Coughlan, M. Franciosi, R. Pardini, J. Rana, and S. Rollenske. On T-divisors and intersections in the moduli space of stable surfaces $\overline{\mathfrak{M}}_{1,3}$. *J. Lond. Math. Soc. (2)*, 107(2):750–776, 2023.
- [10] D. A. Cox, J. B. Little, and H. K. Schenck. *Toric varieties*, volume 124 of *Graduate Studies in Mathematics*. American Mathematical Society, Providence, RI, 2011.
- [11] V. I. Danilov. The geometry of toric varieties. *Uspekhi Mat. Nauk*, 33(2(200)):85–134, 247, 1978.
- [12] K. DeVleming and D. Stapleton. Smooth limits of plane curves of prime degree and markov numbers. *arXiv:2208.10595*, 2022.
- [13] H. Esnault and E. Viehweg. Two-dimensional quotient singularities deform to quotient singularities. *Math. Ann.*, 271(3):439–449, 1985.
- [14] J. D. Evans. *Lectures on Lagrangian torus fibrations*, volume 105 of *London Mathematical Society Student Texts*. Cambridge University Press, Cambridge, 2023.
- [15] M. Franciosi, R. Pardini, J. Rana, and S. Rollenske. I-surfaces with one T-singularity. *Boll. Unione Mat. Ital.*, 15(1-2):173–190, 2022.
- [16] M. Franciosi, R. Pardini, and S. Rollenske. Gorenstein stable surfaces with $K_X^2 = 1$ and $p_g > 0$. *Math. Nachr.*, 290(5-6):794–814, 2017.
- [17] W. Fulton. *Introduction to toric varieties*, volume 131 of *Annals of Mathematics Studies*. Princeton University Press, Princeton, NJ, 1993. The William H. Roever Lectures in Geometry.
- [18] P. Gallardo, G. Pearlstein, L. Schaffler, and Z. Zhang. Unimodal singularities and boundary divisors in the KSBA moduli of a class of Horikawa surfaces. *Math. Nachr.*, 297(2):595–628, 2024.
- [19] M. Gross, P. Hacking, and S. Keel. Birational geometry of cluster algebras. *Algebr. Geom.*, 2(2):137–175, 2015.
- [20] M. Gross, P. Hacking, and S. Keel. Mirror symmetry for log Calabi-Yau surfaces I. *Publ. Math. Inst. Hautes Études Sci.*, 122:65–168, 2015.

- [21] M. Gross, P. Hacking, S. Keel, and M. Kontsevich. Canonical bases for cluster algebras. *J. Amer. Math. Soc.*, 31(2):497–608, 2018.
- [22] P. Hacking. Compact moduli of plane curves. *Duke Math. J.*, 124(2):213–257, 2004.
- [23] P. Hacking and Y. Prokhorov. Degenerations of Del Pezzo surfaces I. *arXiv:math/0509529*, 2005.
- [24] P. Hacking and Y. Prokhorov. Smoothable del Pezzo surfaces with quotient singularities. *Compos. Math.*, 146(1):169–192, 2010.
- [25] E. Horikawa. Algebraic surfaces of general type with small c_1^2 . I. *Ann. of Math. (2)*, 104(2):357–387, 1976.
- [26] E. Horikawa. Algebraic surfaces of general type with small c_1^2 . II. *Invent. Math.*, 37(2):121–155, 1976.
- [27] E. Horikawa. Algebraic surfaces of general type with small c_1^2 . III. *Invent. Math.*, 47(3):209–248, 1978.
- [28] E. Horikawa. Algebraic surfaces of general type with small c_1^2 . IV. *Invent. Math.*, 50(2):103–128, 1978/79.
- [29] E. Horikawa. Algebraic surfaces of general type with small c_1^2 . V. *J. Fac. Sci. Univ. Tokyo Sect. IA Math.*, 28(3):745–755 (1982), 1981.
- [30] N. O. Ilten. Mutations of Laurent polynomials and flat families with toric fibers. *SIGMA Symmetry Integrability Geom. Methods Appl.*, 8:Paper 047, 7, 2012.
- [31] A. Kasprzyk, B. Nill, and T. Prince. Minimality and mutation-equivalence of polygons. *Forum Math. Sigma*, 5:Paper No. e18, 48, 2017.
- [32] K. Kodaira. On compact analytic surfaces: II. *Annals of Mathematics*, 77(3):563–626, 1963.
- [33] J. Kollár. *Families of varieties of general type*, volume 231 of *Cambridge Tracts in Mathematics*. Cambridge University Press, Cambridge, 2023. With the collaboration of Klaus Altmann and Sándor J. Kovács.
- [34] J. Kollár and N. I. Shepherd-Barron. Threefolds and deformations of surface singularities. *Invent. Math.*, 91(2):299–338, 1988.
- [35] T. Mandel. Tropical theta functions and log Calabi-Yau surfaces. *Selecta Math. (N.S.)*, 22(3):1289–1335, 2016.
- [36] M. Manetti. Normal degenerations of the complex projective plane. *J. Reine Angew. Math.*, 419:89–118, 1991.
- [37] M. Manetti. *Degenerations of algebraic surfaces and applications to moduli problems*. PhD thesis, Scuola Normale Pisa, 1996.

- [38] M. Manetti. Degenerate double covers of the projective plane. In *New trends in algebraic geometry (Warwick, 1996)*, volume 264 of *London Math. Soc. Lecture Note Ser.*, pages 255–281. Cambridge Univ. Press, Cambridge, 1999.
- [39] V. Monreal, J. Negrete, and G. Urzúa. Classification of Horikawa surfaces with T-singularities. *In preparation*, 2024.
- [40] J. Rana. A boundary divisor in the moduli spaces of stable quintic surfaces. *Internat. J. Math.*, 28(4):1750021, 61, 2017.
- [41] J. Rana and S. Rollenske. Standard stable Horikawa surfaces. *arXiv:2211.12059*, 2022.
- [42] J. Rana and G. Urzúa. Optimal bounds for T-singularities in stable surfaces. *Adv. Math.*, 345:814–844, 2019.
- [43] M. Symington. Four dimensions from two in symplectic topology. In *Topology and geometry of manifolds (Athens, GA, 2001)*, volume 71 of *Proc. Sympos. Pure Math.*, pages 153–208. Amer. Math. Soc., Providence, RI, 2003.
- [44] I. R. Šafarevič, B. G. Averbuh, Ju. R. Vaňberg, A. B. Žižčenko, Ju. I. Manin, B. G. Moišezon, G. N. Tjurina, and A. N. Tjurin. Algebraic surfaces. *Trudy Mat. Inst. Steklov.*, 75:1–215, 1965.